NHM2018

# 5th International Workshop on Nonhydrostatic Models

November 14-16, 2018

Japan Meteorological Agency, Tokyo, Japan

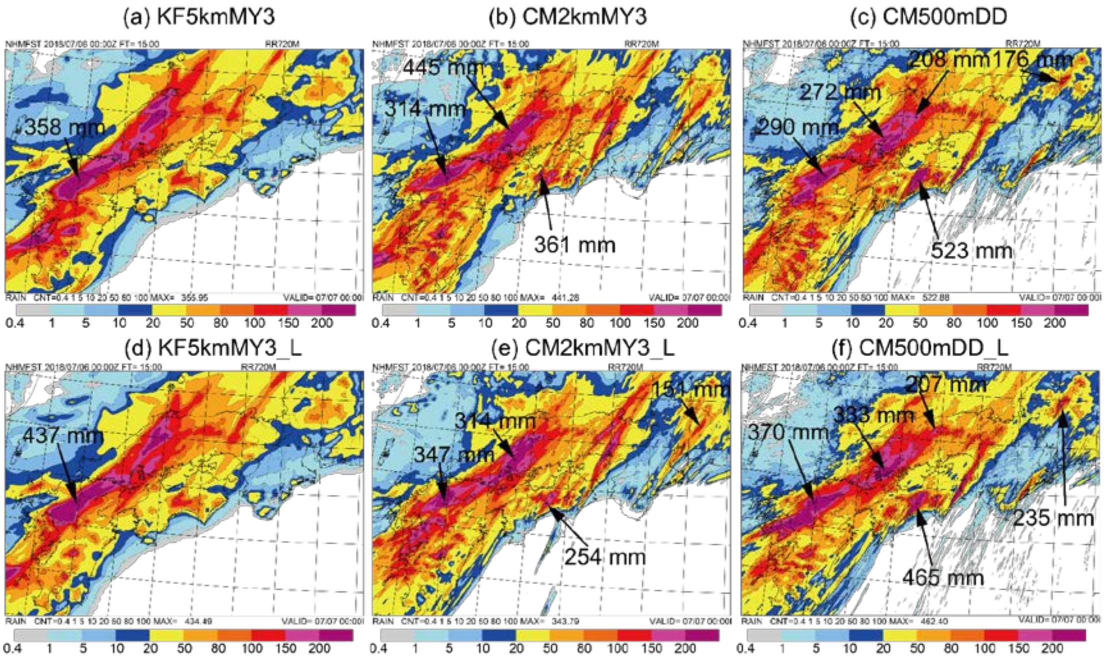


Japan Meteorological Agency, Meteorological Research Institute, JAPAN

Research Group on Non-hydrostatic Numerical Models,

Meteorological Society of Japan

# 5th International Workshop on Nonhydrostatic Models (NHM2018)

## Program and Abstracts

Prepared by Local Organizing Committee of the NHM2018

November 14-16, 2018

Japan Meteorological Agency, Tokyo, Japan

## 5th International Workshop on Nonhydrostatic Model (NHM2018)

The workshop on nonhydrostatic modeling celebrates its 20th anniversary this year. For the past two decades, the non-hydrostatic model has created many scientific achievements and has contributed to society as an operational model of the Japan Meteorological Agency. NHM2018 will focus on all aspects of nonhydrostatic models: from Large Eddy Simulation (LES) models to global models, dynamical frames, physics schemes, data assimilation schemes and regional climate models. Predictability and applications to mesoscale phenomena such as tropical cyclones, heavy precipitations, and shallow clouds are all welcome. The high-performance computing for the meteorological and climate researches in the future is one of our great concerns.

## NHM2018 Local Organizing Committee

Hiromu Seko (Meteorological Research Institute, Japan Meteorological Agency)
Akihiko Murata (Meteorological Research Institute, Japan Meteorological Agency)
Akiyoshi Wada (Meteorological Research Institute, Japan Meteorological Agency)

## Website

http://www.mri-jma.go.jp/Dep/fo/lab2/nhmws/Nonhydrostatic%20Modeling%20Workshop%20(NHM)%202018.html

## Sponsors and Supporters

Japan Meteorological Agency, Meteorological Research Institute, JAPAN
Research Group on Non-hydrostatic Numerical Models, Meteorological Society of Japan

# 5th International Workshop on Nonhydrostatic Models (NHM2018)

## Session Program

### November 14 (Wed)

| | |
|---|---|
| 9:30- 9:50 | Opening |
| | Ken-ichi Kuma (Meteorological Research Institute) |
| 9:50-11:40 Session 1 Global Modelling: | |
| | Chair: Tomoki Miyakawa (The University of Tokyo) |
| 9:50-10:20 | O1.1 An Update on Our Comparison of Alternative Dynamical Frameworks for Global Cloud-Resolving Models |
| | （Invited） David Randall （Colorado State University) |
| 10:20-10:40 | O1.2 Development of nonhydrostatic Double Fourier Series global spectral Model (DFSM) and Global 7km mesh Model Intercomparison Project for improving TYphoon forecast (TYMIP-G7) |
| | Hiromasa Yoshimura (Meteorological Research Institute, Forecast Research Department) |
| 10:40-11:00 | O1.3 The impact of hybrid usage of the Chikira-Sugiyama scheme on tropical convection and large-scale circulations in NICAM |
| | Tomoki Miyakawa (The University of Tokyo, Atmosphere and Ocean Research Institute) |
| 11:00-11:20 | O1.4 A preliminary result in the DYAMOND simulations by NICAM |
| | Ryosuke Shibuya (Japan Agency for Earth-Marine Science and Technology) |
| 11:20-11:40 | O1.5 Initiation processes of the tropical intraseasonal variability simulated in an aqua-planet experiment: Implication for MJO onset |
| | Daisuke Takasuka (The University of Tokyo, Atmosphere and Ocean Research Institute) |
| 11:40-13:00 Lunch time | |
| 13:00-14:50 Session 2 Rainfall event: | |
| | Chair: Tetsuya Takemi (Kyoto University) |
| 13:00-13:30 | O1.6 Tracking of convective rain events in idealized and realistic large eddy simulations |
| | (Invited) Christopher Moseley (Max Planck Institute for Meteorology, Hamburg, Germany Atmosphere in the Earth System) |

| | |
|---|---|
| 13:30-13:50 | O1.7 High-resolution large-eddy simulation of urban atmospheric boundary layer |
| | Antti Hellsten (Finnish Meteorological Institute) |
| 13:50-14:10 | O1.8 Importance of Terrain Representation in Simulating a Stationary Convective System for the July 2017 Northern Kyushu Heavy Rainfall Case |
| | Tetsuya Takemi (Kyoto University, Disaster Prevention Research Institute) |
| 14:10-14:30 | O1.9 Development of a high-resolution cloud-resolving model over complex topography (TaiwanVVM) |
| | Chien-Ming Wu (National Taiwan University,Atmospheric Sciences) |
| 14:30-14:50 | O1.10 Evaluation of WRF and WRF-Hydro Models in Simulating Heavy Rainfall and Streamflow in the Talomo Watershed: A Baseline Study for the Development of a HydroMeteorological Flood Forecasting System for Davao City |
| | Cathrene Ma. Lagare (Ateneo de Davao University, Environmental Science) |
| 14:50-15:10 Break | |
| 15:10-17:00 Session 3 Reanalysis and data assimilation: Chair: Shin Fukui (Tohoku University) | |
| 15:10-15:40 | O1.11 Regional Reanalysis systems and production in Europe |
| | (Invited) Per Unden (SMHI, Research) |
| 15:40-16:00 | O1.12 Towards a long-term high-resolution regional reanalysis over Japan by using NHM-LETKF |
| | Shin Fukui (Tohoku University, Graduate school of Science) |
| 16:00-16:20 | O1.13 Impacts of high-resolution Himawari-8 AMVs assimilation on TC forecast in HWRF |
| | Masahiro Sawada (Meteorological Research Institute, Japan Meteorological Agency, Typhoon Research Department) |
| 16:20-16:40 | O1.14 Regional atmospheric data assimilation coupled with an ocean mixed layer model: a case of typhoon Soudelor (2015) |
| | Kohei Takatama (RIKEN Center for Computational Science) |
| 16:40-17:00 | O1.15 Near-real-time SCALE-LETKF forecasts of the record breaking rainfall in Japan in July 2018 |
| | Takumi Honda (RIKEN Center for Computational Science) |

| 17:00-17:35 | **Poster Session 1** |
|---|---|
| | P1 Establishment of MRV system of greenhouse gas emission from Asian rice paddies by integrating multi-type satellite data and ground flux data |
| | Hironori Arai (the University of Tokyo, Institute of Industrial Science) |
| | P2 Forecast skill of intraseasonal oscillation events over the Maritime Continent in a global cloud-system-resolving model |
| | Tomoe Nasuno (Japan Agency for Marine-Earth Science and Technology, Department of Seamless Environmental Prediction Research) |
| | P3 Continental-scale simulation of diurnal variations in South Asian summer monsoon: Insights from the explicit and parameterized convection experiments |
| | Rakesh Teja Konduru (Tokyo Metropolitan University) |
| | P4 An oceanic impact of the Kuroshio path on snowfall on the Kanto region of Japan in the cold season. |
| | Takuya Yamazaki (Tokyo Metropolitan University, Laboratory of Climatology) |
| | P5 Sensitivity of coastal front simulation to the thermal diffusivity in the PBL scheme |
| | Kento Suzuki (Tohoku University, Atmospheric Science) |
| | P6 Data assimilation and forecast experiments for the record-breaking rainfall event in Japan in July 2018 with NICAM-LETKF at 112-km and 28-km resolution |
| | Koji Terasaki (RIKEN Center for Computational Science) |
| | P7 Data Assimilation Experiments with Himawari-8 Optimal Cloud Analysis Products |
| | Michiko Otsuka (Meteorological Research Institute, Forecast Research Department) |
| | P8 Precipitation nowcasting with Phased-Array Weather Radar: a case of July 2018 record-breaking rainfall in Western Japan |
| | Shigenori Otsuka (RIKEN Center for Computational Science) |
| | P9 Impact of every 30-second phased array weather radar data on simulating a torrential rainfall event on July 6, 2018 around Kobe city |
| | Yasumitsu Maejima (RIKEN Center for Computational Science) |
| | P10 Fine-scale Structure of Mesoscale-beta-scale vortices that caused tornado-like vortices |
| | Eigo Tochimoto (Atmosphere and Ocean Resaerch Institute, The University of Tokyo) |

**November 15 (Thu)**

| | |
|---|---|
| 9:40-11:40 Session 4 Data Assimilation: Chair: Takuya Kawabata (Meteorological Research Institute) | |
| 9:40-10:10 | O2.1 Particle Filters for Convective Scale NWP |
| | (Invited) Potthast Roland (Deutscher Wetterdienst) |
| 10:10-10:40 | O2.2 Regional Weather Forecasting Using the Local Particle Filter |
| | (Invited) Jonathan Poterjoy (University of Maryland, Atmospheric and Oceanic Science) |
| 10:40-11:00 | O2.3 A Study on Non-Gaussian Probability Densities on Convection Initiation and Development using a Particle Filter with a Storm-Scale Numerical Weather Prediction Model |
| | Takuya Kawabata (Meteorological Research Institute, Japan Meteorological Agency, Forecast Research Department) |
| 11:00-11:20 | O2.4 LETKF Perturbations by Ensemble Transform in a Cloud Resolving Model |
| | Kazuo Saito (Japan Meteorological Business Support Center, The University of Tokyo) |
| 11:20-11:40 | O2.5 Model Parameter Estimation with Data Assimilation using NICAM-LETKF |
| | Shunji Kotsuki (RIKEN Center for Computational Science) |
| 11:40-13:00 Lunch time | |
| 13:00-14:50 Session 5 Physics 1: Chair: Wojciech Grabowski (Grabowski Wojciech) | |
| 13:00-13:30 | O2.6 Towards a super dynamics for the gray zone |
| | (Invited) Shian-Jiann Lin (GFDL, The Weather and Climate dynamics division) |
| 13:30-13:50 | O2.7 A three-dimensional turbulence scheme for the gray zone in a convective boundary layer |
| | Yuji Kitamura (Meteorological Research Institute, Japan Meteorological Agency, Atmospheric Environment and Applied Meteorology Research Department) |
| 13:50-14:10 | O2.8 Plumes, thermals and chains: A critical examination of the various conceptual models for moist convection |
| | Hugh Morrison (UCAR) |
| 14:10-14:30 | O2.9 Separating dynamic and thermodynamic impacts of climate change on daytime convective development over land |
| | Wojciech Grabowski(NCAR, MMM Lab) |

| | |
|---|---|
| 14:30-14:50 | O2.10 Super Fine Vertical Resolution Radiative-Convective Equilibrium Experiments on the High-Cloud Response to Sea Surface Temperatures |
| | Tomoki Ohno (The University of Tokyo, Atmosphere and Ocean Research Institute) |
| 14:50-15:10 Break | |
| 15:10-16:40 Session 6 Physics 2: Chair: Tatsuya Seiki (JAMSTEC) | |
| 15:10-15:40 | O2.11 Alleviating low cloud problem in climate and weather forecast models by adaptive vertical grid enhancement |
| | (Invited) Takanobu Yamaguchi (CIRES CU/NOAA ESRL, CSD) |
| 15:40-16:00 | O2.12 Evaluation of microphysics in mixed-phase clouds over the Southern Ocean in NICAM using Joint simulator |
| | Woosub Roh (The University of Tokyo, Atmosphere and Ocean Research Institute) |
| 16:00-16:20 | O2.13 Ice cloud modeling for simulating mixed-phase low-clouds |
| | Tatsuya Seiki (Japan Agency for Marine-Earth Science and Technology, Department of Seamless Environmental Prediction Research) |
| 16:20-16:40 | O2.14 A numerical investigation of the impact of aerosol-induced warming on deep convective updrafts with varying slope and width |
| | Zachary Lebo (University of Wyoming, Department of Atmospheric Science) |
| 16:40-17:15 | **Poster Session 2** |
| | P11 30-second cycle LETKF assimilation of dual-phased array weather radar observations to short-range convective forecasts |
| | James Taylor (RIKEN Center for Computational Science) |
| | P12 Surface flux parameterization for large eddy simulation |
| | Junshi Ito (University of Tokyo, Atmosphere and Ocean Research Institute) |
| | P13 LES analysis of the effect of source heights on the longitudinal distribution of plume concentration in the convective boundary layer capped by a temperature inversion |
| | Hiromasa Nakayama (Japan Atomic Energy Agency, Research Group for Environmental Sciences) |
| | P14 Intercomparison of rainfall simulations using different bulk microphysical models |
| | Yoshinori Yamada (Meteorological Research Institute, Forecast Research Department) |

| | |
|---|---|
| | P15　Revisit of the fixed anvil temperature hypothesis from nonhydrostatic global simulations |
| | Akira Noda (Japan Agency for Marine-Earth Science and Technology, Project Team for Advanced Climate Modeling) |
| | P16　High resolution simulation of the west Japan heavy rainfall in July 2018 |
| | Tsutao Oizumi (Japan Agency for Marine-Earth Science and Technology, Project Team for HPC Advanced Predictions utilizing Big Data) |
| | P17　Development and validation of a diagonal ensemble transform Kalman filter |
| | Le Duc (Japan Agency for Marine-Earth Science and Technology, Department of Seamless Environmental Prediction Research) |
| | P18　4DEnVar with Iterative Calculation of Nonlinear Nonhydrostatic Model Compared to En4DVar |
| | Sho Yokota (Meteorological Research Institute, Forecast Research Department) |
| | P19　Ensemble-based Singular Value Decomposition Analysis to Clarify Relationship between the Atmospheric State and the Hydrometeors |
| | Sho Yokota (Meteorological Research Institute, Forecast Research Department) |
| | P20　Dense precipitation radar data assimilation with an ensemble Kalman filter: an observing system simulation experiment for a typhoon case |
| | Atsushi Okazaki (RIKEN Center for Computational Science) |
| | P21　Assimilating every-10-minute Himawari-8 infrared radiances to improve convective predictability |
| | Yohei Sawada(Meteorological Research Institute, Japan Meteorological Agency, Forecast Research Department) |
| 18:00-20:00 Buffet | |

## November 16 (Fri)

| | |
|---|---|
| 9:40-11:40 Session 7 Dynamics: Chair: John McGregor (CSIRO, Oceans and Atmosphere) | |
| 9:40-10:10 | O3.1 Some preliminary results from Global SAM |
| | (Invited) Marat Khairoutdinov (School of Marine and Atmospheric Sciences, Stony Brook University) |
| 10:10-10:40 | O3.2 Atmospheric modelling on the equal-area cubed-sphere |
| | (Invited) John McGregor (CSIRO, Oceans and Atmosphere) |
| 10:40-11:00 | O3.3 A shallow-water model using the B-grid staggering on the spherical icosahedral grid |
| | Hiroaki Miura (The University of Tokyo, Graduate School of Science) |
| 11:00-11:20 | O3.4 A nestable, multigrid-friendly grid on a sphere for global spectral models based on Clenshaw-Curtis quadrature. |
| | Daisuke Hotta (Meteorological Research Institute, Japan Meteorological Agency, Forecast Research Department) |
| 11:20-11:40 | O3.5 Coupling isobaric physics with isochoric dynamics |
| | Youhei Kawano (Japan Meteorological Agency, Forecast Department) |
| 11:40-11:50 | Closing |
| | Toshiki Iwasaki (Tohoku University) |

# Open Seminar

## Advancements of non-hydrostatic modeling and its future perspectives for numerical weather forecasting

**Date** : November 16 (Fri)

**Purpose of this seminar**

The workshop on nonhydrostatic modeling celebrates its 20th anniversary this year. For the past two decades, the non-hydrostatic model has created many scientific achievements and has contributed to society as an operational model of the Japan Meteorological Agency. At this open seminar, we will introduce topics on leading-edge technologies and social contributions regarding nonhydrostatic modeling to the general public.

## Program of Open Seminar

| | |
|---|---|
| **13:30-13:45**<br>**Opening**<br><br>**Kazuo Saito**<br>(Japan Meteorological Business Support Center, The university of Tokyo) | |
| **13:45-14:20**<br>**Research and development of a basic library and environment SCALE for next-generation meteorological simulations**<br><br>**Seiya Nishizawa PhD**<br>(RIKEN Center for Computational Science)<br><br>What will be possible in next-generation weather and climate simulation? What are the challenges for realizing that? This talk introduces the possibilities and challenges revealed thorough our research, such as high resolution simulations using the SCALE. |  |

**14:20-14:55**
**Global Cloud-Resolving Simulations by the Nonhydrostatic Icosahedral Atmospheric Model, NICAM**

**Masaki Satoh Prof.**

(Atmosphere and Ocean Research Institute, The University of Tokyo)

NICAM realistically simulates clouds over the globe with a km scale mesh covering the entire earth. This talk introduces NICAM simulations of multi-scale convective systems including the Madden-Julian oscillations and tropical cyclones.

**14:55-15:30**
**Data assimilation research using NICAM and SCALE**

**Takemasa Miyoshi PhD**

(RIKEN Center for Computational Science)

Data assimilation connects computer model simulations and measurement data and plays a central role in prediction. This talk focuses on data assimilation research using the NICAM and SCALE models.

**15:30-15:40**
**Break**

**15:40-16:15**
**Development of JMA operational limited-area NWP systems**

**Tadashi Fujita Senior Scientific Officer**

(JMA Forecast Department)

This talk presents about development of the JMA operational Meso-scale and Local NWP systems aimed at enhancement of disaster prevention and aviation forecast.

**16:15-16:30**
**Efforts of the Japan Meteorological Agency for the numerical weather models**

**Masaki Hasegawa Senior Coordinator for Research and Development**

(JMA Administration Department)

| | |
|---|---|
| The Japan Meteorological Agency are promoting any developments based on "JMA NWP Strategic Plan Toward 2030" for contributing to the prevention and reduction of weather disasters, and improvement of productivity in socioeconomic activities. This talk introduces efforts of the Japan Meteorological Agency on this strategic plan and also explains a perspective of the developments of numerical modeling, which is one of essential technologies for numerical weather system. | |
| **16:30-16:35**<br>**Closing** | |

# Venue

## *Conference room (2F), Japan Meteorological Agency*

*Address: 1-3-4 Otemachi, Chiyoda-ku, Tokyo 100-8122, Japan*
*Website: http://www.jma.go.jp/jma/en/Access/indexe_acs.html*


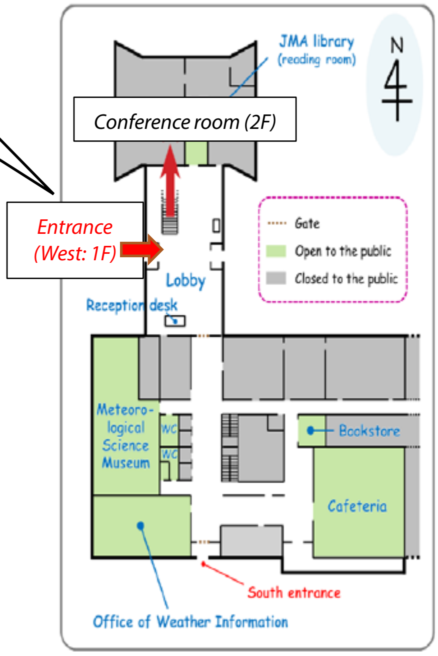


# Buffet *(Pre-registration only)*

## *PRONTO, Otemachi Conference Center B1F*

Date and Time:

1800-2000 JST, 15th November, 2018

Fee: ¥7,000 per person (¥5,000 per student)

*Please pay the fee at the registration.*

After https://tabelog.com/tokyo/A1310/A131002/13097960/dtlphotolst/1/smp2/

# Access

## *From Narita International Airport*

*Narita International Airport is about 60 km east of central Tokyo. A variety of public transport connects Narita International Airport to central Tokyo.*

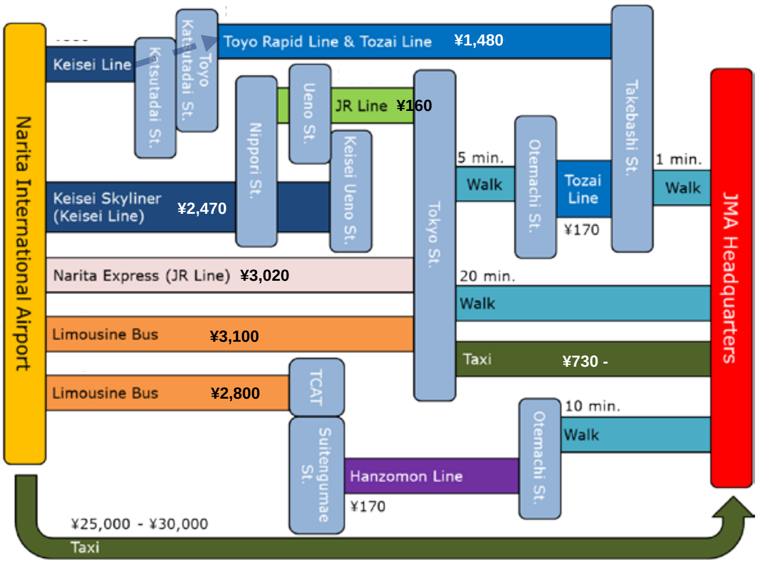


## Railways

JR East (East Japan Railway Company) and Keisei Electric Railway Co., Ltd. operate express train services between Narita International Airport and central Tokyo. ※Discount service is available when using a prepaid IC card such as Suica and Pasmo.

### JR Lines

The Narita Express train connects Narita International Airport to Tokyo, Shinagawa, Yokohama, Shinjuku and Ikebukuro (all trains stop at Tokyo Station). The station at Narita International Airport is located under the terminal building. It takes about an hour between Tokyo and Narita with a fare of 3,020 yen (as of October 2018).

### Keisei Lines

Keisei Electric Railway Co., Ltd. runs Skyliner express trains between Narita International Airport and Keisei Ueno Station. It takes about an hour between Narita and Ueno with a fare of 2,470 yen (as of October 2018). Standard express trains also run every 20 minutes, connecting Narita and Ueno in 70 minutes at 840 yen (as of October 2018). Passengers can board the Keisei Skyliner at Keisei Narita Airport Station, located under the terminal building. The train runs all the way to Keisei Ueno Station in Tokyo. The JR Ueno and Ueno subway stations are within a short walking distance of Keisei Ueno Station. The Keisei line connects with JR lines at Nippori Station.

## Bus transportation

Limousine bus services are available between Narita Airport and Tokyo City Air Terminal (TCAT), Tokyo Station and other places around Tokyo.

## Tokyo City Air Terminal (TCAT)

TCAT is located at Hakozaki, about a 10-minute drive from Tokyo Station. TCAT is directly connected to Suitengumae Station on the Hanzomon Subway Line, which leads to central Tokyo.

## *From Tokyo International Airport (Haneda Airport)*

*Tokyo International Airport (Haneda Airport) is about 20 km south of central Tokyo. A variety of public transport connects Tokyo International Airport to central Tokyo.*

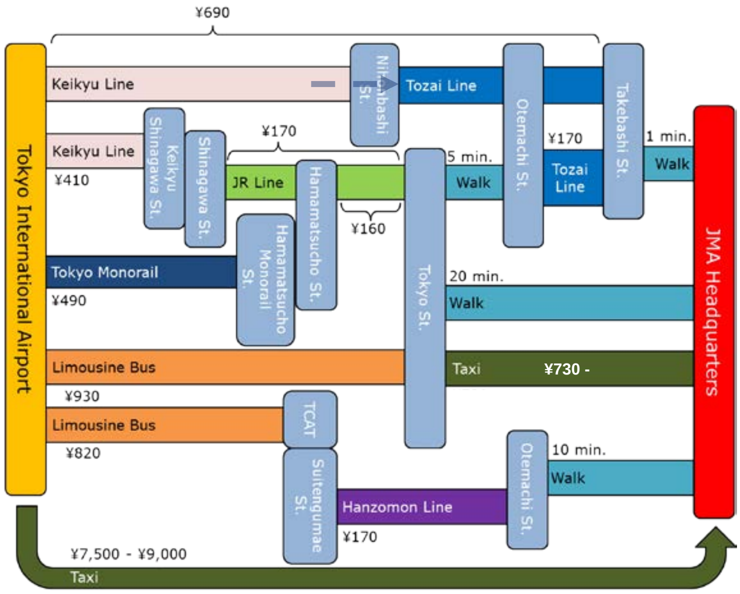


## Railways

Keikyu Corporation, Tokyo Monorail Co., Ltd. and JR East (East Japan Railway Company) operate train services between Tokyo International Airport (Haneda Airport) and central Tokyo. ※Discount service is available when using a prepaid IC card such as Suica and Pasmo.

### Keikyu Lines

Keikyu Corporation runs Airport Limited express trains between International Terminal and Keikyu Shinagawa Station. It takes about 12 minutes between Tokyo International Airportand Shinagawa with a fare of 410 yen (as of October 2018). Passengers can board the Keikyu line at Keikyu Haneda Airport International Terminal Station, located under the terminal building. The JR Shinagawa station is within a short walking distance of Keikyu Shinagawa Station. The Keikyu line also connects with the Tokyo Metro Tozai Line at Nihonbashi Station. It takes about 40 minutes between Tokyo International Airport and Takebashi Station with a fare of 690 yen (as of October 2018).

### Tokyo Monorail

The Tokyo Monorail runs between Tokyo International Airport (Haneda Airport International Terminal) and Hamamatsucho Monorail Station. It takes about 15 minutes between Tokyo international Airport and Hamamatsucho with a fare of 490 yen (as of October 2018). Passengers can board the Tokyo Monorail at Haneda Airport International Terminal Monorail Station on the third floor of the terminal building. The JR Hamamatsucho station is within a short walking distance of Monorail Hamamatsucho Station.

## Bus transportation

Limousine bus services are available between Tokyo International Airport and Tokyo City Air Terminal (TCAT), Tokyo Station and other places around Tokyo.

## Tokyo City Air Terminal (TCAT)

TCAT is located at Hakozaki, about a 10-minute drive from Tokyo Station. TCAT is directly connected to Suitengumae Station on the Hanzomon Subway Line, which leads to central Tokyo.

# November 14, 2018 (Wednesday)

O1.1

# An Update on Our Comparison of Alternative Dynamical Frameworks for Global Cloud-Resolving Models

David Randall, Celal Konor, Ross Heikes, and Joon-Hee Jung

Department of Atmospheric Science
Colorado State University
Fort Collins, Colorado 80523
Email: david.randall@colostate.edu

## Abstract

Various approaches are being explored in the rapidly evolving world of dynamical cores for global cloud-resolving models. Issues include alternative equation sets (fully compressible versus sound-proof), alternative choices of prognostic variables (momentum versus vorticity), alternative methods to discretize the sphere itself (icosahedral versus cubic), and alternative vertical staggerings (Lorenz versus Charney-Phillips). In this talk we will show comparisons of cloud-resolving simulations with different dynamical cores but identical physics for both idealized (e.g., bubble) and realistic (e.g., TWP-ICE) cases.

We are comparing the merits of several prognostic variables to represent the wind field. These include:

- the momentum vector,
- the vertical component of the vorticity and the horizontal divergence as in the Z-grid model of Randall (1994),
- the horizontal vorticity vector as in the "vector vorticity model" (VVM) of Jung and Arakawa (2008), and finally
- the curl of the horizontal vorticity vector combined with the vertical component of the vorticity.

The momentum equation is being tested with the fully compressible system of equations, and also the anelastic system and the "Unified System" of Arakawa and Konor (2009).

The other three choices are tested only with the anelastic and Unified systems.

All of the dynamical cores currently use the Lorenz grid, although we plan to test the Charney-Phillips grid in the future.

All of the dynamical cores have  been coupled with the physical parameterizations of the System for Atmospheric Modeling (SAM; Khairoutdinov and Randall, 2003). We are also comparing our results with comparable simulations using SAM.

The cores are being tested with Cartesian grids on a plane, hexagonal grids on a plane, and geodesic grids. Test cases include dry bubbles, radiative-convective equilibrium, cases based on field data, e.g., TWP-ICE (Fridlind et al., 2012), and idealized baroclinic waves on the sphere.

**References:**


Arakawa, A. and Konor, C.S., 2009. Unification of the anelastic and quasi-hydrostatic systems of equations. *Monthly Weather Review*, *137*(2), pp.710-726.

Fridlind, A.M., Ackerman, A.S., Chaboureau, J.P., Fan, J., Grabowski, W.W., Hill, A.A., Jones, T.R., Khaiyer, M.M., Liu, G., Minnis, P. and Morrison, H., 2012. A comparison of TWP-ICE observational data with cloud-resolving model results. *Journal of Geophysical Research: Atmospheres*, *117*(D5).

Jung, J.H. and Arakawa, A., 2008. A three-dimensional anelastic model based on the vorticity equation. *Monthly Weather Review*, *136*(1), pp.276-294.

Khairoutdinov, M.F. and Randall, D.A., 2003. Cloud resolving modeling of the ARM summer 1997 IOP: Model formulation, results, uncertainties, and sensitivities. *Journal of the Atmospheric Sciences*, *60*(4), pp.607-625.

Randall, D.A., 1994. Geostrophic adjustment and the finite-difference shallow-water equations. *Monthly Weather Review*, *122*(6), pp.1371-1377.

O1.2

# Development of nonhydrostatic Double Fourier Series global spectral Model (DFSM) and Global 7km mesh Model Intercomparison Project for improving TYphoon forecast (TYMIP-G7)

Hiromasa Yoshimura[1], Akiyoshi Wada[1], Masuo Nakano[2], Ryo Onishi[2], Masayuki Nakagawa[1], Tomoe Nasuno[2], Masato Sugi[1], Masahiro Sawada[1], Koji Goto[3], Kenta Sakauchi[3]

1. Meteorological Research Institute, Japan Meteorological Agency, Tsukuba
2. Japan Agency for Marine-Earth Science and Technology, Japan
3. NEC, Ltd.

Email: hyoshimu@mri-jma.go.jp

**Abstract**

Based on the Japan Meteorological Agency Global Spectral Model (JMA GSM), we have developed a nonhydrostatic Double Fourier Series Model (DFSM) (Yoshimura 2012), where double Fourier series (DFS) are used as basis functions instead of spherical harmonics. The use of DFS reduces computational cost in high resolutions.

We had used the DFS basis functions of Cheong (2000) until recently. For improvement near the North and South poles, we have developed and introduced a new method using different basis functions. In the basis functions of Cheong (2000), scalar variables are expanded with $\sin n\varphi$ in the meridional direction for odd $m\,(\geq 3)$, where $\varphi$ is colatitude, $n$ is a meridional wavenumber, and $m$ is a zonal wavenumber. $U = u\,\sin\varphi$ and $V = v\,\sin\varphi$ are also expanded with $\sin n\varphi$, where $u$ and $v$ are westerly and southerly winds respectively. Therefore $u$ and $v$ are not zero at the poles ($\varphi = 0, \pi$) for odd $m \geq 3$, and $u$ and $v$ are not continuous at the poles. In the new method, scalar variables are expanded with $\sin^2\varphi \sin n\varphi$ in the meridional direction for odd $m \geq 3$. $u$ and $v$ are expanded with $\sin\varphi \sin n\varphi$. Therefore $u$ and $v$ are zero at the poles for odd $m \geq 3$, and the vector $(u, v)$ is continuous at the poles. This contributes to remove high zonal wavenumber noise near the poles. In the new method the least squares method is used for the calculation of DFS coefficients to make the error small.

In the Global 7km mesh Model Intercomparison Project for improving TYphoon forecast (TYMIP-G7), we conducted typhoon forecast experiments using the following three 7km mesh nonhydrostatic global atmospheric models: DFSM, the Nonhydrostatic

ICosahedral Atmospheric Model (NICAM), and the Multi-Scale Simulator for the Geoenvironment (MSSG) (Nakano et al. 2017). In DFSM, the development of typhoons tended to be excessive compared to NICAM and MSSG. One of the reasons seems to be that air-sea sensible heat flux around the storm center in DFSM was larger than in NICAM and MSSG. In the experiment with SST uniformly decreased by 2 degrees, the excessive development of the typhoon Lionrock in DFS was alleviated due to suppressed sensible and latent heat fluxes (Fig. 1). We will conduct experiments using high resolution atmospheric-ocean coupled models to consider SST cooling due to typhoons.

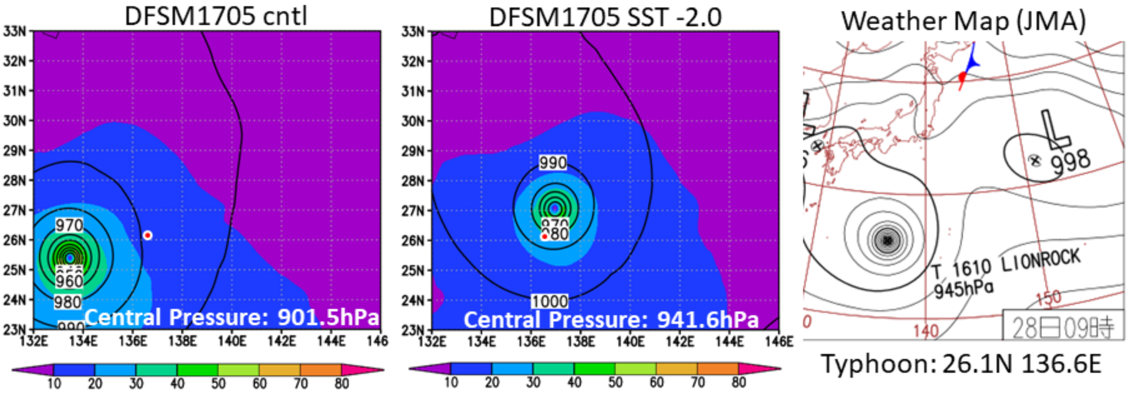


Figure 1. [Left and Middle] 120 hour forecasts of sea level pressure and surface wind velocity from initial condition of 00UTC 23 August 2016 in the control experiment (left) and the experiment with SST uniformly decreased by 2 degrees (middle). Red points show the observed position of Lionrock. [Right] Weather map at 00UTC 28 August 2016.

Acknowledgement. This study was partly supported by 'The Earth Simulator Proposed Research Project.' Numerical experiments were run on the Earth Simulator.

**References:**

Cheong, H.-B.: Application of double Fourier series to the shallow water equations on a sphere. *J. Comput. Phys.* 2000, **165**, 261–287. doi:10.1006/jcph.2000.6615

Nakano, M., A. Wada, M. Sawada, H. Yoshimura, R. Onishi, S. Kawahara, W. Sasaki, T. Nasuno, M. Yamaguchi, T. Iriguchi, M. Sugi, and Y. Takeuchi: Global 7-km mesh nonhydrostatic Model Intercomparison Project for improving Typhoon forecast (TYMIP-G7): Experimental design and preliminary results. *Geosci. Model Dev.* 2017, **10**, 1363-1381. doi:10.5194/gmd-10-1363-2017

Yoshimura, H.: Development of a nonhydrostatic global spectral atmospheric model using double Fourier series. *CAS/JSC WGNE Research Activities in Atmospheric and Ocean Modeling* 2012, **42**, 3.05–3.06.

O1.3

# The impact of hybrid usage of the Chikira-Sugiyama scheme on tropical convection and large-scale circulations in NICAM

Tomoki Miyakawa[1], Akira T. Noda[2], Chihiro Kodama[2]

1. Atmosphere and Ocean Research Institute, the University of Tokyo, Japan
2. Japan Agency for Marine-Earth Science and Technology, Japan

## Abstract

The impact of activating the Chikira-Sugiyama (CS) scheme in the global Nonhydrostatic Icosahedral Atmospheric Model (NICAM) coupled with a 1D mixed-layer ocean model is assessed using a cloud-system resolving, 14-km mesh. The CS scheme, which employs an entrainment rate sensitive to the humidity of the environment, is known to produce congestus clouds in the tropics when used in conventional global climate models, which are under-resolved in the default 14-km mesh NICAM. In this study, boreal-summer NICAM simulations were carried out with and without the CS scheme, and several different scheme parameters were also evaluated. Results showed that the horizontal scale of convection and precipitable water increased in the tropics when using the CS scheme. Model adjustments were apparent at two different timescales; a rapid adjustment within the first week, and a slower adjustment at one to two months. Both effects were magnified in simulations that applied smaller values for the parameter that defined the fraction of loss of buoyancy-generated energy in the parameterized convection. The upward branch of the Hadley circulation shifted northward and the Walker circulation was enhanced when the CS scheme was activated. These large scale adjustments suggested that increased moisture and deeper atmospheric heating in the tropics tended to favor larger organized convective activities, which require a rich moisture supply; in this case available to the north of the equatorial West Pacific Ocean.

O1.4

# A preliminary result in the DYAMOND project by NICAM

Ryosuke Shibuya[1], Chihiro Kodama[1], and Masaki Satoh[1,2]

1. Japan Agency for Marine-Earth Science and Technology, Japan

2. Atmosphere and Ocean Research Institute, the University of Tokyo, Japan

Email: shibuyar@jamstec.go.jp

## Abstract

Project DYAMOND (Dynamics of the Atmospheric general circulation Modeled On Non-hydrostatic Domains) is an inter-comparison project which describes a framework for the inter-comparison of an emerging class of atmospheric circulation models resolving a non-hydrostatic scale in the atmospheric motion. The first stage of the Project DYAMOND is based on a 40-day-simulation initialized on 1 August 2016 by NICAM (Satoh et al., 2014) with dx~3.5 km and 7.0 km, ICON (Zängl et al., 2014) with dx~2.5 km and 5.0 km, SAM (Khairoutdinov et al., 2001) with 4.0 km, and FV-3 (Harris and Lin, 2013) with 3.25 km. It is confirmed that the global mean Outgoing Long Radiation (OLR) and precipitation agree surprisingly well among models, despite none of the models was tuned. Note that the global mean precipitation in the models is slightly higher than in GPCP, which is consistent with past inferences that GPCP underestimates the amount of precipitation. In addition, the structure of the tropical cyclone "Howard" is successfully simulated by all models after 36h forecast time as a hindcast experiment. However, some notable differences in the horizontal map of precipitation are found over Bay of Bengal and the Western North Pacific, in terms of the location of the local maximum and the degree of the aggregation. This is likely attributable both to difference in the representation of the large-scale circulation associated with the Asian monsoon, and that in the cloud-radiation interaction resolved by different microphysics schemes in the models. In addition, the distribution of the ice clouds over the warm pool is simulated few times and at lower heights in ICON, many times and at higher heights in NICAM, and moderate in SAM and FV3. These preliminary results suggest that, even though the global averaged OLR and precipitation is quite similar, the horizontal/vertical distribution of clouds which are simultaneously generated in the models is not deterministic in the global atmospheric models with the storm resolving scales. Further analysis will be made about the explicitly resolved momentum/specific humidity transport by convection.

**References:**

Satoh, M., H. Tomita, H. Yashiro, H. Miura, C. Kodama, T. Seiki, A. T. Noda, Y. Yamada, D. Goto, M. Sawada, T. Miyoshi, Y. Niwa, M. Hara, T. Ohno, S. Iga, T. Arakawa, T. Inoue and H. Kubokawa: The Non-hydrostatic Icosahedral Atmospheric Model: description and development. *Progress in Earth and Planetary Science* 2014, **1**:18. doi: 10.1186/s40645-014-0018-1

Zängl G, Reinert D, Rípodas P, Baldauf M, 2014: The ICON (ICOsahedral Non-hydrostatic) modelling framework of DWD and MPI-M: Description of the non-hydrostatic dynamical core. Quart J Roy Meteor Soc, doi:10.1002/qj.2378.

Khairoutdinov, M. F., and D.A. Randall, 2001: A cloud resolving model as a cloud parameterization in the NCAR Community Climate System Model: Preliminary Results. Geophys. Res. Lett., 28, 3617-3620.

Harris, L. M., & Lin, S.-J., 2013: A two-way nested global-regional dynamical core on the cubed-sphere grid. Monthly Weather Review,141(1), 283–306.

O1.5

# Initiation Processes of the Tropical Intraseasonal Variability Simulated in an Aqua-Planet Experiment: Implication for MJO onset

Daisuke Takasuka[1], Masaki Satoh[1], Tomoki Miyakawa[1], Hiroaki Miura[2]

1. Atmosphere and Ocean Research Institute, the University of Tokyo, Japan

2. Department of Earth and Planetary Science, the University of Tokyo, Japan

Email: takasuka@aori.u-tokyo.ac.jp

## 1. Introduction

The Madden-Julian Oscillation (MJO) is a dominant intraseasonal variability in the tropics, which is characterized as the eastward propagation of large-scale convective envelopes coupled with an overturning zonal circulation. Since the active cumulus convection associated with the MJO has a great impact on the global weather and climate systems, the physical mechanism or the predictability of MJO onset is one of the interesting issues in tropical meteorology.

Previous studies have proposed many kinds of theories about the MJO initiation such as the influences of the equatorially circumnavigating Kelvin waves (e.g., Hendon & Salby, 1994; Kikuchi & Takayabu, 2004), the discharge-recharge mechanism (e.g., Bladé & Hartmann, 1993; Benedict & Randall, 2007), moistening via horizontal advection (e.g., Zhao et al. 2013; Maloney & Wolding, 2015), and the tropical-extratropical interaction as a trigger for tropical convection (e.g., Hsu et al., 1990; Ray & Zhang, 2010). However, a consensus on its essential mechanisms has yet to be reached partly because of the diversity of MJO behavior affected by the seasonality or land-sea distributions.

To help overcome this situation and get an intrinsic insight into the MJO onset, we examined a set of initiation processes of the MJO-like disturbances in 10 year aqua-planet experiments under an idealized SST distribution mimicking the real warm pool distribution (Takasuka et al., 2018).

## 2. Experimental Design and Analysis Method

We used the Nonhydrostatic Icosahedral Atmospheric Model (NICAM) with an approximately 56 km horizontal mesh. In this study, we adopted an aqua-planet configuration with perpetual March 20 solar insolation with diurnal cycles. The use of the zonal non-uniform SST distributions in the tropics and an explicit cloud scheme (NSW6; Tomita, 2008) led to reproducing the MJO-like disturbances over the western warm pool region. Although the 56 km mesh is clearly too coarse to treat the cloud physics explicitly, an explicit cloud scheme appears to be valid in realizing MJO-like disturbances even in low-resolution simulations (e.g., Holloway et al., 2013; Takasuka et al., 2015). Thus, we performed a 10 year simulation under the above setting as the control experiment.

We detected the simulated MJO-like disturbances using outgoing longwave radiation in the tropics, and conducted a lagged-composite analysis with reference to the onset date of each case.

## 3. Main Results

In the control experiment, there were the 34 MJO-like disturbances that propagate eastward at about 4 m $s^{-1}$. We particularly focused on the following three points: (1) moistening processes, (2) convective triggering mechanism, and (3) convective organization feedback processes.

We first recognized the mid-tropospheric moistening in the initiation region 5‑9 days before the onset, which made a favorable condition for deep convective outbreaks. This moistening was mainly caused by horizontal moisture advection due to cross-equatorial shallow circulations associated with mixed Rossby-gravity waves, as well as anomalous flows of a negative Rossby response to suppressed convection as documented previously (Figure 1). After that, the intrusion of low sea level pressure anomalies of circumnavigating Kelvin waves triggered active convection through the low-level convergence. Finally, the large-scale convective organization in the initial and later stages was efficiently driven by surface latent heat flux (LHF) and cloud-radiation feedbacks, respectively.

Based on the above results in the control experiment, we conducted two sensitivity experiments that assess the two processes related to the convective onset: the roles of circumnavigating Kelvin waves and the LHF feedback. The comparison of the results between control and sensitivity experiments showed that the Kelvin waves effectively regulate the periods of the MJO-like disturbance, and that the LHF feedback contributes to the rapid convective organization. Meanwhile, it was also suggested that neither is essential for the existence of the MJO.

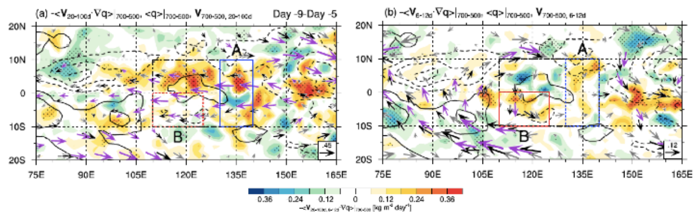


**Figure 1.** 700-500 hPa moisture (contours) and its horizontal advection anomalies (shading) by a) 20-100-day and b) 6-12-day component flows (vectors). A black square shows the initiation region.

## 4. Concluding Remarks

This study investigated the intrinsic mechanism of MJO onset with 10-year NICAM aqua-planet simulations. In spite of adopting a relatively coarse resolution, we successfully reproduced the disturbances with similar characteristics to the real MJO. The results have informative implications for interpreting the observed MJO onset processes, including the scale interaction between the MJO and mixed Rossby-gravity waves or the role of equatorial circumnavigation of Kelvin waves. In future, we will examine the resolution dependence of the structure or physical processes of the MJO-like disturbances simulated at multiple resolutions.

**References:**

Takasuka, D., M. Satoh, T. Miyakawa, and H. Miura (2018), Initiation processes of the Tropical Intraseasonal Variability Simulated in an Aqua-Planet Experiment: What is the Intrinsic Mechanism for MJO Onset? *Journal of Advances in Modeling Earth Systems*, **10**, 1047−1073. doi:10.1002/2017MS001243

O1.6

# Tracking of convective rain events in idealized and realistic large eddy simulations

Christopher Moseley[1], Olga Henneberg[2], Jan O. Haerter[2]

1. Max Planck Institute of Meteorology, Hamburg, Germany

2. Niels Bohr Institute, Copenhagen, Denmark

Email: christopher.moseley@mpimet.mpg.de

## Abstract

Object oriented analysis methods are increasingly favored tools for statistical evaluations of data sets showing complex convective environments. These could be both model data as well as observations like radar data sets. I present a tracking algorithm that is particularly suited for the study of convective rainfall events and their interaction with neighboring convective cells. While some of these cells just form, grow, and finally disappear without interacting with other cells, others merge with their neighbors to form larger, more intense cells. In particular, repeated merging may be regarded as the preliminary stage of clustering and convective aggregation, as it is e.g. found in simulations of radiative convective equilibrium (RCE).

I will first discuss the properties of the tracking method on the basis of an application to idealized large eddy simulations (LES). For tracks that do not merge or split (termed "solitary"), many of these quantities show generic, often nearly linear relations that hardly depend on the forcing conditions of the simulations, such as surface temperature (Fig. 1). Furthermore, I will present a more realistic application on a limited area simulation with ICON for a domain covering Germany with 600 m grid spacing: In a land use change experiment, the whole domain is afforested by mixed forest, and the feedback on convection is investigated. It was found that convective cells are more intense in the afforested simulation, compared to the control simulation.

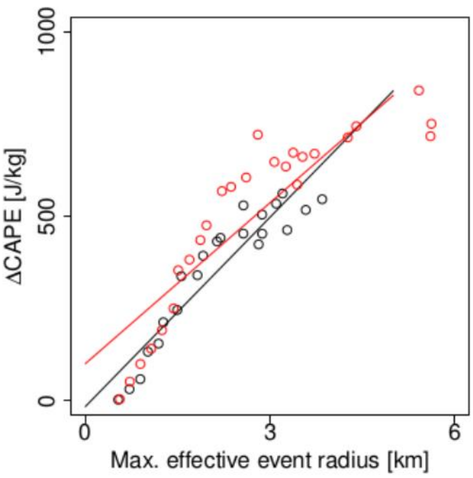


Fig.1: Approximately liner relation between the maximal extent of an isolated convective rain event, and the difference in Convective Available Potential Energy (CAPE) between the beginning and the end of the rainfall event. Two simulations are shown, one with 2 K higher surface temperature (red circles) compared to the other (black circles). The relation remains surprisingly robust with respect to the surface forcing (Moseley et al., 2018).

An important factor for the organization of convection is the role of cold pools. Similar as the convective cells that they originate from, cold pools can be regarded as individuals. As an outlook, I will discuss a tracking methods for cold pools, and speculate how it could be combined with the presented rain cell tracking into one single framework.

**References:**


Moseley, C., O. Henneberg, and J. O. Haerter (2018): Amplified convective precipitation from multi-merging, *Under revision at Journal of Advances in Modeling Earth Systems*. Preprint available at: https://arxiv.org/abs/1809.03840

Moseley, C., C. Hohenegger, P. Berg, and J. O. Haerter (2016): Intensification of convective extremes driven by cloud–cloud interaction, *Nature Geoscience* 9, 748–752

O1.7

# High-resolution large-eddy simulation of urban atmospheric boundary layer

Antti Hellsten[1], Mikko Auvinen[1,2], Mia Aarnio[1], Mona Kurppa[2], Sasu Karttunen[2]

1. Finnish Meteorological Institute, Helsinki, Finland

2. Institute for Atmospheric and Earth System Research (INAR), University of Helsinki, Finland

Email: antti.hellsten@fmi.fi

## Abstract

The main interests of our research group are Urban Atmospheric Boundary Layer (Urban ABL, UABL), wind flow, turbulence and various transport phenomena within the UABL, and application of high-resolution Large-Eddy Simulation (LES) to study these phenomena. We are motivated to study these problems both from the scientific and applied points of view. Our central modelling idea is as follows. We include the whole vertical extent of the ABL in a large LES domain in order to realistically resolve the large, strongly elongated turbulent structures of the ABL. While using a large domain, we also use high resolution in order to capture at least the most important part of the turbulent motion within street canyons and courtyards etc. in the urban canopy in the area of primary interest. These requirements together would lead to a huge number of grid nodes without the self nesting method which we have developed especially for urban LES (Hellsten et al., 2017). The nesting method allows us to use a large outer domain with a compromised resolution and a smaller higher-resolution nest-domain for the area of principal interest. Several nest domains can be set in a cascading chain or in parallel. We typically use set ups with two domains (root and nest) or three cascading domains (root, 1st nest and 2nd nest) to achieve a sufficiently large model domain and high resolution within the area of principal interest. The modelling system includes a realistic model for the urban geometry including terrain shape and buildings and also trees. Currently we are working e.g. on implementing aerosol physics modelling in PALM.

The PALM LES model (Maronga et al., 2015) forms the core of our modeling system. It is a highly versatile LES model for ABL and UABL problems with very effient parallelization based on the Message Passing Interface (MPI) scalable up to tens of thousands of processes.

We have so far applied the PALM system to the following UABL problems. We have developed a source-area estimation method for greenhouse-gas flux measurements in urban environment based on high-resolution LES with coupled Lagrangian-stochastic (LS) particle modelling (Auvinen et al., 2017). We have applied PALM to a practical air quality study for a certain city planning purpose in collaboration with the City of Helsinki (Kurppa et al., 2018). Currently we are studying UABL LES sensitivity to various modelling choices such as ABL depth (often unknown), details of tree modelling and grid resolution. Moreover, we are looking for an optimal layout of street canyon vegetation from the air quality point of view in collaboration with the City of Helsinki. We are also currently developing a new precomputed LES-LS based model for hazardous material release accidents.

**References:**

Auvinen, M., L. Järvi, A. Hellsten, Ü. Rannik, and T. Vesala: Numerical framework for the computation of urban flux footprints employing large-eddy simulation and Lagrangian stochastic modeling. *Geosci. Model Dev*. 2017, **10**, 4187-4205, https://doi.org/10.5194/gmd-10-4187-2017.

Hellsten, A., K. Ketelsen, F. Barmpas, G. Tsegas, N. Moussiopoulos and S. Raasch: Nested Multi-Scale System Implemented in the PALM Large-Eddy Simulation Model. *Klemens, M., Kallos, G., Eds. In: Air Pollution Modelling and its Application XXV*. 2017, pp. 287-292. ISBN 978-3-319-57644-2. Springer.

Kurppa, M., A. Hellsten, M. Auvinen, S. Raasch, T. Vesala, and L. Järvi: Ventilation and Air Quality in City Blocks Using Large-Eddy Simulation—Urban Planning Perspective. *Atmosphere*. 2017, **9**(2), 65. https://doi.org/10.3390/ atmos9020065

Maronga, B., M. Gryschka, R. Heinze, F. Hoffmann, F. Kanani-Sühring, M. Keck, K. Ketelsen, M.O. Letzel, M. Sühring, and S. Raasch: The Parallelized Large-Eddy Simulation Model (PALM) version 4.0 for atmospheric and oceanic flows: model formulation, recent developments, and future perspectives, *Geosci. Model Dev.* 2015, **8**, 2515-2551, https://doi.org/10.5194/gmd-8-2515-2015

O1.8

# Importance of terrain representation in simulating a stationary convective system for the July 2017 Northern Kyushu Heavy Rainfall case

Tetsuya Takemi

Disaster Prevention Research Institute, Kyoto University, Japan

Email: takemi@storm.dpri.kyoto-u.ac.jp

## Abstract

Stationary convective systems are one of the major extreme-rain-producing storms. From a statistical point of view, Tsuguti and Kato (2014) examined warm-season heavy rain events in Japan and suggested that there is a topographical influence on the generation of stationary rain events. Unuma and Takemi (2016) examined stationary meso-$\beta$-scale convective systems, called as quasi-stationary convective clusters (QSCCs), during the warm season and mentioned that the locations of QSCC occurrence correspond to regions with high elevation.

An extreme, damaging rainfall occurred in northern Kyushu in July 2017. This case produced extreme rainfalls in northern Kyushu and spawned damaging floods and landslides. The case developed under influences of a stationary front: during the southward movement of the Baiu front the heavy rainfall occurred. Among the raingauge stations, the heaviest rainfall was measured at the Asakura station: the maximum accumulated rainfalls for 24, 48, and 72 hours were 545.5 mm (by 1140 JST 6 July), 600.5 mm (by 1040 JST 7 July), and 616.0 mm (by 0600 JST 7 July), respectively, all of which are the highest records at the station.

Whether such an extreme rainfall is quantitatively captured by numerical models is a challenging issue. We investigate the influences of terrain representation in simulating a stationary convective system and the resulting heavy rainfall for this case by conducting a series of 167-m-resolution numerical experiments. The model used is the Weather Research and Forecasting (WRF) model Version 3.6.1. Two-way nesting was used to set four computational domains: the outermost domain (Domain 1) covers most of the Japanese islands at the 4.5-km horizontal grid, the second domain (Domain 2) Kyushu Island at the 1.5-km grid, the third domain (Domain 3) the northern half of

Kyushu Island at the 500-m grid, and the innermost domain (Domain 4) focuses northern Kyushu at the 167-m grid. The model topography was generated with a coarser-resolution digital elevation model (DEM) dataset and a higher-resolution DEM dataset. The topography in Domain 1 and 2 was generated with the global DEM data having a horizontal grid spacing of 30 arc-seconds (about 1 km) (referred to as G30) provided by the United States Geological Survey, while the topography in Domain 3 and 4 was created with the 50-m horizontal resolution DEM data provided by the Geospatial Information Authority of Japan (referred to as GSI); this GSI dataset is a digital version of the GSI maps created by ground-based measurements. To examine the sensitivity to the choice of the elevation dataset, we used the G30 data to create the model topography not only in Domain 1 and 2 but also in Domain 3 and 4 and conducted sensitivity experiments.

By employing the high-resolution elevation dataset as well as a double-moment cloud microphysics scheme, the control experiment successfully reproduced the stationary, linear-shaped convective system and the associated heavy rainfall. When the model terrain was created by a coarser-resolution elevation dataset, the 167-m-resolution experiment underestimated the accumulated rainfall, because of discretely developing convection and weaker intensities of the rainfall. These impacts of the terrain representation were confirmed to be robust through conducting another experiments with a different microphysics scheme.

The sensitivity experiments demonstrated that the representation of model terrain is critically important in reproducing stationary convective systems and quantitatively the resulting heavy rainfall in convection-resolving simulations at a $O$(100 m) grid spacing.

This work has been published in Takemi (2018).

**References:**

Takemi, T.: Importance of terrain representation in simulating a stationary convective system for the July 2017 Northern Kyushu Heavy Rainfall case. *SOLA* 2018, **14**, 153-158, doi:10.2151/sola.2018-027.

Tsuguti, H., and T. Kato: Objective extraction of heavy rainfall events and statistical analysis on their characteristic features. *Tenki* 2014, **61**, 455-469. (in Japanese)

Unuma, T., and T. Takemi: Characteristics and environmental conditions of quasi-stationary convective clusters during the warm season in Japan. *Quart. J. Roy. Meteor. Soc.* 2016, **142**, 1232-1249.

# O1.9

Development of a high-resolution cloud-resolving model over complex topography (TaiwanVVM)

Chien-Ming Wu

Department of Atmospheric Sciences, National Taiwan University, Taipei, Taiwan

Abstract

In this study, we present a high-resolution (500 m in the horizontal) vorticity equation based cloud resolving model covering the whole Taiwan area with the following features:
Representation of surface topography in the vector vorticity equation model (VVM) is updated with a partial step approach using the immersed boundary method (Chien and Wu, 2016). Compared with the full step approach, the partial step approach provides additional topography forcing to represent micro mountains while preserving the same grid structure by interpolating from adjacent grid points. It maintains the characteristics of dynamics and physics of VVM and improves the representation of gentle slope topography without increasing vertical resolution. Representation of land surface processes is updated with the Noah land surface model (LSM) using the surface properties in 500 m horizontal resolution in Taiwan (Wu et al. 2018). This approach produces reasonable diurnal cycle evolution of the boundary layer and local circulation which is crucial in the development of local afternoon thunderstorms. Representation of microphysical processes is updated with the Predicted Particle Properties scheme (P3, Morrison and Milbrandt, 2014). Idealized experiments are performed to evaluate the aerosol effects on precipitation hotspots of afternoon thunderstorms over Taiwan. Preliminary results show that under a dirty environment, the timing of precipitation over Taiwan is delayed with enhanced diurnal precipitation peak compared with a clean environment. In the future, the model will be used to investigate changes with precipitation hotspots associated with local circulation under pseudo global warming.

References:

Chien, M.-H., and C.-M. Wu (2016): Representation of topography by partial steps using the immersed boundary method in a vector vorticity equation model (VVM), J. Adv. Model. Earth Syst., 8, 212–223, doi:10.1002/2015MS000514.

Morrison, H., and J. A. Milbrandt, 2014: Parameterization of cloud microphysics based on the prediction of bulk ice particle properties. Part I: Scheme description and idealized tests. J. Atmos. Sci., 72, 287–311.

Wu C.-M., Lin, H.-C., M.-H. Chien, and F.-Y. Cheng (2018): Implementation of the land surface processes into a vector vorticity equation model (VVM) to study its impact on afternoon thunderstorms over complex topography in Taiwan. Submitted to APJAS.

O1.10

# Evaluation of WRF and WRF-Hydro Models in Simulating Heavy Rainfall and Streamflow in the Talomo Watershed: A Baseline Study for the Development of a Hydro –Meteorological Flood Forecasting System for Davao City

Ma. Cathrene S. Lagare[1], Rochelle C. Coronel[1]

1. Environmental Science Department, Ateneo de Davao University, Philippines

Email: cathrenelagare@gmail.com

## 1. Introduction

The increasing occurrence of river flooding in Davao City, Philippines brings up the need for a hydro-meteorological forecasting system that integrates the relationship of atmospheric phenomena and the streamflow within the Davao City's watershed area. This study aims to evaluate the performance of the Weather and Research Forecasting (WRF) and the WRF-Hydro models in simulating heavy rainfall and streamflow events in Davao City, respectively. The models were configured to simulate the observed intense precipitation and streamflow event in the Talomo River in 01 August 2015.

## 2. Experimental Design

Using Final (FNL) Operational Global Analysis as global forcing, numerical experiments were performed following the best WRF model setups of past studies for heavy rainfall events (Skamarock, 2008; Cruz and Narisma, 2016; Kaewmesri et al., 2017; Olaguera, 2015). Sensitivity to initial time of simulation, initial and lateral boundary conditions, and horizontal resolutions (9-, 3-, 1-km resolution) were conducted on the model configurations used in the numerical experiments. The WRF output from the experiment with the least bias was then utilized as input to the WRF-Hydro simulation. The results from the previous experiments determined the model setup used in the rainfall and streamflow forecasting. The initial and boundary conditions for the forecasting were provided by Global Forecast System (GFS) and Global Data Assimilation System (GDAS)

## 3. Results and Discussion

A set of numerical experiments and sensitivity tests with model validation were performed to determine the optimal model setup for Davao City rainfall. The numerical run with the highest horizontal resolution and both WRF 1 (with WSM6 as microphysics scheme; New Tiedtke as cumulus scheme; RRTMG as long and short wave radiations schemes; Yonsei University as PBL scheme; Noah LSM as land surface scheme) and WRF 4 (with Goddard as microphysics scheme; Grell 3D Ensemble as cumulus scheme; RRTM as long wave radiation scheme; Dudhia as short wave radiation schemes; Yonsei University as PBL scheme; Noah LSM as land surface scheme) of WRF outperforms other test simulations (Figure 1). Output from WRF 1 and WRF 4 were then utilized as forcing to the hydrological model to simulate streamflow and forecast possible flood events within the city. As shown in Figure 2, results from WRF-Hydro simulations show the capability of the model to recreate the observed hourly pattern of strong streamflow in the Talomo River during the first 12 hours of the simulations but had difficulty in modeling the forecasts (after 12 hours).

## 4. Conclusion

Among the numerical experiments, WRF 1 and WRF 4 (refer to Figure 1) has showed promising results in simulating rainfall patterns. However, based on the hydrograph (Figure 2), the model captured higher discharge values during the initial simulation but was unable to simulate peaks at the forecast. Further tuning of the meteorological and hydrological models is needed to improve the accuracy of the output. Nevertheless, this study introduces numerical tools and baseline results to be used in developing a hydro-meteorological flood forecasting system among the major rivers of Davao City.

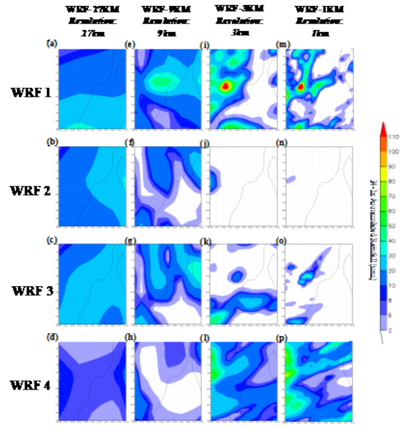


Figure 1. Accumulated rainfall (mm) on 01 AUGUST 2015 over Davao City for each simulation experiment at 27-km resolution (a-d), 9-km resolution (e-h), 3-km resolution (i-l), and 1-km resolution (m-p)

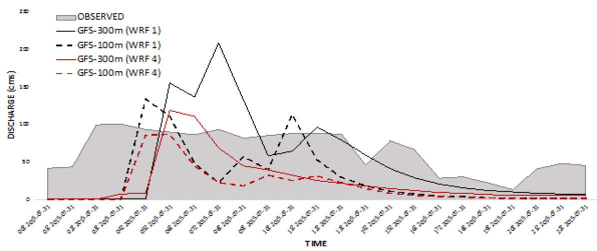


Figure 2. Observed and simulated (GFS) hydrograph for the period of 31 JULY 2015 00Z to 01 AUGUST 2015 09Z

## References:

Cruz, F. T., & Narisma, G. T. (2016). WRF simulation of the heavy rainfall over Metropolitan Manila, Philippines during tropical cyclone Ketsana: a sensitivity study. *Meteorology and Atmospheric Physics,* 128(4), 415–428.

Kaewmesri, P., Humphries, U.W., & Sooktawee S. (2017). Simulation on high-resolution WRF model for an extreme rainfall event over the southern part of Thailand. *International Journal of ADVANCED AND APPLIED SCIENCES*, 4(9), 26–34.

National Centers for Environmental Prediction NOAA, U.S. Department of Commerce, N. W. S. (2000). NCEP **FNL** Operational Model Global Tropospheric Analyses, continuing from July 1999. Boulder, CO: Research Data Archive at the National Center for Atmospheric Research, Computational and Information Systems Laboratory.

National Centers for Environmental Prediction NOAA, U.S. Department of Commerce, N. W. S. (2015). NCEP **GFS** 0.25 Degree Global Forecast Grids Historical Archive. Boulder, CO: Research Data Archive at the National Center for Atmospheric Research, Computational and Information Systems Laboratory.

National Centers for Environmental Prediction NOAA, U.S. Department of Commerce, N. W. S. (2015). NCEP **GDAS**/FNL 0.25 Degree Global Tropospheric Analyses and Forecast Grids. Boulder, CO: Research Data Archive at the National Center for Atmospheric Research, Computational and Information Systems Laboratory.

Olaguera, L. (2015). Improving Extreme Weather Forecast Through Observation Data Assimilation (Master's Thesis). Ateneo de Manila University, Quezon City, Philippines.

Skamarock, W. C., Klemp, J. B., Dudhi, J., Gill, D. O., Barker, D. M., Duda, M. G., & Powers, J. G. (2008). A Description of the Advanced Research WRF Version 3. Technical Report, (June), 113.

O1.11

# Regional European Reanalysis systems and production

Per Undén[1], Martin Ridal[1], Esbjörn Olsson[1] , Richard Renshaw[2], Peter Jermey[2], Andrea Kaiser-Weiss[3], Michael Borsche[3], Else van den Besselaar[4], Gerard van der Schrier[4], Gé Verver[4], Cristian Lussana[5], Patrick Le Moigne[6], Eric Bazile[5], Francesco Isotta[7]

1. Swedish Meteorological and Hydrological Institue, Sweden
2. Met Office, United Kingdom
3. Deutsher Wetterdienst, Germany
4. KNMI, Netherlands
5. MET, Norway
6. Météo-France, France
7. Meteo Swiss, Switzerland

Email: Per.Unden@smhi.se

## Abstract

Global Reanalyses have been carried out at ECMWF since the end of the 1970's and then at both NCEP and JMA. There have been several generations and periods of these analyses and with ever increasing resolution . In the later decades, from the end of 1990's a number of projects for regional reanalyses were launched to allow much higher horizontal resolution as well as certain additional local observation or particular coupling or downscaling reanalyses. Examples of these will be shown from the EU FP7 EURO4M project where both the Met Office and SMHI built and performed 3-dimensional reanalyses covering the whole Europe (EU-CORDEX) while Météo-France and SMHI built a surface downscaling system with analysis at even higher resolution of near surface observations and precipitation.

In the follow-on EU FP7 project UERRA (2014-2017) more model and data assimilation systems were employed, thereby adding a multi-model dimensionality to cover and gauge the inherent uncertainties. The reanalysis systems also included ensemble assimilation for all or parts of the period. The assimilation systems and the observations used will be described. The Met Office used a 4DEnsVar to estimate both error covariances for the 4D-VAR and uncertainties in the reanalysis. SMHI used the ALADIN 3D-VAR and DWD a nudging ensemble assimilation. The computation efforts were extensive and this could be a problem for state-of -the-art reanalysis systems at

high resolution.

The downscaling reanalysis at Météo-France was used to force a surface model and in turn a hydrological model and this was used to validate run-off and discharge in certain rivers.
There was an extensive evaluation across all the systems (also the DWD reanalysis together with their German COSMO high resolution reanalysis). The resulting reanalyses were in general similar and agreed quite well with special observation sets although wind-sheers, diurnal variations and extreme values were not always accurate. Particularly climate indices were difficult to reproduce. Still the data sets have proven a valuable source for consistent gridded data over many decades. Some problems have been revealed afterwards so it is vital to do an extensive monitoring during the production.

The SMHI ALADIN-HARMONIE reanalysis system with the MF downscaling is now continuing under a Copernicus Climate Change Service (C3S) contract financed by the EC and managed by ECMWF. The new system will be at 5.5 km with 106 levels and 10 ensemble members. More observations are used with many remote sensing data. Emphasis is put on data access and user support for the community at large.

It should also be mentioned that there are other sub-European reanalyses, like the afore mentioned COSMO but also the Irish MÉRA 2.5 km reanalysis.

Rescue of historical observations for climate research and reanalyses was also part of EURO4M and UERRA.

**References:**

Borsche, M, A. K. Kaiser-Weiss, P. Undén, and F. Kaspar: Methodologies to characterize uncertainties in regional reanalyses. Adv. Sci. Res., 12, 207-218, 2015 www.adv-sci-res.net/12/207/2015/doi:10.5194/asr-12-207-2015.

Soci, Cornel, Bazile, E., Besson, F and Landelius, T.: High-resolution precipitation re-analysis system for climatological purposes. Tellus A 2016, 68, 29879, http://dx.doi.org/10.3402/tellusa.v68.29879

Undén, P. et al.: UERRA Project. Deliverables and reports, http://www.uerra.eu

O1.12

# Towards a long-term high-resolution regional reanalysis over Japan by using NHM-LETKF

Shin Fukui[1], Toshiki Iwasaki[1], Kazuo Saito[2,3], Hiromu Seko[3]

1. Graduate School of Science, Tohoku University, Japan

2. Atmosphere and Ocean Research Institute, the University of Tokyo, Japan

3. Meteorological Research Institute, Japan

Email: fukui@tohoku.ac.jp

## Abstract

We are investigating the feasibility of regional reanalysis covering Japan and its surrounding area with a 5-km grid spacing over ~60 years (Fukui et al., 2018). Such long-term high-resolution reanalysis datasets are expected to be useful for various purposes, such as researching past extreme events, monitoring local responses on the climate change, and developing schemes to apply meteorological data. The regional reanalysis system that we are developing consists of the JMA's nonhydrostatic model (NHM) nested in JRA-55 (equivalent to a 55 km gird spacing) and the local ensemble transform Kalman filter (LETKF). The NHM-LETKF is optimized for long-term regional reanalysis in terms of first guesses, lateral boundary perturbations and the ensemble size. The assimilated data are limited to the conventional observations, such as surface pressure observations and radiosonde observations, in order to keep the consistency of the reanalysis in quality throughout the entire reanalysis period, which enables us to detect signals of climate change and to compare past extreme events.

Towards a long-term reanalysis, regional reanalysis experiments covering one summer (August 2014) and one winter (January 2016) were conducted. We assessed the system, paying special attention to its reproducibility of precipitation. Dynamical downscaling experiments were also conducted to validate the values of the regional reanalysis.

First, we confirmed that the system worked stably for the experimental period, using the JMA's operational Mesoscale Analysis (MA), where the observations with satellites and radars as well as the conventional observations are assimilated. The root mean square differences (RMSD) to MA for mean sea level pressure were ~0.9 hPa on average

and stable over the period. The RMSDs were comparable to the RMSDs of JRA-55 and significantly smaller than the RMSDs of the dynamical downscaling experiment.

Then, the simulated precipitation over the Japan islands were verified using the JMA's precipitation data (R/A), which are based on radar observations calibrated with rain gauge observations. The bias scores of the regional reanalysis are stable, whereas those of JRA-55 were gradually smaller for higher precipitation in both season. The threat scores of the regional reanalysis is higher in both seasons than those of JRA-55 and the dynamical downscaling experiments. The higher-resolution model resolved better not only the topography but also mesoscale phenomena, such as vortex over the Japan sea in winter and typhoons. The assimilation of the conventional observations improved some individual mesoscale phenomena that were difficult to simulate with dynamical downscaling where no observation was assimilated, although the difficulty remained in simulating of the phenomena over the area where observations are sparse, such as the ocean to the south of the Japan islands.

**Acknowledgement:**

This study was funded by the social and scientific priority issues (Theme 4) to be tackled by using post K computer of the FLAGSHIP2020 Project (ID: hp150287, hp160230, hp170246, hp180194) and JSPS KAKENHI Grant Number 16H04054. This work was done as part of a joint research project between Tohoku Univ. and MRI The experiments were partly conducted with the supercomputing resources at Cyberscience Center, Tohoku Univ. and the ES under the Strategic Project with Special Support.

**References:**

Fukui, S., T. Iwasaki, K. Saito, H. Seko, and M. Kunii, 2018: A feasibility study on the high-resolution regional reanalysis over Japan assimilating only conventional observations as an alternative to the dynamical downscaling. *J. Meteor. Soc. Japan*, **96** doi: 10.2151/jmsj.2018-056.

O1.13

# Impacts of high-resolution Himawari-8 AMVs assimilation on TC forecast in HWRF

Masahiro Sawada[1], Ryo Oyama[2], Kazuki Shimoji[1], Zaizhong Ma[3,4], Avichal Mehra[4], Vijay Tallapraga[4]

1. Numerical Prediction Division, Japan Meteorological Agency, Japan

2. Meteorological Research Institute, Japan Meteorological Agency, Japan

3. I.M. Systems Group, Inc., USA

4. Environmental Modeling Center, National Center for Environmental Prediction, USA

Email: msawada@mri-jma.go.jp

## 1. Introduction

Accurately estimating the tropical cyclone (TC) intensity and structure is essential to improve TC forecasts and to diagnose numerical model characteristics. Several previous studies show the data assimilation (DA) of atmospheric motion vectors (AMVs) derived from consecutive satellite images benefits TC forecasts using HWRF (Velden et al. 2017, Zhang et al. 2018). Himawari-8 provides high spatiotemporal resolution AMVs and these have a potential to better capture the TC structure and initial conditions of the surrounding environment, leading to more skillful forecasts. Therefore, purposes of this study are to assess the capability of DA for the Western Pacific TCs, to investigate what impacts of assimilating the high resolution Himawari-8 AMVs have on the TC forecasts, and to understand how the impacts arise.

## 2. Model description and experimental design

NCEP Operational hurricane model, Hurricane Weather Research and Forecasting Model (HWRF), is used in this study. The configuration of the model is the same as the 2017 operational version, except for the ocean model. Initial condition for outermost domain comes from global forecast system (GFS) analysis with vortex initialization. Forecast length for each experiments is 126 hours. The total number of cycles is 26. Target case is typhoon Meranti (2016), which experienced extreme rapid intensification (RI). Its maximum intensification rate reached 70 kt / day.

Control experiment and four sensitivity experiments are conducted. CTL is control experiment which does not use DA for initialization. Two ensemble-variational hybrid DA configurations, based on the Grid-point Statistical Interpolation (GSI), are used for the sensitivity experiments. One is using background error covariance generated from global ensemble forecast system (GEFS), gDA experiment. The other is generated from HWRF ensembles, hDA experiment. The assimilated observation data are the same as those in the GFS analysis. Two additional sensitivity experiments (gDA-AMV and hDA-AMV experiments) with high-resolution Himawari-8 AMVs (H8AMV) are conducted. In the gDA-AMV and hDA-AMV experiments, H8AMV are added to the gDA and hDA experiment, respectively.

## 3. Results

A track verification shows hDA-AMV experiment provided the best track forecast for longer forecast lead time (Fig. 1a). Track error was smaller in the hDA-AMV than that in the gDA-AMV experiments. It implies that the assimilation of high-resolution Himawari-8 AMVs (H8AMV) with the covariance generated from HWRF ensembles can benefit the track forecast skill. On the other hand, track error was larger in the gDA than in the CTL experiment for almost all forecast lead time, indicating DA in high resolution grid space cannot improve track forecast in this case and in this configuration at least. A intensity verification shows gDA and gDA-AMV had larger intensity errors than that CTL, gDA, and gDA-AMV for shorter-range lead time. The assimilation with the covariance generated from GEFS could not improve the intensity forecast, even if H8AMV was assimilated. The intensity forecast biases in the all experiments were negative partly because the extreme RI could not captured (not shown). We will discuss what processes account for these impacts in the presentation.

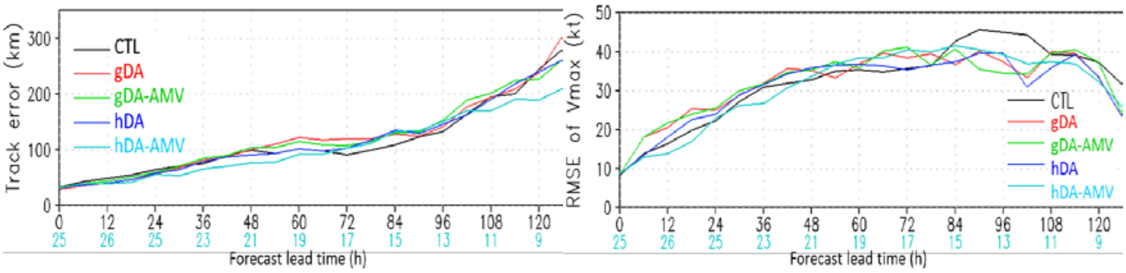


Fig. 1 (a) Statistics of (a) track error, and (b) RMSE of maximum wind speed with reference to the best-track data of JTWC. Figures at bottom show number of sample.

## References:


Velden, C., W. E. Lewis, W. Bresky, D. Stettner, J. Daniels, and S. Wanzong, 2017: Assimilation of High-Resolution Satellite-Derived Atmospheric Motion Vectors: Impact on HWRF Forecasts of Tropical Cyclone Track and Intensity. Mon. Wea. Rev., 145, 1107–1125.

Zhang, S., Z. Pu, and C. Velden, 2018: Impact of Enhanced Atmospheric Motion Vectors on HWRF Hurricane Analyses and Forecasts with Different Data Assimilation Configurations. Mon. Wea. Rev., 146, 1549–1569.

O1.14

# Regional atmospheric data assimilation coupled with an ocean mixed layer model: a case of typhoon Soudelor (2015)

Kohei Takatama[1], Takumi Honda[1], Takemasa Miyoshi[1]
1. RIKEN Center for Computational Science
Email: kohei.takatama@riken.jp

## Abstract

This study investigates the effect of atmosphere-ocean coupling in a regional atmospheric data assimilation system for a case of Typhoon Soudelor (2015). A simple ocean mixed layer model, known as the Price-Weller-Pinkel (PWP) model (Price et al. 1986), has been implemented into a regional atmospheric data assimilation system SCALE-LETKF (Lien et al. 2017), composed of the regional atmospheric model SCALE-RM and the local ensemble transform Kalman filter (LETKF). It is expected that the ocean mixed layer model brings more realistic physics to the simulation and modifies the ensemble spread, particularly near the ocean surface.

The numerical experiments were conducted at 15 km resolution with 50 ensemble members. The ocean states were prescribed in an experiment named CTL and calculated by the ocean mixed layer model in an experiment named PWP. We performed data assimilation cycles with conventional observations from the NCEP PREPBUFR dataset for 2 weeks starting at 0000UTC 25 July 2015 after a 1-day spin-up.

Although the sea surface temperatures (SSTs) in PWP change depending on the atmospheric-flow, the mixed layer model does not improve the track and intensity of the typhoon (Fig. 1). This can be explained by a decrease of the SSTs and by a decrease of the ensemble spread of the near surface atmospheric temperature (SAT) compared with those in CTL (Fig. 2). In the atmosphere-ocean coupling system, the stronger a typhoon, the cooler the SSTs via heat releases from the ocean surface and via vertical mixing of the upper ocean. These processes induce negative feedback for the typhoon development, so that the typhoon growth rates are suppressed (enhanced) in ensemble members with strong (weak) typhoon. This results in more similar typhoon intensities among ensemble members. Therefore, the coupled system reduces the ensemble spreads in the atmospheric fields associated with typhoon.

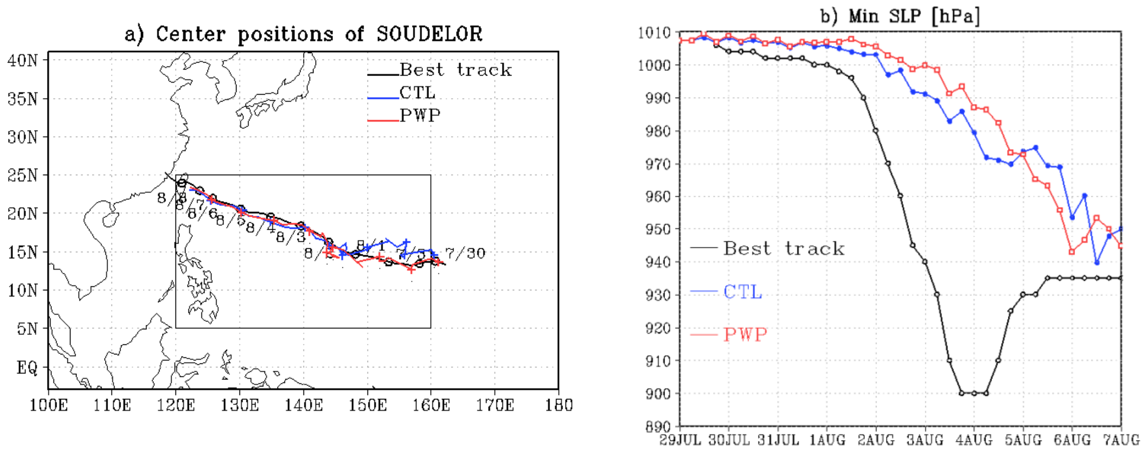


Fig. 1. a) Tracks and b) minimum sea level pressures (SLP, the unit is hPa) of the Typhoon Soudelor (2015). Black lines denote the data obtained from the best track, blue lines CTL, and red lines PWP. The rectangle region in panel a) is used for statistics.

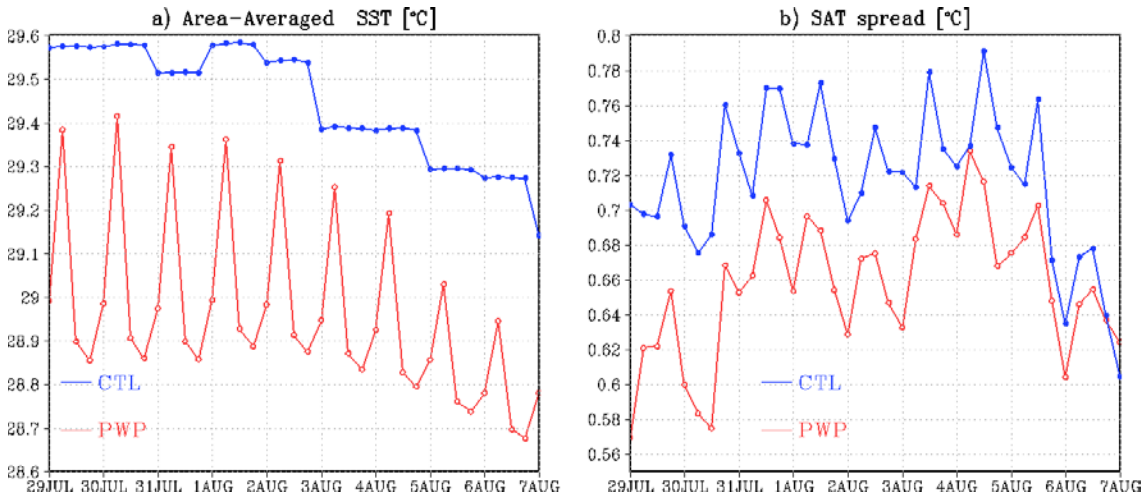


Fig. 2 a) Area averaged SSTs and b) SAT spreads over the rectangle region in Fig. 1a (the units are °C). Line colors are same as those in Fig. 1.

## References


Lien, G.-Y., T. Miyoshi, S. Nishizawa, R. Yoshida, H. Yashiro, S. A. Adachi, T. Yamaura, and H. Tomita, 2017: The near-real-time SCALE-LETKF system: A case of the September 2015 Kanto-Tohoku heavy rainfall. *SOLA*, **13**, 1–6.

Price, J. F., R. A. Weller, and R. Pinkel, 1986: Diurnal cycling: Observations and models of the upper ocean response to diurnal heating, cooling, and wind mixing. *J. Geophys. Res.*, **91**, 8411-8427.

O1.15

# Near-real-time SCALE-LETKF forecasts of the record breaking rainfall in Japan in July 2018

Takumi Honda[1], Guo-Yuan Lien[2,1], Takemasa Miyoshi[1]
1. RIKEN Center for Computational Science, Kobe, Japan
2. Central Weather Bureau, Taipei, Taiwan
Email: takumi.honda@riken.jp

## Abstract

In July 2018, a stationary precipitation band associated with the Baiu front induced a record breaking rainfall and caused catastrophic destruction in Japan. This event was successfully captured by the near-real-time SCALE-LETKF system (Lien et al. 2017) consisting of the Scalable Computing for Advanced Library and Environment-Regional Model (SCALE-RM, Nishizawa et al. 2015; Sato et al. 2015) and the Local Ensemble Transform Kalman Filter (LETKF, Hunt et al. 2007; Miyoshi and Yamane 2007). This system has been operated since 2015 with an 18-km mesh model domain and the ensemble size of 50. In this system, only conventional observations are assimilated every 6 hours. This study aims to investigate predictability of this torrential rainfall event by conducting a series of 50-member ensemble forecasts from the 6-hourly SCALE-LETKF analyses. In general, the SCALE-LETKF system provides skillful ensemble forecasts of the rainfall a few days in advance. Interestingly, the forecast skill exhibits sudden improvement due to assimilating conventional observations far from the peak accumulated rainfall location. Forecast differences suggest that an extratropical cyclone over the Sea of Japan and a trough near Taiwan play important roles in determining the front location.

**References:**

Hunt, B. R., E. J. Kostelich, and I. Szunyogh, 2007: Efficient data assimilation for spatiotemporal chaos: A local ensemble transform Kalman filter. *Physica D*, **230**, 112–126, doi: 10.1016/j.physd.2006.11.008.

Miyoshi, T., and S. Yamane, 2007: Local ensemble transform Kalman filtering with an AGCM at a T159/L48 resolution. *Mon. Wea. Rev.*, **135**, 3841 – 3861, doi: 10.1175/2007MWR 1873.1.

Lien, G.-Y., T. Miyoshi, S. Nishizawa, R. Yoshida, H. Yashiro, S. A. Adachi, T. Yamaura, and H. Tomita, 2017: The near-real-time SCALE-LETKF system: A case of the September 2015 Kanto- Tohoku heavy rainfall. *SOLA*, **13**, 1–6, doi: 10.2151/ sola.2017-001.

Nishizawa, S., H. Yashiro, Y. Sato, Y. Miyamoto, and H. Tomita, 2015: Influence of grid aspect ratio on planetary boundary layer turbulence in large-eddy simulations. *Geosci. Model Dev.*, **8**, 3393–3419, doi: 10.5194/gmd-8-3393-2015.

Sato, Y., S. Nishizawa, H. Yashiro, Y. Miyamoto, Y. Kajikawa, and H. Tomita, 2015: Impacts of cloud microphysics on trade wind cumulus: which cloud microphysics processes contribute to the diversity in a large eddy simulation? *Prog. Earth Planet. Sci.*, **2**, 23, doi: 10.1186/s40645-015-0053-6

# November 15, 2018 (Thursday)

O2.1

# Particle Filters for Convective Scale NWP

Roland Potthast[1,2]

1. Deutscher Wetterdienst, Offenbach, Germany

2. University of Reading, Reading, United Kingdom

Email: roland.potthast@dwd.de

## Abstract

We discuss the setup of the ensemble data assimilation (EDA) and forecasting systems (EPS) which have been developed and are under development at the German Weather Service DWD and its COSMO partners.

DWD operates the ICON global+mesoscale model (two-way nested), 13km/6.5km resolution, with its hybrid ensemble variational data assimilation (LETKF+EnVAR) run on a 3h cycle, and the ensemble prediction system ICON EPS. Second, this system drives the high-resolution ensemble data assimilation system COSMO-KENDA (Kilometer Scale Ensemble Data Assimilation) with 2.2km operational resolution at DWD and up to 1km resolution at further members of the COSMO consortium (Germany, Switzerland, Italy, Russia, Poland, Romania, Greece and Israel) to provide initial conditions for the high-resolution ensemble forecasting systems, e.g. the operational COSMO-D2-EPS or experimental ICON-LAM EPS. The system is also successfully run on GPU based supercomputers.

Central part of the talk is to discuss and show results on the tests of localized adaptive particle filter (LAPF) and a localized Markov chain particle filter (LMCPF), which are being tested for the convective scale as well as global model setup, currently in the standard experimental global resolutions of 2.8km over central Europe and on the 40km resolution globally.

We discuss how to overcome filter collapse or divergence by adaptive rejuvenation, mapping into ensemble space based on spread estimators. We also discuss how to keep balances intact when drawing from probability distributions in combination with

localization. We employ incremental analysis update (IAU) for the ICON model system, whereas IAU is not used for COSMO on the convective scale. The LMCPF incorporates model error and explicitly calculates a posterior distribution in ensemble space based on radial basis function approximations of the prior. We show new results on the particle filter on the convective scale, where LMCPF now also shows stable behavior and good scores.

Different further versions of particle-filters and hybrid ensemble-particle filters are under test both for ICON on the global scale as well as for COSMO or ICON-LAM on the convective scale in collaboration with colleagues from ETH, Reading and Potsdam.

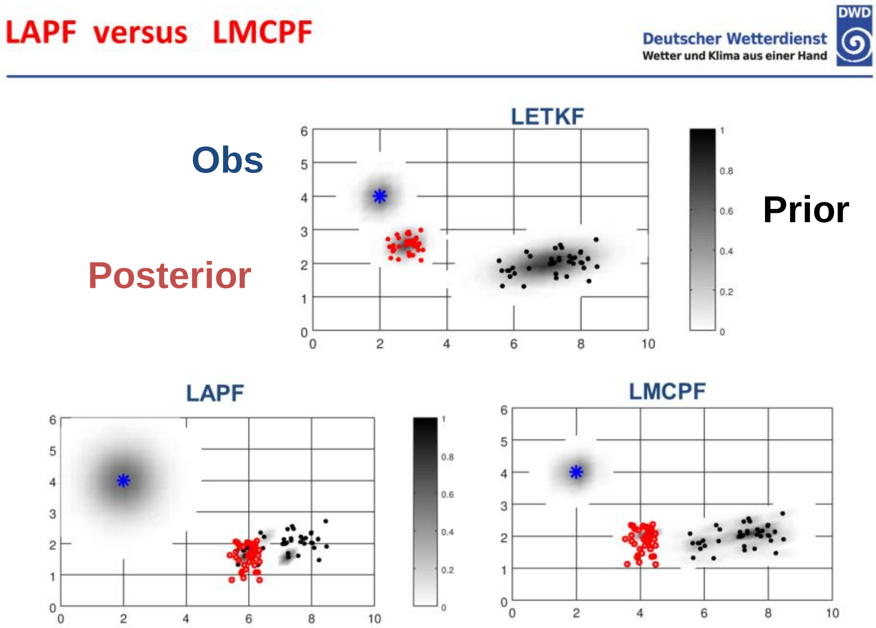


**Figure:** Basic Idea of LETKF, LAPF and LMCPF applied to a simple prior distribution and a measurement in tw o dimensions. Including Model error for each particle leads to the shift of particles in ensemble space for the LMCPF.

**References:**


- Roland Potthast, Anne Walter and Andreas Rhodin: A Localised Adaptive Particle Filter within an Operational NWP Framework. Monthly Weather Review 2018.
- Christoph Schraff, Hendrik Reich, Andreas Rhodin, Annika Schomburg, Klaus Stephan, Africa Perianez and Roland Potthast: Kilometer Scale Ensemble Data Assimilation for the COSMO Model (KENDA), QJRMS, Volume 142, Issue 696, pages 1453–1472, April 2016 Part A.

O2.2

# Regional Weather Forecasting Using the Local Particle Filter

Jonathan Poterjoy[1,2]
1. University of Maryland, United States
2. National Oceanographic and Atmospheric Administration (NOAA) Atlantic Oceanographic and Meteorological Laboratory, United States
Email: poterjoy@umd.edu

## Abstract

Particle filters (PFs) are sequential Monte Carlo methods that can solve data assimilation problems characterized by non-Gaussian error distributions for prior model variables or measurements. From the perspective of a geoscientist, PFs contain several theoretical properties that make them attractive for research and environmental prediction. Namely, they preserve dynamical balances during data assimilation update steps; they require no special treatment for nonlinear measurement operators or non-Gaussian errors; and they provide an elegant solution to the underlying Bayesian filtering problem. Recent efforts applying PFs for geophysical models have resulted in "localized" PFs, which approximate a given data assimilation application as a large set of loosely coupled problems that can be solved independently using relatively small ensembles – an approach long used for ensemble Kalman filters (EnKFs). While localization delivers a potentially transformative strategy for implementing PFs for high-dimensional systems, its use for real geophysical applications has been limited to small-scale, easily localized fluid motions such as moist convection in atmospheric models.

This seminar reveals findings from synoptic-scale weather forecasting experiments performed with a localized PF. The experiments use a modified version of the Poterjoy (2016) local PF (see Poterjoy et al. 2018), which is implemented in a community data assimilation package used operationally in the United States. Experiments are carried out using the Hurricane Weather Research and Forecasting (HWRF) model with an extensive domain that covers most of the Atlantic hurricane basin. To measure potential benefits of the new system, medium-range HWRF ensemble forecasts generated from

local PF members are scrutinized alongside forecasts generated using EnKF members. These forecasts occur over a four-week period that features the formation and evolution of several major tropical cyclones from the 2017 season. The experiment poses a challenging geophysical data assimilation problem, owing to strong nonlinearity in the system dynamics and the extensive use of indirect remotely-sensed measurements from satellites. This research identifies several advantages of the local PF for an application known to pose challenges for Gaussian filters and smoothers, and describes broader implications of PFs for environmental prediction.

**References:**

Poterjoy, J., 2016: A localized particle filter for high-dimensional nonlinear systems. Mon. Wea. Rev., 144, 59 – 76.

Poterjoy, J., L. Wicker, and M. Buehner, 2018: Progress toward the application of a localized particle filter for numerical weather prediction. Mon. Wea. Rev., in press

O2.3

# A Study on Non-Gaussian Probability Densities on Convection Initiation and Development using a Particle Filter with a Storm-Scale Numerical Weather Prediction Model

Takuya Kawabata[1], Genta Ueno[2]

1. Meteorological Research Institute, Japan Meteorological Agency, Japan

2. The Institute of Statistical Mathematics, ROIS/ SOKENDAI (The Graduate University for Advanced Studies), Japan

Email: tkawabat@mri-jma.go.jp

## Abstract

Non-Gaussian probability densities in convection initiation (CI) and development are investigated using a sampling importance resampling particle filter with a nonhydrostatic numerical weather prediction model (NHM-PF). An observation system simulation experiment (OSSE) is conducted with a short assimilation period (90 min), a small domain (48×48×50 grids) with a storm scale of 2 km grid spacing and relatively small number of observations (54) and large number of particles (1,000), to avoid the 'curse of dimensionality' in particle filters. The observations are created from a nature run, which simulates a well-developed cumulonimbus, and factors of the observations are pseudo surface observations of potential temperature (PT), winds (U, V), water vapor (QV) at the lowest height level, and pseudo radar observations of rainwater (QR) at four height levels of the low troposphere. The results of the OSSE are verified with root mean square errors against the nature run in comparison with ensemble simulations without any observations (NoDA). The verifications show that PF significantly improves NoDA (Fig. 1) and the spreads of PF are smaller than that of NoDA. PDFs on grids over the CI area are examined in detail. For evaluation of non-Gaussianity of the ensembles, we proposed to apply the Bayesian Information Criterion to compare the goodness of fit of Gaussian, two-Gaussian mixture and histogram models. The PDFs become strongly non-Gaussian, when NHM-PF produces diverse particles over the CI period. This is led by non-Gaussian PDF of updraft at the beginning, and then the upper-bounded PDF of relative humidity, which creates non-Gaussian PDFs of QV and PT (Fig. 2). These are strongly connected with each other

through saturation and condensation processes. The PDFs of cloud water and QR are quite far from Gaussian distributions throughout the experimental period. Part of PDFs of QC and QR still remain in no-water region, thus, we see bimodal distributions with distant peaks in the development stage. From these examination, it is concluded that the source of non-Gaussian in the CI is updraft.

**References:**


Kawabata, T., and G. Ueno: A Study on Non-Gaussian Probability Densities on Convection Initiation and Development using a Particle Filter with a Storm-Scale Numerical Weather Prediction Model. (*submitted*)


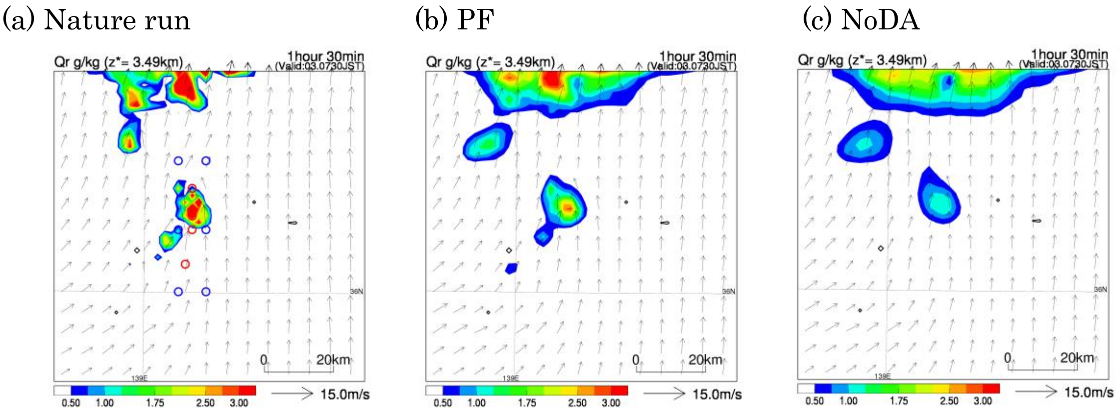


Fig. 1 Horizontal distributions of mixing ratio of rainwater (color shade) and horizontal winds (arrows) at 3.49 km height.

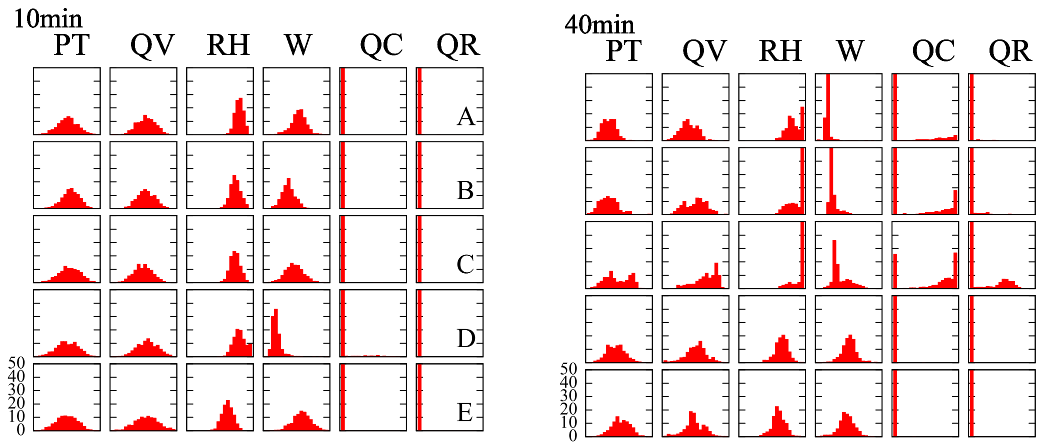


Fig. 2 Probability densities of PT, QV, RH, W, QC and QR on grids from south (lower) to north (upper) in the convection initiation region.

O2.4

# LETKF Perturbations by Ensemble Transform in a Cloud Resolving Model

Kazuo Saito[1,2,3], Le Duc[4,2], Sho Yokota[2,3] and ho Takumi Matsunobu[5]

1. Atmosphere and Ocean Research Institute, the University of Tokyo, Japan
2. Meteorological Research Institute, Japan Meteorological Agency
3. Japan Meteorological Business Support Center
4. Japan Agency for Marine-Earth Science and Technology
5. University of Tsukuba, Japan

Email: k_saito@aori.u-tokyo.ac.jp

## Abstract

In ensemble data assimilation, the forecast error is estimated by perturbations of the ensemble forecast, while characteristics of the ensemble forecast strongly depend on how the initial ensemble was generated. The ensemble transform (ET) is widely used as the initial ensemble perturbation generator, however, in the previous studies for the mesoscale ensemble system (Saito et al. 2011, 2012; Duc et al. 2015), perturbations from LETKF were not necessarily better than other methods as the initial perturbations. Non-diagonal components in the transform matrix likely contaminate the synoptic scale structure of the bred vectors in the ensemble forecast in the assimilation window.

Recently, Duc et al. (2018) presented the mathematical basis of the diagonally predominance property of the ensemble transform matrix and reported that initial perturbations obtained from a diagonal matrix produce better ensemble forecasts than the ones obtained from the conventional ET in experiments using real observations. In this paper, we show detailed structures of perturbations by LETKF and by diagonal transform matrix, and compare their evolution in a cloud resolving model with deep convection.

**References:**

Duc, L., T. Kuroda, K. Saito and T. Fujita, 2015: Ensemble Kalman Filter data assimilation and storm surge experiments of tropical cyclone Nargis. *Tellus*, 67, 25941, doi: 10.3402/tellusa.v67.25941.

Duc, L., K. Saito and D. Hotta, 2018: The diagonally predominant property of the positive symmetric ensemble transform matrix and its application in ensemble forecast. *Mon. Wea. Rev.* (in revision)

Saito, K., M. Hara, M. Kunii, H. Seko, and M. Yamaguchi, 2011: Comparison of initial perturbation methods for the mesoscale ensemble prediction system of the Meteorological Research Institute for the WWRP Beijing 2008 Olympics Research and Development Project (B08RDP). *Tellus*, 63A, 445-467.

Saito, K., H. Seko, M. Kunii and T. Miyoshi, 2012: Effect of lateral boundary perturbations on the breeding method and the local ensemble transform Kalman filter for mesoscale ensemble prediction. *Tellus*, 64, 11594, doi:10.3402/tellusa.v64i0.11594.

O2.5

# Model Parameter Estimation with Data Assimilation using NICAM-LETKF

Shunji Kotsuki[1], Yousuke Sato[2], Koji Terasaki[1], Hisashi Yashiro[1], Hirofumi Tomita[1], Masaki Satoh[3,4], and Takemasa Miyoshi[1,4,5]

1. RIKEN Center for Computational Science, Japan
2. Graduate School of Engineering, Nagoya University, Japan
3. Atmosphere and Ocean Research Institute, the University of Tokyo, Japan
4. Japan Agency for Marine-Earth Science and Technology, Japan
5. Department of Atmospheric and Oceanic Science, University of Maryland, U. S.

Email: shunji.kotsuki@riken.jp

## Abstract

This study aims to improve forecasts of numerical weather prediction (NWP) models by optimizing model parameters with data assimilation. Kotsuki et al. (2018a, JGR) succeeded in improving global precipitation forecasts at 112-km-resolution NICAM (Nonhydrostatic ICosahedral Atmospheric Model) by estimating a parameter called B1 of Berry (1967)'s large-scale condensation scheme using satellite-observed precipitation data and the Local Ensemble Transform Kalman Filter (LETKF).

Extending the previous study, this study explores to improve the forecasts further using other satellite observations. This study estimates the parameter B1 as a global-constant parameter with cloud liquid water (CLW) data observed by GCOM-W/AMSR2. The parameter estimation successfully reduces excessive bias in CLW (Figs. 1 a, b, d) although precipitation forecasts are degraded. In addition, this study extends to estimate spatial distributions of the B1 parameter. The spatially-varying B1 parameter shows the best agreement to the spatial pattern of observed LWP (Figs. 1 c, d). This presentation will include the most recent progress up to the time of the workshop.

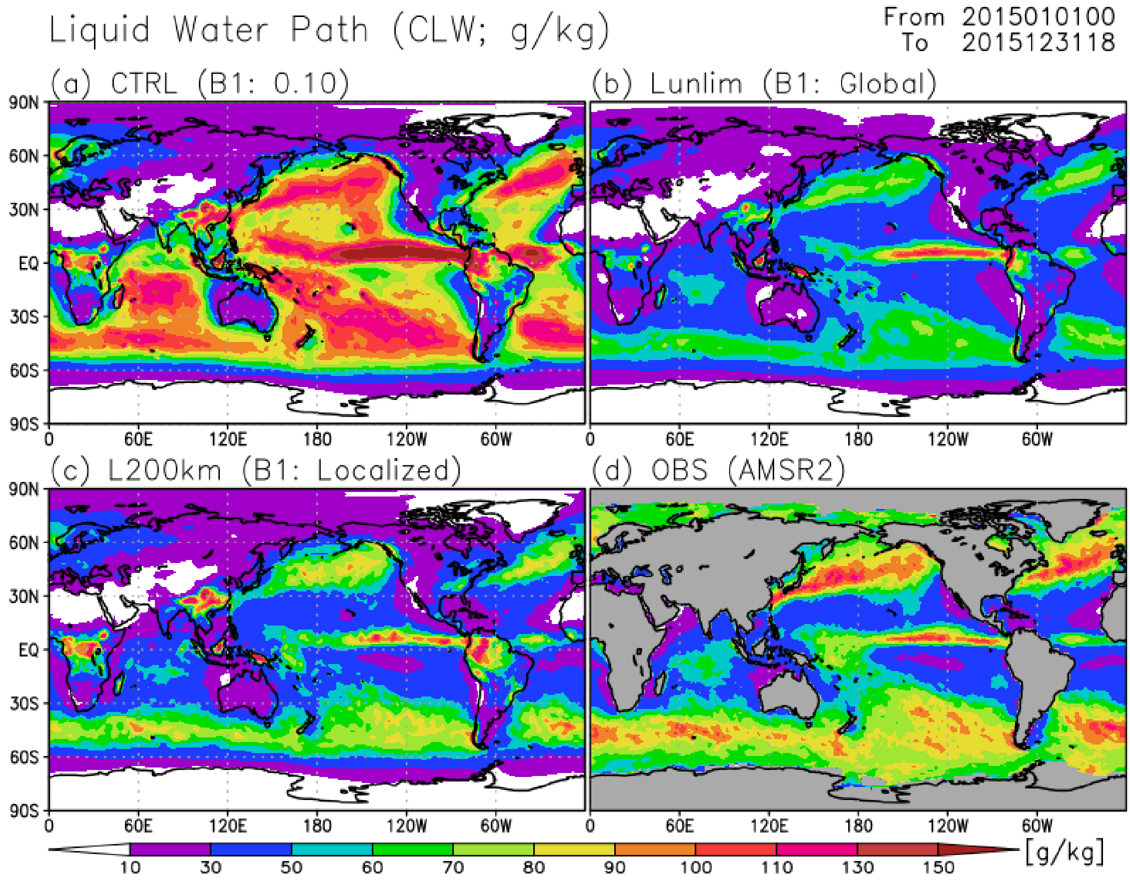


Fig. 1 Global patterns of the time-mean liquid water path (LWP; g kg-1) for (a) control experiment without parameter estimation, (b) parameter estimation as a global-constant parameter, (c) parameter estimation as spatially-varying parameter, and (d) GCOM-W/AMSR2 observation, averaged over 12 months from January to December 2015. According to Kotsuki et al. (2018b)

**References:**

Kotsuki, S., K. Terasaki, H. Yashiro, H. Tomita, M. Satoh, and T. Miyoshi (2018a): Online Model Parameter Estimation with Ensemble Data Assimilation in the Real Global Atmosphere: A Case with the Nonhydrostatic Icosahedral Atmospheric Model (NICAM) and the Global Satellite Mapping of Precipitation Data. *J. Geophys. Res.* 123, 7375-7392.

Kotsuki, S., Y. Sato, and T. Miyoshi (2018b): Localizing parameterization with data assimilation: A case with Berry's large scale condensation scheme. (in preparation)

O2.6

# Towards a super dynamics for the gray zone

Shian-Jiann Lin
GFDL, The Weather and Climate dynamics division

## Abstract

In climate and weather modeling, the “dynamics" and "physical parameterizations" are traditionally separated due do both scientific and software engineering concerns. As sciences and supercomputing hardware evolve in time, this strict separation may actually become counterproductive limiting scientist's imagination and even freedom. A small group of scientists at GFDL have been recently working on a radically new approach merging physics and a (nonhydrostatic) dynamics for the goal of achieving optimal performance in simulation quality and computational performance. We have attempted to embed sub-grid physical-dynamical processes into the Finite-Volume Dynamical core on the cubed-sphere (FV3) thus breaking the boundary between the physics and the dynamics. Since truly sub-grid processes (designed for gray zone) are becoming part of the new dynamics we shall call this merged model the "super dynamics".

O2.7

# A three-dimensional turbulence scheme for the gray zone in a convective boundary layer

Yuji Kitamura[1]
[1]Meteorological Research Institute, Japan Meteorological Agency, Japan
Email: kitamura@mri-jma.go.jp

While a convective flow in a planetary boundary layer can be partly captured with the horizontal resolution less than 1 km, a turbulence scheme suitable for such the resolution is not sufficiently established. This issue is often called the gray zone problem for a boundary layer. Several schemes applicable to the gray zone has been proposed in recent years. Most of them are designed on the basis of a vertically one-dimensional (1D) scheme which is usually employed for a RANS model. On the other hand, Honnert and Masson (2014) indicated that the effect of the horizontal shear production, which cannot be taken into account in a 1D model, is not negligible in the gray zone.

Kitamura (2016) proposed a three-dimensional (3D) turbulence scheme based on the Deardorff (Deardorff 1980) model. While this model improves the representation of the resolved motion in the gray zone, it tends to underestimate the vertical gradient of the temperature in the surface layer and cannot reproduce a weak stable region seen in the upper part of the mixed layer for coarser model resolution. In the present study, we modify the three-dimensional (3D) scheme proposed by Kitamura (2016). First, the upper limit of the vertical length in the surface layer is given independently of the horizontal resolution, because the length scale should be determined by the height from the ground rather than the horizontal resolution. Second, the countergradient term by Troen and Mahrt (1986) is introduced to the vertical temperature flux.

We examined the numerical experiments for an unstable boundary layer using ASUCA which is an NWP model developed by Japan Meteorological Agency. In the experiments, the surface temperature is prescribed as an external forcing. The horizontal grid spacings of 125, 250, 500 and 1000 m are performed.

Figure 1 shows the ratio of the subgrid scale (SGS) components to the total turbulence kinetic energy (TKE) and vertical heat flux. Honnert et al. (2011) reported that the ratio could be well represented as a function of the horizontal resolution normalized by the boundary layer height and proposed the empirical functions for these SGS ratios. The ratio of the SGS component calculated by the present model is consistent with their empirical functions while that by the MYNN level 3 model (Nakanishi and Niino 2009) which is employed in the operational use is insensitive to the horizontal resolution and is overestimated in finer resolutions. Furthermore, The effect of the horizontal shear production in the new 3D scheme is analyzed. The ratio of the shear production to the total TKE production is displayed in Figure 2. The horizontal shear production is comparable to the vertical one and is not negligible in comparison with the buoyancy production in the gray zone. This result suggests that use of a 1D model induces underestimation of the SGS TKE because the effect of the horizontal shear production does not contribute to increasing the SGS TKE in the 1D model.

**References:**

Deardorff, J. W., 1980: Stratocumulus-capped mixed layers derived from a three-dimensional model. *Boundary-Layer Meteorol.*, **18**, 495–527.

Honnert, R., and V. Masson, 2014: What is the smallest physically acceptable scale for 1D turbulence schemes? *Front. Earth Sci.*, **2**, 27.

Honnert, R., V. Masson, and F. Couvreux, 2011: A diagnostic for evaluating the representation of turbulence in atmospheric models at the kilometric scale. *J. Atmos. Sci.*, **68**, 3112–3131.

Kitamura, Y., 2016: Improving a turbulence scheme for the terra incognita in a dry convective boundary layer. *J. Meteor. Soc. Japan*, **94**, 491–506.

Nakanishi, M., and H. Niino, 2009: Development of an improved turbulence closure model for the atmospheric boundary layer. *J. Meteor. Soc. Japan*, **87**, 895–912.

Troen, I., and L. Mahrt, 1986: A simple model of the atmospheric boundary layer; sensitivity to surface evaporation. *Boundary-Layer Meteorol.*, **37**, 129–148.

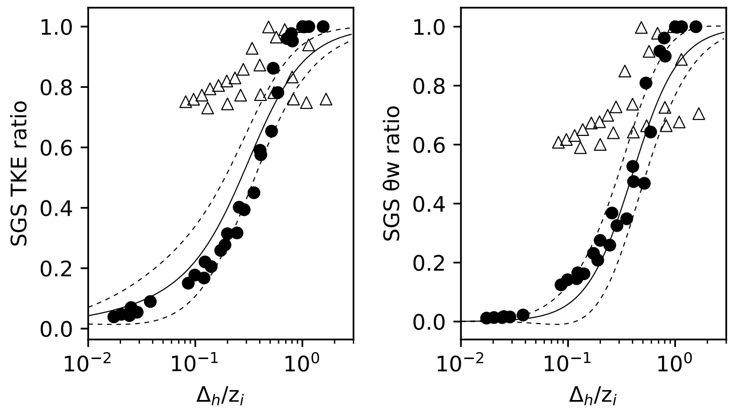


Figure 1: The ratio of the SGS components to the total TKE (left) and vertical heat flux (right). The abscissa indicates the horizontal grid size normalized by the height of the boundary layer. The open triangles and filled circles display the results for the MYNN level 3 model and the proposed model, respectively. The solid line shows the empirical function proposed by Honnert et al. (2011).

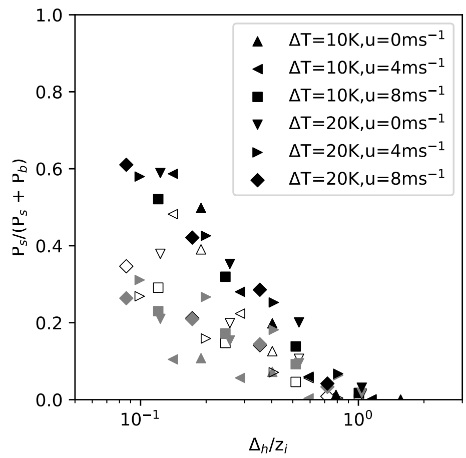


Figure 2: The ratio of the shear production to the total TKE production. The black, gray and open markers display the total shear production, the vertical and horizontal parts of the shear production.

O2.8

# Plumes, thermals and chains: A critical examination of the various conceptual models for moist convection

Hugh Morrison (morrison@ucar.edu)
National Center for Atmospheric Research,
Mesoscale and Microscale Meteorology Laboratory

Since the 1950's two primary conceptual models have served as a basis for understanding the structure and behavior of moist convection in the atmosphere. The first is the steady-state plume, and the second is the isolated rising thermal. These models have markedly different structural and flow characteristics, and debate has continued as to which one provides a better framework for understanding and parameterizing moist convection. Based on theory, high resolution large eddy simulations, and observations, we argue that moist updrafts have characteristics of both plumes and thermals, with neither alone providing a satisfactory description. More plume-like versus thermal-like updrafts occur as conditions vary (e.g., environmental relative humidity), and the transition between thermal-like and plume-like updrafts is characterized by a succession of rising bubbles which we call a "thermal chain". Although thermal chains share common features with both plumes and thermals they also have several unique characteristics, particularly with regard to entrainment. We derive approximate analytic solutions to the governing momentum, mass continuity, and cloud thermodynamic equations for a cloudy updraft, and show that thermal chains are a characteristic feature of these solutions under a wide range of conditions. Although dry convective updrafts can also occur as thermal chains under certain conditions, they are primarily a feature of moist convection owing to the feedback between entrainment, evaporation, buoyancy, and flow structure. A conceptual model based on these ideas will be presented, and implications for improving convection parameterizations and interpreting results from nonhydrostatic convection-permitting models will be discussed.

O2.9

# Separating dynamical and thermodynamical impacts of climate change on clouds and precipitation for daytime convective development over land

Wojciech W. Grabowski and Andreas F. Prein
Mesoscale and Microscale Meteorology Laboratory
National Center for Atmospheric Research, USA
Email: grabow@ucar.edu

## Abstract

This presentation will discuss results from high-resolution simulations applying piggybacking methodology to separate dynamical and thermodynamical impacts of climate change on convection developing during daytime over summertime continents. Dynamical impacts include an increase of convective updraft strength due to an increase of CAPE in a warmer climate. Thermodynamic impacts concern an increase of cloudiness and surface precipitation resulting from the increase of water vapor that the warmer atmosphere can hold and convection can work with. The main idea behind the piggybacking method is to use two sets of thermodynamic variables in a single cloud field simulation. The first set is coupled to the dynamics and drives the simulation (set D, as in Driving), and the second set piggybacks the simulated flow and does not affect it (set P, as in Piggybacking). Because the two sets are driven by the same flow, the methodology allows assessing the impact of initial thermodynamic profiles with high accuracy. The impact on the dynamics is assessed by performing a second simulation with thermodynamic sets swapped so the D set becomes the P set, and vice versa. This presentation will discuss application of the piggybacking method to the case of a global climate-model predicted change of the temperature and moisture profiles (the sounding) in the Amazon region. The CoNTRol sounding (CNTR hereafter) initiates the model with a profile that was observed at sunrise during the Large-Scale Biosphere–Atmosphere (LBA) field project in Rondonia (Brazil). This sounding was previously used in studies of convective development over summertime continents. The CLimate CHange sounding (CLCH hereafter) comes from adding climate change signal over the Amazon at the end of the 21$^{st}$ century as shown in Fig. 1 to the CNTR sounding. The CLCH initial sounding features increased CAPE (from ~1300 to ~2500 J kg$^{-1}$) and CIN (from ~20 to ~40 J kg$^{-1}$).

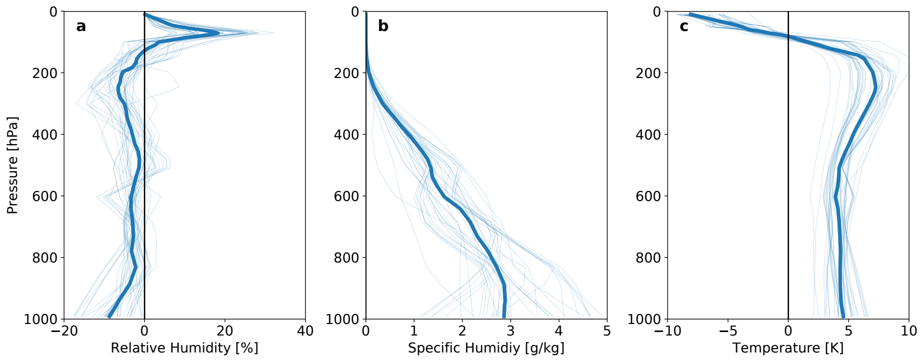


Figure 1. Differences in the relative humidity, specific humidity, and temperature between ends of the 21st and 20th-century climate over the Amazon as simulated by CMIP5 RCP8.5 global climate model ensemble. Thin lines represent individual model results. The thick line is the median used in LES simulations.

Figure 2 shows the impact of CNTR and CLCH soundings on the simulated convective development. Because of the differences in the low-level humidity, clouds in the CLCH environment develop later and have higher cloud bases regardless which set drives the simulation. Because of higher CAPE, deep convection is stronger in CLCH and transports more water into the upper atmosphere. The latter leads to deeper and more extensive anvils at the end of simulations. Reduced initial upper tropospheric humidity (cf. Fig. 1) results in reduced anvil coverage in CLCH at hour 12, again regardless which set drives the simulation. Other details of the simulations (e.g., surface rain accumulations), as well as results of sensitivity simulations with additional sounding modifications, will be discussed at the meeting.

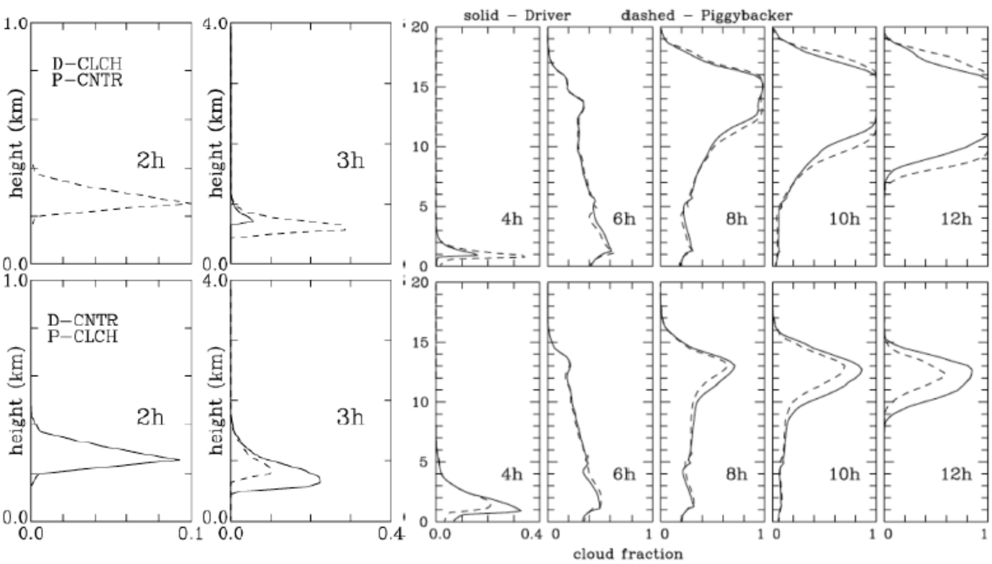


Figure 2. Evolution of cloud fraction profiles in piggybacking simulations applying CNTR and CLCH initial soundings. Driver/piggybacker results are shown with solid/dashed line. CNTR drives and CLCH piggybacks in lower panels (D-CNTR/P-CLCH); the reverse is in the upper panels, D-CLCH/P-CLTR.

O2.10

# Super Fine Vertical Resolution Radiative-Convective Equilibrium Experiments on the High-Cloud Response to Sea Surface Temperatures

Tomoki Ohno[1], Masaki Satoh[1,2]

1. Japan Agency for Marine-Earth Science and Technology, Japan

2. Atmosphere and Ocean Research Institute, the University of Tokyo, Japan

Email: t-ohno@jamstec.go.jp

## Abstract

As the high clouds have large impacts not only on shortwave and longwave radiation, but also on the environmental fields for the convective activity, it is important to improve the understanding of the high cloud changes in response to warmer climates. Radiative-convective equilibrium (RCE) experiments are a unique set of experiments to study uncertainties of cloud feedback, particularly that of high clouds associated with deep moist convection.

As the vertical resolution has large impacts on the representability of high clouds, it is expected to have impacts on high-cloud amount responses on global warming. In this study, we examined the vertical resolution dependency of high-cloud amount response on sea surface temperature (SST) changes. We conducted simulations with RCE configurations on the earth-like sphere domain using a nonhydrostatic global circulation model (the Nonhydrostatic Icosahedral Atmospheric Model; NICAM) and a two-moment bulk cloud microphysics scheme. Constant SSTs of 300 and 304 K were used as lower boundary conditions. We compare responses with five vertical layer configurations where the layer depths are about 1 km to 50 m.

We found that although high-cloud amounts decrease with the SST increase using relatively lower vertical resolutions configuration, they increase using higher vertical resolution configurations. A budget analysis of ice water condensate and sensitivity experiments revealed that the variability of responses were caused by the differences in the interactions between the

turbulent mixing and the cloud microphysics. The results speculate that the climate sensitivity depends on the natures of both turbulence and cloud microphysics at the high altitude through the high-cloud amount responses.

O2.11

# Alleviating low cloud problem in climate and weather forecast models by adaptive vertical grid enhancement

Takanobu Yamaguchi[1,2], Peter Bogenschutz[3], Yaosheng Chen[1,2], Ryuji Yoshida[1,2], Graham Feingoldtoh[2], Daniel Martin[4], Hsiang-He Lee[3], Peter Schwartz[4]

1. Cooperative Institute for Research in Environmental Sciences, University of Colorado Boulder, USA
2. NOAA Earth System Research Laboratory, Boulder, CO, USA
3. Lawrence Livermore National Laboratory, Livermore, CA, USA
4. Lawrence Berkeley National Laboratory, Berkeley, CA, USA

Email: tak.yamaguchi@noaa.gov

## Abstract

Low cloud bias in atmospheric models for climate and weather remains as an unsolved problem. Considering decades of community effort for developing and advancing boundary layer and microphysics parameterizations, one realizes how persistence the low cloud problem is. In this presentation, the first focus is impact of vertical resolution on representation of low clouds for these large scale models. For these models, sensitivity of vertical resolution on simulated boundary layer is a relatively less explored aspect due to limitation of computational resources. We will discuss how low cloud representation is improved by simply increasing vertical resolution for the Energy Exascale Earth System Model (E3SM) (Fig. 1) and its single column model. Second, we will introduce a new computational method, Framework for Improvement by Vertical Enhancement (FIVE; Yamaguchi et al. 2017) coupled with Adaptive Vertical Grid (AVG). This method will offer better representation of atmospheric boundary layer clouds while limiting additional increase of computational cost due to increased number of levels. Last, we will discuss a path to E3SM coupled with FIVE-AVG and challenges for developing a computationally efficient FIVE-AVG and current progress of the development.

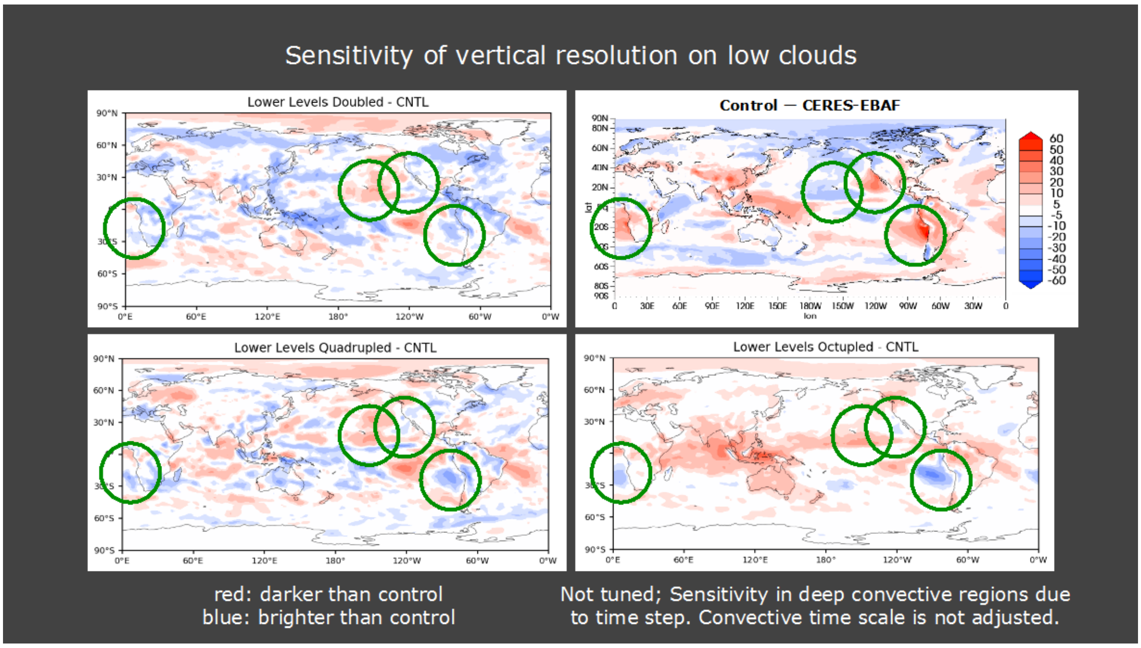


Fig. 1: Sensitivity of vertical resolution for E3SM.

**References:**

Yamaguchi, T., G. Feingold, and V. E. Larson: Framework for improvement by vertical enhancement: A simple approach to improve representation of low and high-level clouds in large-scale models, *J. Adv. Model. Earth Syst.* 2017, **9**(1), 627-646. doi: 10.1002/2016MS000815

O2.12

# Evaluation of microphysics in mixed-phase clouds over the Southern Ocean in NICAM using Joint simulator

Woosub Roh[1], Tatsuya Seiki[2], Masaki Satoh[1,2], Tempei Hashino[3]

1. Atmosphere and Ocean Research Institute, the University of Tokyo, Japan

2. Japan Agency for Marine-Earth Science and Technology, Japan

3. Nagoya university, Japan

Email: ws-roh@aori.u-tokyo.ac.jp

## Abstract

It is important to evaluate and improve the cloud properties in global non-hydrostatic models like a Nonhydrostatic ICosahedral Atmospheric Model (NICAM, Satoh et al. 2014) using observation data. One of the methods is a radiance-based evaluation using satellite data and a satellite simulator (here Joint simulator, Hashino et al. 2013), which avoids making different settings of the microphysics between retrieval algorithms and NICAM.

One of challenging issues is an evaluation of mixed-phase clouds, which consist of water vapor, ice particles, and supercooled water droplets. It is known one of the main reasons why climate models reveal large errors about the reflection of solar radiation over the Southern Ocean and Arctic.

This study is an evaluation and improvement of mixed-phase clouds over Southern Ocean in NICAM using a Cloud-Aerosol Lidar and Infrared Pathfinder Satellite Observation (CALIPSO) and a satellite simulator. We evaluated thermodynamics phase of mixed phases clouds over the Southern Ocean in a regional version of NICAM between 45°S to 65°S and 170°E to 170°W following Yoshida et al. (2010) method. We found underestimation of super cooled water clouds in our single moment scheme. We improved the single moment microphysics scheme using a double moment microphysics and a single column model. And we expand the global simulation to investigate impact of the mixed phase clouds on OSR and OLR in NICAM.

**References:**

Hashino, T., M. Satoh, Y. Hagihara, T. Kubota, T. Matsui, T. Nasuno, and H. Okamoto:

Evaluating cloud microphysics from NICAM against CloudSat and CALIPSO. *J. Geophys. Res.2013, 118, 1-20, doi:10.1002/jgrd.50564.*

Satoh, M., H. Tomita, H. Yashiro, H. Miura, C. Kodama, T. Seiki, A. T. Noda, Y. Yamada, D. Goto, M. Sawada, T. Miyoshi, Y. Niwa, M. Hara, T. Ohno, S. Iga, T. Arakawa, T. Inoue and H. Kubokawa: The Non-hydrostatic Icosahedral Atmospheric Model: description and development. *Progress in Earth and Planetary Science* 2014, **1**:18. *doi: 10.1186/s40645-014-0018-1*

Yoshida, R., H. Okamoto, Y. Hagihara, and H. Ishimoto:: Global analysis of cloud phase and ice crystal orientation from cloud-aerosol lidar and infrared pathfinder satellite observation (CALIPSO) data using attenuated backscattering and depolarization ratio, *J. Geophys. Res 2010., 115, D00H32, doi:10.1029/2009JD012334.*

O2.13

# Ice cloud modeling for simulating mixed-phase low-clouds

Tatsuya Seiki[1], Woosub Roh[2]

1. Japan Agency for Marine-Earth Science and Technology, Japan
2. Atmosphere and Ocean Research Institute, the University of Tokyo, Japan

Email: tseiki@jamstec.go.jp

## Abstract

This study improved a single-moment bulk cloud microphysics scheme (SM) to realistically simulate supercooled-liquid water within low-level mixed-phase clouds in polar regions. Low-level clouds in polar regions are known to have unique structure: Cloud ice slowly settles down to cloud bottom while super-cooled liquid water remains near the cloud top. CMIP5 GCMs poorly simulated this cloud structure because of difficulty in simulation using their simple cloud microphysics [e.g., Williams et al., 2013]. As a result, they underestimated low-level cloud fraction over the polar region, and hence, cloud radiative forcing was significantly biased [e.g., Bodas-Salcedo et al., 2012]. The same issue also arises in a global high-resolution GCM NICAM [Kodama et al., 2015; Hashino et al., 2016], which uses single-moment cloud microphysics schemes (SMs) with five categories of hydrometeors [Lin et al., 1983; Tomita, 2008; Roh and Satoh, 2014]. Recently, Seiki and Nakajima [2014] implemented a double-moment bulk cloud microphysics scheme (DM) based on Seifert and Beheng [2006]. Seiki et al. [2015a] achieved more realistic simulation of global cloud distribution using the DM scheme. We found that low-level clouds over the Southern Ocean was also simulated well (See Fig. 1).

We used a single column model to evaluate ice cloud microphysics of the SM [Roh and Satoh, 2014] and DM. The model only includes microphysics and gravitational sedimentation with no external forcing. Initial condition was given by simplifying a vertical column at 60 S in a global simulation [Seiki et al., 2015b] (see Figs. 2a; 2b): a cloud layer exists from 1000 m to 2000m altitude, atmospheric temperature slightly fell below the freezing level in the cloud layer, cloud water linearly decreases from cloud top to cloud bottom with cloud top mixing ratio of $3.5e^{-4}$ kg $kg^{-1}$. The super-cooled liquid water is maintained unless ice hydrometeors initiate and consume ice supersaturation.

We found that a significant difference in super cooled liquid water between the SM and DM was observed quickly after running the single column model. Thus, the bias in NICAM originated from artificial settings in the SM scheme rather than the boundary layer processes. Budget analysis showed that underestimation of supercooled liquid water originated from strong Bergeron-Findeisen process when using the SM. We newly introduced several thresholds to suppress growth of cloud ice, snow, and graupel.

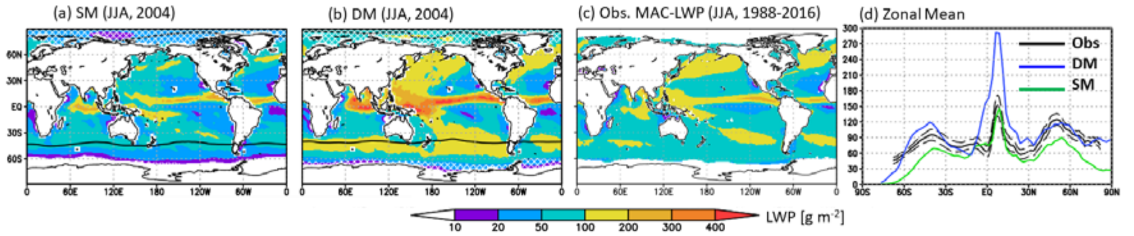


Figure 1. Global distribution of liquid water path [g $m^{-2}$] on JJA from (a) the SM experiment, (b) DM experiment, and (c) satellite product of MAC-LWP [Elsaesser et al., 2017]. Polar regions covered by sea-ice was shown by white tiles and the freezing level at 850 hPa was shown by black solid lines in (a) and (b).

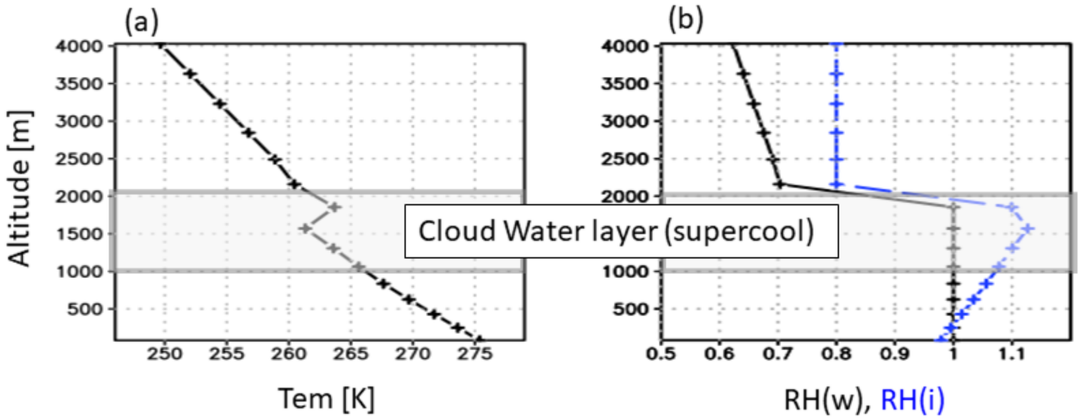


Figure 2. Initial condition of the single column model: (a) the vertical profiles of the atmospheric temperature and (b) relative humidity with respect to liquid cloud (black line) and with respect to ice cloud (blue line).

O2.14

# A numerical investigation of the impact of aerosol-induced warming on deep convective updrafts with varying slope and width

Zachary J. Lebo[1]

1. Department of Atmospheric Science, University of Wyoming, Laramie, Wyoming, USA

Email: zlebo@uwyp.edu

## Abstract

An idealized but accurate numerical approach is utilized to examine changes in updraft velocities in deep convective updrafts due to differences in updraft slope, updraft width, and aerosol-induced warming, i.e., invigoration (Lebo 2018). Because updraft width and slope are tightly coupled to the ambient environmental conditions, this approach provides a rigorous way to examine potential indirect impacts of changes in aerosol loading on updraft velocities relative to those expected from changes in environmental conditions, which vary both spatially and temporally. We show that the updraft slope and width parameter space is complex, whereby changes in updraft width have little to not impact on updraft velocities for a given slope, and vice versa. The results also indicate that prior idealized modeling results of the effect of aerosol-induced warming on updraft velocities are

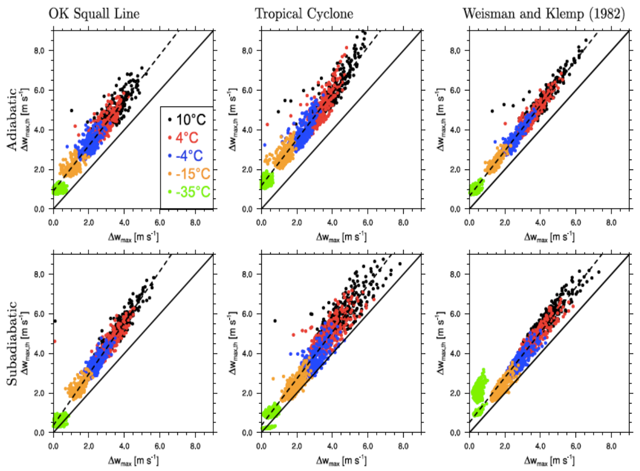


Figure 1: Comparison between theoretical changes in maximum vertical velocity ($\Delta w_{max,th}$) and the predicted change in maximum vertical velocity ($\Delta w_{max}$) for warming at different temperatures levels (colors), different soundings (columns), and both adiabatic (top) and

overestimated by as much as 100% due to neglecting the buoyant perturbation pressure field (Figure 1). We show that the impacts of aerosol-induced warming on convective updraft strength is largely outweighed by small changes in updraft width and slope, and we relate the changes to changes in environmental conditions (Figure 2).

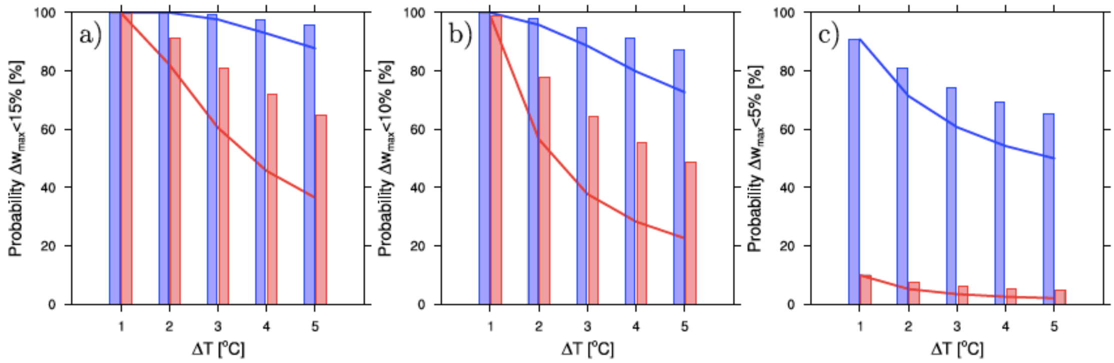


Figure 2: Probability of $\Delta w_{max}$ exceeding thresholds determined by realistic changes in $w$ for small environmentally variability as a function of the aerosol-induced warming. Cumulative probability is shown by the bars, individual probabilities shown by the lines. Colors indicate warm (red) and mixed-phase (blue) invigoration.

**References:**


Lebo, Z., 2018: A Numerical Investigation of the Potential Effects of Aerosol-Induced Warming and Updraft Width and Slope on Updraft Intensity in Deep Convective Clouds. *J. Atmos. Sci.,* **75**, 535–554,

# November 16, 2018 (Friday)

O3.1

# Some preliminary results from Global SAM


Marat Khairoutdinov

School of Marine and Atmospheric Sciences, Stony Brook University


## Abstract


A new version of the System for Atmospheric Modeling extended to the latitude-longitude grid will be introduced. The model features an anelastic dynamical core, which is unusual for a global model. The results of several standard dynamical-core tests, such as Jablonowsi's hydrostatic and baroclinic instability test as well as the Held and Suares' dry test among others will be shown. Some results from a recent DYAMOND GCRM intercomparison as well as some preliminary results of using GSAM for hurricane prediction will be discussed.

O3.2

# Atmospheric modelling on the equal-area cubed-sphere

John L. McGregor
CSIRO Oceans and Atmosphere, Melbourne, Australia
Email: John.McGregor@csiro.au

## Abstract

The Conformal-Cubic Atmospheric Model (CCAM) was the first atmospheric global model to be formulated on a cubed-sphere grid. CCAM employs semi-Lagrangian, semi-implicit dynamics (McGregor, 2005a), which handles the finer resolution near the vertices without a time step penalty. It also uses reversible staggering in the horizontal (McGregor, 2005b) to achieve good dispersion properties and good kinetic energy spectra.

The CCAM code has recently been generalized to provide a version on the Uniform Jacobian (UJ) arrangement of the cubed-sphere grid. This grid was modified from the conformal-cubic grid to provide equal area for every grid cell (Purser and Rancis, 2011); a similar grid was derived by Tsugawa et al. (2008),. Since the grid lines are no longer orthogonal, covariant and contravariant velocity components are required. Despite the complications of the non-orthogonality, most of the CCAM semi-Lagrangian approach may be used, including reversible staggering of the contravariant velocity components to switch between values at cell centres and cell edges. The solver for the Helmholtz equation is a little more complicated than for CCAM, but is well handled by the multigrid approach.

Both of these versions of CCAM include the Miller and White (1984) non-hydrostatic formulation, which provides extremely economical solutions in the context of semi-Lagrangian time differencing.

A second dynamical core has also been developed on the UJ grid. This version employs the primitive equations in conservative form, providing extra appeal for climate studies and for modelling trace gases and chemistry. Split-explicit time stepping is used, with small time steps for the fast gravity waves processes and longer time steps for the slow

advective processes and for the physical parameterizations. Flux-corrected-transport is employed to better preserve any sharp gradients in the advected fields. It also employs the reversible staggering technique for the contravariant wind components

Both new dynamical cores produce very acceptable climatologies. Results from the various dynamical cores will be shown, and their relative advantages and disadvantages discussed.

**References:**

McGregor, J. L.: C-CAM: Geometric aspects and dynamical formulation. CSIRO Atmospheric Research Tech. Paper No. 70, 43 pp. https://publications.csiro.au/rpr/pub?list=BRO&pid=procite:eb33ff33-c6d6-4779-8b82-867b2ca6e112, 2005a.

McGregor, J. L.:: Geostrophic adjustment for reversibly staggered grids. *Mon. Wea. Rev.*, **133**, 1119-1128, 2005b.

Miller, M. J. and A. A. White: On the non-hydrostatic equations in pressure and sigma coordinates. *Q. J. R. Meteor. Soc.*,, **110**, 515-533, 1984.

Purser, R. J. and M. Rancic: A standardized procedure for the derivation of smooth and partially overset grids on the sphere, associated with polyhedra that admit regular griddings of their surfaces. Part I: Mathematical principles of classification and construction. *NOAA/NCEP Office Note 407*, 58 pp., 2011.

Tsugawa, M., Y. Tanaka and T. Matsuno: An ocean general circulation model on a quasi-homogeneous cubic grid. *Ocean Modelling*, **22**, 66-86, 2008.

O3.3

# A shallow-water model using the B-grid staggering on the spherical icosahedral grid

Hiroaki Miura
The University of Tokyo, Graduate School of Science

## Abstract

A shallow water model using the hexagonal synchronized B grid (SB grid) is developed and tested on the spherical icosahedral mesh. The SB grid adopts the same variable arrangement as the ZM grid, but does not suffer from a computational mode problem of the ZM grid since an extra coupling of velocity fields through the nonlinear terms is excluded. Some standard tests are performed to examine the model. The model is almost second order accurate if the initial conditions and the surface topography are sufficiently smooth. The SB-grid model is superior to a hexagonal C-grid model regarding the convergence of error norms in a steady-state geostrophically balanced flow test, while it is inferior to that concerning conservation of total energy in a case of flow over an isolated mountain. An advantage of the new model is that both accuracy and stability are only weakly sensitive to whether a grid optimization is applied or not.

O3.4

# A nestable, multigrid-friendly grid on a sphere for global spectral models based on Clenshaw-Curtis quadrature

Daisuke Hotta[*1,2], Masashi Ujiie[2]

1. Meteorological Research Institute, Japan Meteorological Agency, Japan

2. Numerical Prediction Division, Japan Meteorological Agency, Japan

[*]Email: dhotta@mri-jma.go.jp

## Extended Abstract

### 1. Introduction

Global spectral models typically adopt Gaussian quadrature in performing spherical harmonics transforms, with the consequence of the nodes (grid-points) placed on irregularly-spaced Gaussian latitudes. As we move into very high resolutions, it becomes necessary to accurately represent the nature's nonhydrostatic aspects into the model. Semi-implicit time-stepping applied to nonhydrostatic equations necessitates solution of non-constant coefficient Helmholtz-type problem, which is difficult to solve efficiently by the current massively parallel HPC architecture. A promising approach with demonstrably high parallel efficiency to this type of problem is the multigrid, which exploits the hierarchy of grids to accelerate iterative elliptic solvers. However, a multigrid approach is difficult to implement on the current global spectral models because the Gaussian grids do not nest.

In this study we propose a new, nestable grid on a sphere which would allow straight multigrid implementation. The proposed grid and quadrature rules are implemented on a shallow-water equations (SWE) model and a three-dimensional hydrostatic primitive equations (HPE) model. Detailed description of this work can be found in our recent publication [1].

### 2. Grid and Quadrature formulation

In the proposed scheme, numerical integration in the meridional direction is performed using a variant of Clenshaw-Curtis-type quadrature (Fejér's second rule) [2] instead of the conventional Gauss-Legendre rule. With this quadrature rule, the nodes are aligned on colatitudes $\theta_j = \frac{j\pi}{J+1}$ $(j = 1, \cdots, J)$, meaning that the grid does not include that poles and the latitudinal grid points are equidistant. This grid is nestable since the grid points for $J/2$ nodes can be constructed by skipping every other grid of the nodes for $J$-point rule starting from $j$=2. One shortcoming of this grid is that $J \geq 2N+1$ meridional nodes are required to ensure exact transform for the truncation total wavenumber of $N$, unlike the Gaussian grid which requires only $(2N-1)/2$ nodes.

## 3. Numerical orthonormality and aliasing errors on nonlinear terms

The proposed grid and quadrature are implemented on the code of the operational global model of Japan Meteorological Agency (JMA-GSM) and tested for numerical orthonormality of the associated Legendre functions. The orthonormality is found to be satisfied up to machine precision as long as the condition $J \geq 2N+1$ is met. The proposed quadrature formally incurs aliasing errors for nonlinear terms of quadratic or higher orders, but the relative errors caused by the aliasing are found to be small (at most $O(10^{-3})$ in practice.

## 4. Test case results

An SWE model and an HPE model based on JMA-GSM are adapted to use the proposed Clenshaw-Curtis grid and are compared with their original Gaussian-grid versions within the framework of idealized test cases ([3,4] for SWE and [5] for HPE) with various horizontal resolutions up to Tc479 ($\Delta x$～20 km). The integration results from the two versions of the models are confirmed to be nearly identical for any of the investigated test cases.

## 5. Future direction: Multigrid-based grid-spectral hybrid model

The proposed grid can be adapted to take a structured form (e.g., as in Fig.1). We postulate that employing the pseudo-spectral multigrid method will foster smooth and gradual transition from spectral to grid-based modelling since the pseudo-spectral horizontal derivatives can be readily replaced by local, stencil-based horizontal derivatives. Given that grid-based elliptic solvers tend to be less efficient at larger scale, as grid/spectral hybrid approach, where a grid-based multigrid method with shallow layers is combined with a spectral elliptic solver used only at the coarsest grid with moderate resolution, would be a reasonable strategy that compromises the need to avoid global inter-node communications and to maintain high accuracy and fast convergence rate.

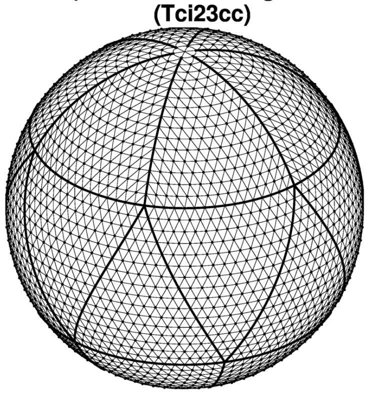


Fig1:Icositetrahedral (24-face polyhedral) Clenshaw-Curtis grid.

**References:**

[1] Hotta and Ujiie (2018) *QJRMS*. **144**:1382–1397 https://doi.org/10.1002/qj.3282

[2] Clenshaw and Curtis (1960) *Numerische Mathematik*, **2**:197–205.

[3] Williamson *et al*. (1992) *J. Comput. Phys*., **102(88)**:211–224.

[4] Galewsky *et al*. (2004) *Tellus*, **56A**:429–440.

[5] Jablonowski and Williamson (2006) *QJRMS*, **132**:2943–2975.

O3.5

# Coupling isobaric physics with isochoric dynamics

Kohei Kawano
Numerical Prediction Division, Japan Meteorological Agency
Email: k_kawano@met.kishou.go.jp

## Abstract

A regional nonhydrostatic model of the Japan Meteorological Agency employs constant height-based coordinate. The model couples physical processes that used to be adopted by the former operational models with hydrostatic assumption and pressure-based vertical coordinate. In converting tendencies evaluated by physics to those of prognostic variables of the dynamical core, differences of some assumptions between the dynamics and the physics have to be taken into account. Because the dynamical core adopts the finite volume method and employs total density as a prognostic variable, it is the simplest way to assume that total density in each cell is kept constant. With this coupling method, latent heat released by the microphysics process makes the pressure increased in constant volume cells, and then the local high pressure is mitigated through the following dynamics steps, which often causes acoustic waves. Since this representation of the process seems to be unrealistic, we are exploring a new way to consider the difference of assumption between the isochoric dynamics and the isobaric physics in the coupling.

A new coupling way which incorporates the change of cell volume in physical processes is tested. In the new experimental coupling, when the dynamics receives tendency $d\theta$ from physics in a cell in which condensation is occurred, tendency $d\rho$ is diagnosed assuming that pressure in the cell is kept constant. Then the change of cell volume is also diagnosed from the tendency $d\rho$, with simple assumption that the cell expands only in upward at same column. Considering the change of each cell volume in a column, total mass in a column is redistributed to each cell. Through the idealized warm-bubble test, it has been confirmed that the experimental coupling can keep the representation of essential features of rising warm-bubble and suppress acoustic noises which are seen in the test with the current coupling.

In the presentation, we will talk about details of the new experimental coupling and some test results.

# Poster sessions

## P1-P10 November 14, 2018 (Wednesday)
## P11-21 November 15, 2018 (Thursday)

P1

# Establishment of MRV system of greenhouse gas emission from Asian rice paddies by integrating multi-type satellite data and ground flux data

Hironori Arai[1,3], Wataru Takeuchi[1], Kei Oyoshi[2], Lam Dao Nguyen[4], Towa Tachibana[5], Ryuta Uozumi[6], Koji Terasaki[3], Hisashi Yashiro[3], Takemasa Miyoshi[3], Kazuyuki Inubushi[7]

1. Institute of Industrial Science, the University of Tokyo, Japan
2. Earth Observation Research Center, Japan Aerospace Exploration Agency, Japan
3. Advanced Institute for Computational Science, RIKEN, Japan
4. Ho Chi Minh Space Technology Application Center, Vietnam National Space Center, Vietnam
5. Faculty of Law, Politics and Economics, Chiba University, Japan
6. Uozumi Sustainability Research Institute, Japan
7. Graduate School of Horticulture, Chiba University, Japan

Email: hiroarai@iis-u.tokyo.ac.jp

## Abstract

Greenhouse gas (GHG) emission observation/reduction technologies are attracting greater deal of attention from policy makers to achieve Sustainable Development Goals. In terms of GHG accounting, Monitoring, Reporting and Verification (MRV) systems have become significantly important for the countries which ratified Paris Agreement by promising Intended Nationally Determined Contributions (INDC). Not only evaluation of the amount of GHG emitted from the countries, but also the mitigation's effect and its dissemination status need to be monitored by the policy makers. In this regard, the societies require the MRV systems with transparency and high cost-performance.

To address such concern, the authors are building an efficient/transparent MRV system in a tropical rice cropping system based on satellite remote sensing data. We are developing a long-term consistent bottom-up approaching method with high spatio-temporal resolution, based on the Japanese earth observation technology (e.g., ALOS-2, AMSR-E/2, GCOM-C). In order to validate the outputs from the bottom-up approaching method, Now we are also challenging to build an independent top-down approaching method based on the other satellites data (GOSAT,SCIAMACHY,AIRS) using NICAM-LETKF with 1way-multivariate variable localization, which can estimate the surface fluxes without requiring any direct observation or a-priori information of the fluxes with K-computer. In this presentation, we would like to discuss the development plan and expected integration with further cross-disciplinary studies.

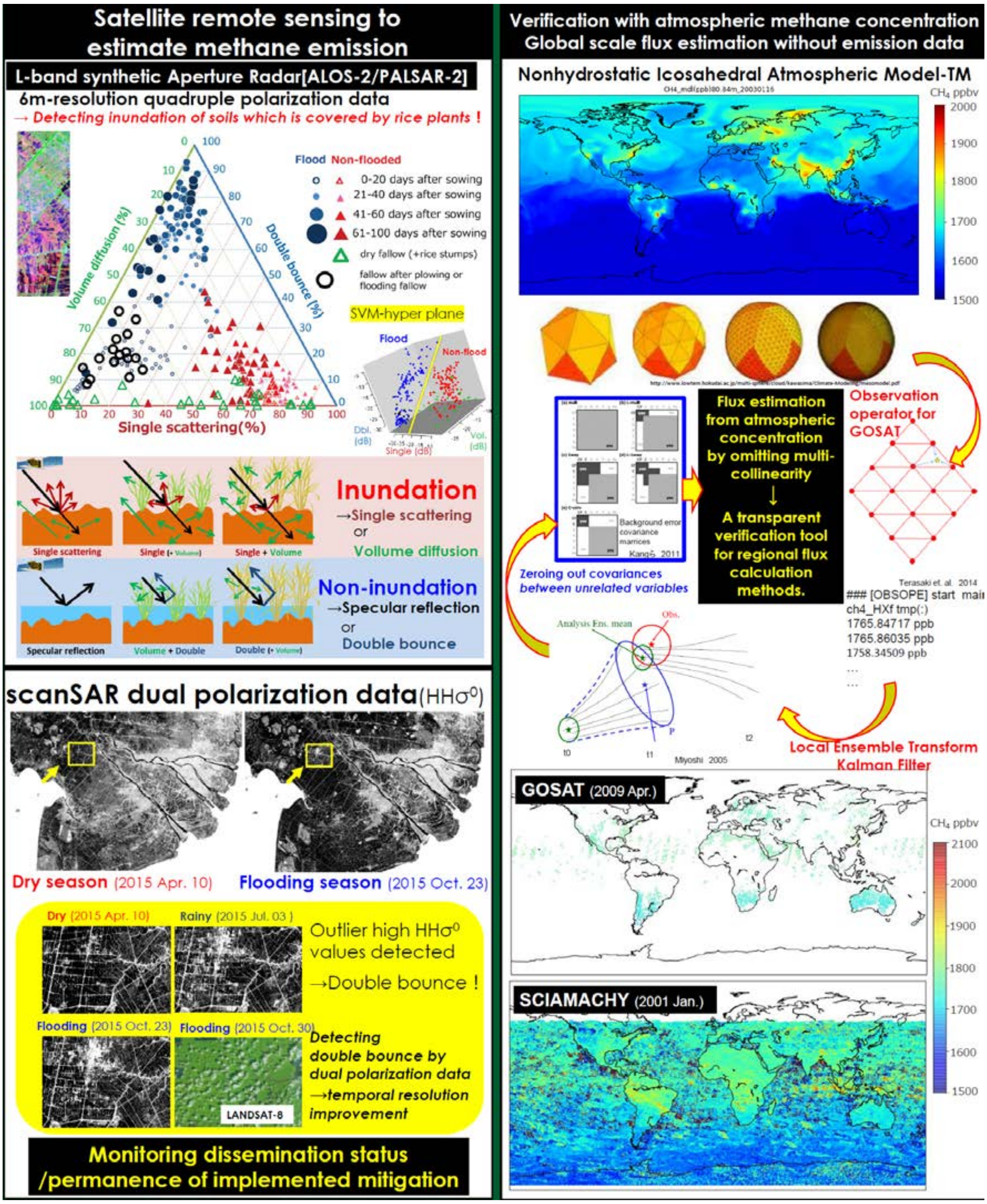


Japanese satellite based methane emission status evaluation methods. Left figure presents bottoming up approach method with ALOS-2 evaluating soil inundation status which controls methane emission. Right figure shows the top down approach method with GOSAT and NICAM-TM-LETKF using K computer.

P2

# Forecast skill of intraseasonal oscillation events over the Maritime Continent in a global cloud-system-resolving model

Tomoe Nasuno[1], Masuo Nakano[1], Kazuyoshi Kikuchi[2], Tim Li[2], Mio Matsueda[3]

1. Japan Agency for Marine-Earth Science and Technology, Japan

2. International Pacific Research Center, University of Hawaii, USA

3. University of Tsukuba, Japan

Email: nasuno@jamstec.go.jp

## Abstract

Forecast skill of the intraseaonal oscillation (ISO) events in Nonhydrostatic Icosahedral Atmospheric Model (NICAM [1]) simulations during the Years of the Maritime Continent (YMC) JAMSTEC field campaign period [2] is evaluated in comparison with observations, analysis, and operational forecasts. We aim to understand what is important to realistically simulate the ISO event, by specifying reasons for higher and lower skill simulation cases.

Global 14-km (7-km) mesh 30-day (14-day) long near real-time forecasts were run on daily basis during the 2015 (2017) campaign period from November to January next year. The initial condition for the forecasts were interpolated using 1.0° x 1.0° gridded NCEP final analysis [3], and sea surface temperature was given by the daily climatology plus initial anomaly.

During the 2015 campaign under a peak El Nino condition, convection was stagnant over the Indian Ocean, but a robust ISO event developed in mid-December and crossed over the Maritime Continent (MC) keeping its magnitude. During the 2017 campaign under a La Nina condition, convection was generally active over the MC and ISO signals were less distinct than in 2015. A moderate ISO developed in late November.

The ISO simulation for the 2015 case tended to be disrupted by dry environment over the MC. The good cases successfully simulated the large-scale circulation and the southward path of convective envelope over the ocean surrounding the MC, whereas the poor cases missed the large-scale circulation and quick eastward shift of convection without significant development along an equatorial path. These are supportive of the

arguments in previous studies. As to the 2017 ISO case, the model captured the amplification of the event but with a tendency of overdevelopment, which was opposite to operational forecasts. We speculate that the erroneous ISO behavior was related to the mean biases of stronger lower tropospheric westerlies to the east (west) of the MC in 2015 (2017), which induce stronger convergence and moistening further to the east of (over) the MC through non-linear effects. The mean bias suggests a tendency of excessively strong coupling between convection and circulation in the model. It is suggested that adequate strength of coupling between convection and circulation was important to the successful simulation of the ISO.

**References:**

[1] Satoh, M., H. Tomita, H. Yashiro, H. Miura, C. Kodama, T. Seiki, A. T. Noda, Y. Yamada, D. Goto, M. Sawada, T. Miyoshi, Y. Niwa, M. Hara, T. Ohno, S. Iga, T. Arakawa, T. Inoue and H. Kubokawa: The Non-hydrostatic Icosahedral Atmospheric Model: description and development. *Progress in Earth and Planetary Science* 2014, **1**:18. doi: 10.1186/s40645-014-0018-1

[2] YMC web (http://www.jamstec.go.jp/ymc/index.html)

[3] The data is provided by the Data Support Section of the Computational and Information Systems Laboratory at the National Center for Atmospheric Research in Boulder, Colorado. (https://rda.ucar.edu/datasets/ds083.2/)

P3

# Continental-scale simulation of diurnal variations in South Asian summer monsoon: Insights from the explicit and parameterized convection experiments

Rakesh Teja Konduru[1] and Hiroshi G. Takahashi[1]

[1]Department of Geography, Tokyo Metropolitan University, 1-1 Minami-Osawa, Hachioji, Tokyo, 192-0397, Japan.

Email:- konduru-rakeshteja@ed.tmu.ac.jp

## 1. *Introduction*

In South Asian Summer Monsoon (SASM), Indian summer monsoon (ISM) is a most crucial season in the annual cycle over the south Asian region, with 80% of the annual precipitation received during ISM (Jain and Kumar, 2012). Gadgil *et al.* (2003) stated that the simulation and prediction of ISM on all scales could be improved. It is requisite to understand the significance of deep convection in the tropics. The representation of such convection in the climate models is a chief source of miscalculation (Sherwood *et al.* 2014). Palmer *et al.* (2007) Showed that the errors in the convection simulation in climate models are due to miss-representation of small-scale processes in convection like diurnal cycle etc. by a physical process. In connection with Indian summer monsoon, the diurnal cycle of convection is the fundamental mode of variability controlled by the solar insolation. Therefore, it is essential for proper simulation of diurnal scale processes in either regional climate models or global climate models (Prein *et al.* 2015; Takahashi *et al.* 2016). In this study, a sensitivity of the diurnal cycle of precipitation to with and without convection parameterized simulations and with variable model resolutions is evaluated.

## 2. *Numerical setup and analysis*

A suite of three ensemble experiments conducted at different spatial resolutions (25km, 12.5km, and 6.25km), with (convection on, CON) and without cumulus parameterization scheme (convection off, COFF). These continental scale simulations forced by Era-interim six hourly datasets for a period April 1 to October 31. The evaluation performed on peak south Asian summer monsoon season (July-August) and, compared with Tropical Rainfall Measuring Mission (TRMM) three hourly datasets. Harmonic analysis is implemented to assess model simulated diurnal cycle with TRMM precipitation dataset. COFF simulations were performed to know the sensitivity of convection off on diurnal cycle as compared to the utilization of convection parameterization scheme.

## 3. *Results and discussion*

Simulated precipitation shows that COFF simulations added value in the representation of precipitation diurnal maxima and diurnal phase. Over core monsoon region, the diurnal peak of precipitation is realized around afternoon or later afternoon in COFF simulations especially at 6.25km (fig 1). However, in CON experiments diurnal peak is seen 3-6 hours earlier around noon/afternoon. It is also clear that the fine model resolution does not show any notable improvements in the diurnal cycle

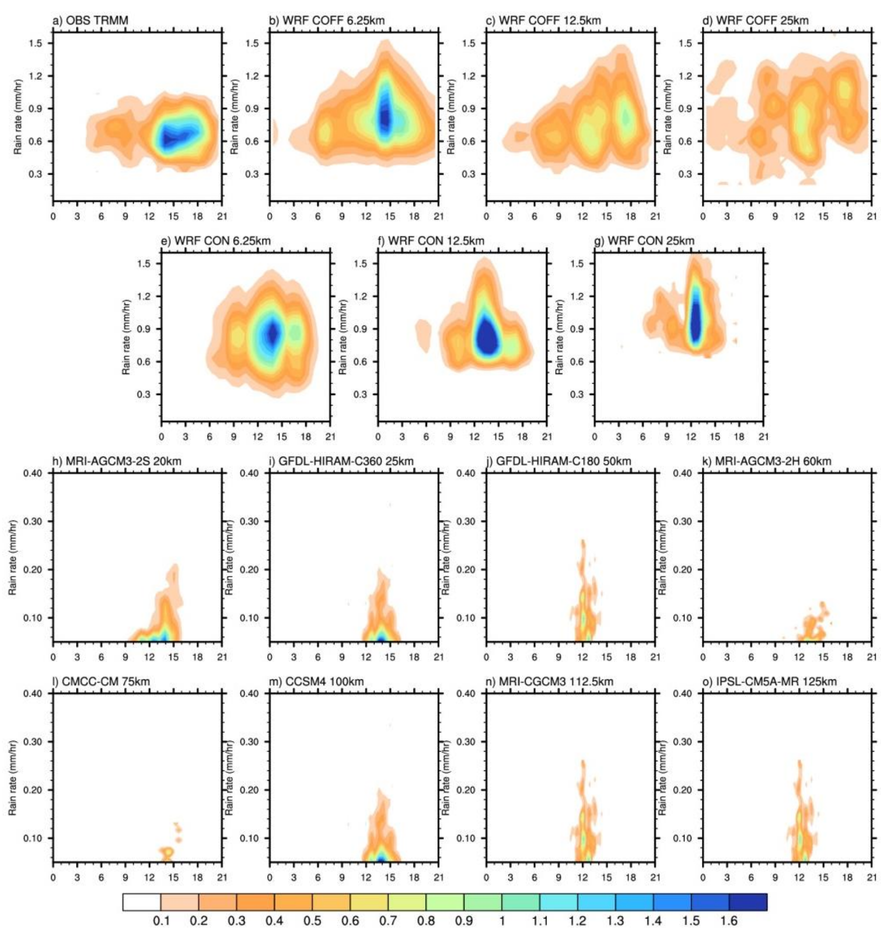


**Figure 1:-** Joint Probability distribution calculated for diurnal cycle of precipitation with TRMM, WRF simulations and for AMIP models.

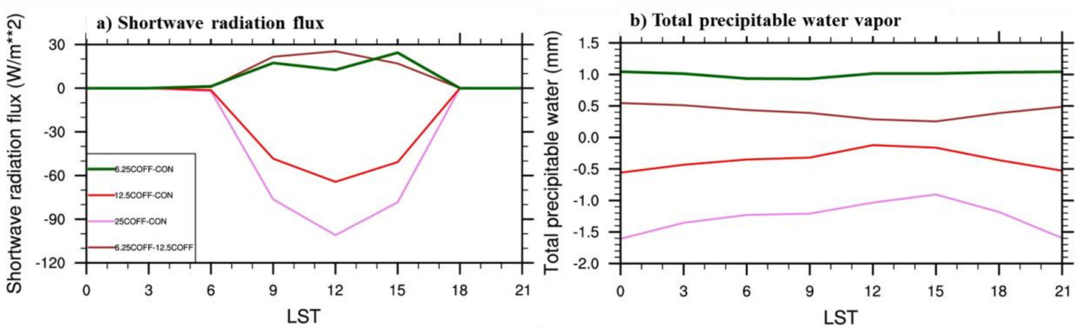


**Figure 2**:- It shows COFF minus CON diurnal cycle at 6.25km (green), 12.5km (red), and 25km (magenta) respectively. Brown color line shows difference between 6.25km COFF and 12.5km COFF.

phase and magnitude of precipitation. The diurnal cycle of precipitation in eight CMIP AGCM models as well failed to simulate the afternoon/late afternoon precipitation over Indian land region during ISM, except MRI-AGCM3-2S 20km model with afternoon diurnal precipitation peak.

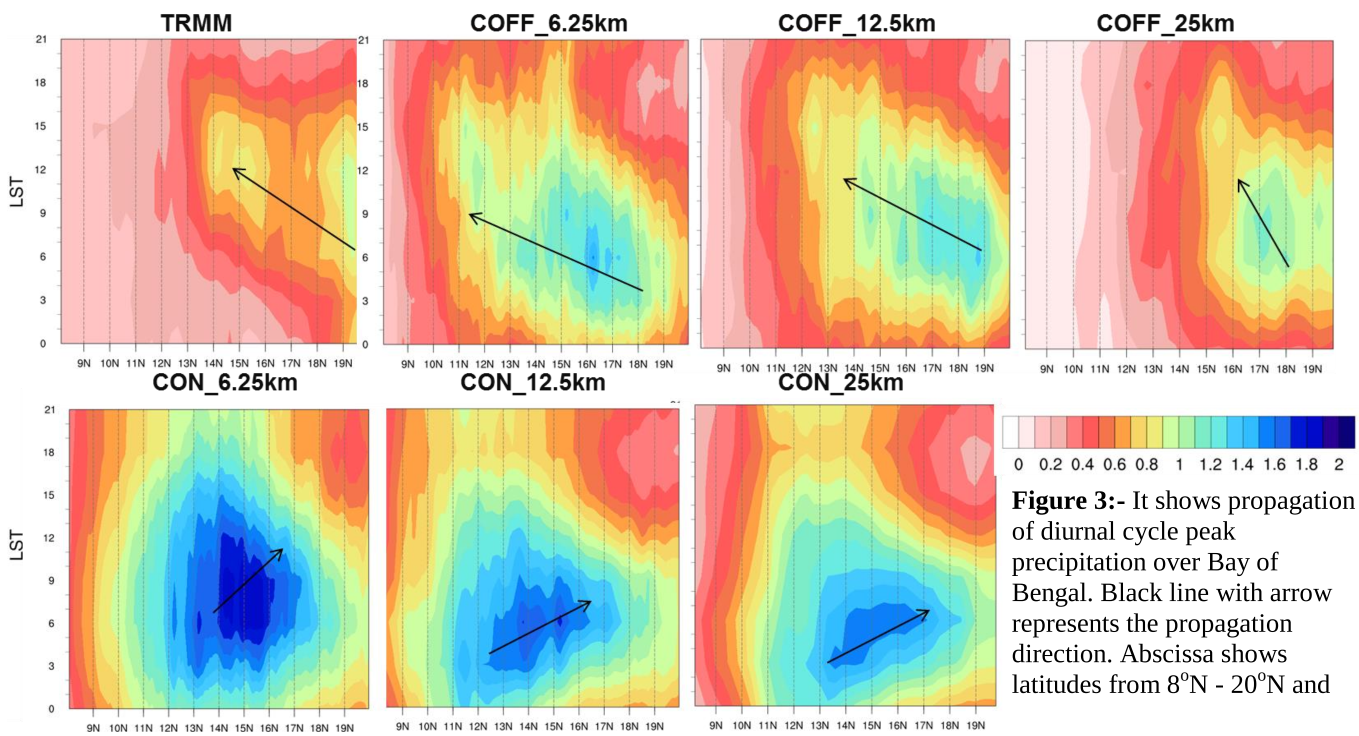


**Figure 3:-** It shows propagation of diurnal cycle peak precipitation over Bay of Bengal. Black line with arrow represents the propagation direction. Abscissa shows latitudes from 8°N - 20°N and

Over Indian land region, in explicit simulations (fig 2), higher solar insolation increased the surface air temperature, which deepened the monsoon trough. As a result, moisture transport to the land from ocean amplified the amount of available water vapor, and availability of sufficiently higher convective available potential energy triggered convection in the late afternoon. Nevertheless, this late afternoon convection is absent in convection parameterized simulations. On the other hand, over ocean regions like the Bay of Bengal, exhibits two diurnal peaks in the observations during early morning and afternoons, this is evident only in the COFF experiments. Besides, the southward propagation of the diurnal peak precipitation is convincingly captured over the Bay of Bengal in the explicit simulations (fig 3). However, in the convection-parameterized experiments, northward propagation of the diurnal peak precipitation simulated over the Bay of Bengal, which is not realistic. This southward propagation of diurnal peak of precipitation in COFF is associated with the mesoscale convective systems that form over North Bay of Bengal in the early morning time and propagate by afternoon to the south of Bay of Bengal. This improvement in the explicit simulations regarding southward propagation of the diurnal peak over the ocean was due to the presence of a southward component of wind at the 600 hPa; this component is no simulated in the CON experiments. These results outline the prominence of the explicit or modified convection schemes in the models to represent a realistic diurnal cycle of precipitation in Indian summer monsoon, which could simulate monsoon-related precipitation variability accurately

### 4. *References*


Sugimoto, S. *et al*., 2016: Effect of spatial resolution and cumulus parameterization on simulated precipitation over south Asia. *SOLA*, **12A**, 7-12.

Prein et al., 2015: A review on regional convection-permitting climate modeling demonstration, prospects and challenges. *Rev. Geophys*., **53,** 323-361.

P4

# An oceanic impact of the Kuroshio path on snowfall on the Kanto region of Japan in the cold season

Takuya Yamazaki [1], Hiroshi G. Takahashi [1,2]

1. Laboratory of Climatology, Tokyo Metropolitan University, Japan

2. Japan Agency for Marine-Earth Science and Technology, Japan

Email: yamazaki-takuya1@ed.tmu.ac.jp

## Abstract

Over the Kanto region of Honshu Island, Japan, in the northern fall, winter and spring the Japanese southern-coastal cyclones (extra-tropical cyclone) sometimes bring heavy rainfall and snowfall. These heavy rainfall and snowfall events induce traffic problem in the Kanto region of Japan. Previous researches showed that the two types of Kuroshio path (i.e., large meander and non-large meander paths) have a different impact on southern-coastal cyclone activity and snowfall in Tokyo (Nakamura et al. 2012 and Hayasaki et al. 2013). However, a relationship between the Kuroshio path and snowfall in the Kanto region is still unclear.

To understand an impact of Kuroshio path south of the Pacific coast of Japan during winter on heavy rainfall and snowfall on the Kanto region, this study conducted 5-km resolution experiments by a non-hydrostatic regional model ARW-WRF (Skamarock et al. 2008). A control simulations (CTL) driven by ERA-Interim reanalysis data and the monthly National Oceanic and Atmospheric Administration Optimum Interpolation sea surface temperature (SST) dataset was performed. We focus on a severe snowfall event in February 7$^{th}$ and 8$^{th}$, 2014. In this case, the SST pattern is similar to that during the large meander path. We conducted 9-member ensemble experiments with the different initial time (00UTC February 1st, 06UTC, 12UTC, 18UTC, 00UTC February 2nd, 06UTC, 12UTC, 18UTC, 00UTC February 3rd). In addition, a series of Kuroshio non-large meander experiments (NLM) was performed. The numerical design of NLM experiments was the same as that of CTL, except that SST over the whole domain was replaced by the SST values in 2012. 2012 was not the large meander period of the Kuroshio. The difference between these two simulation sets is analyzed to determine the sensitivity of surface temperature and snowfall in the Kanto region to the SST difference.

Results showed that the CTL simulations represented spatial and temporal variations

in surface temperature well, yielding realistic surface temperature values with observations (not shown). In addition, the location and strength of the simulated extra-tropical cyclones are basically reproduced in both CTL and NLM experiments, which implies that there is no distinct modifications of the extra-tropical cyclone due to the SST changes.

The prescribed SST values south and east of the Kanto region are warmer in the NLM experiments, compared with those in the CTL experiments. As the result of sensitivity experiments, surface air temperature at Tokyo in the NLM experiments tends to be higher than that in the CTL experiments during almost snowfall period. We will discuss the changes in rainfall and snowfall.

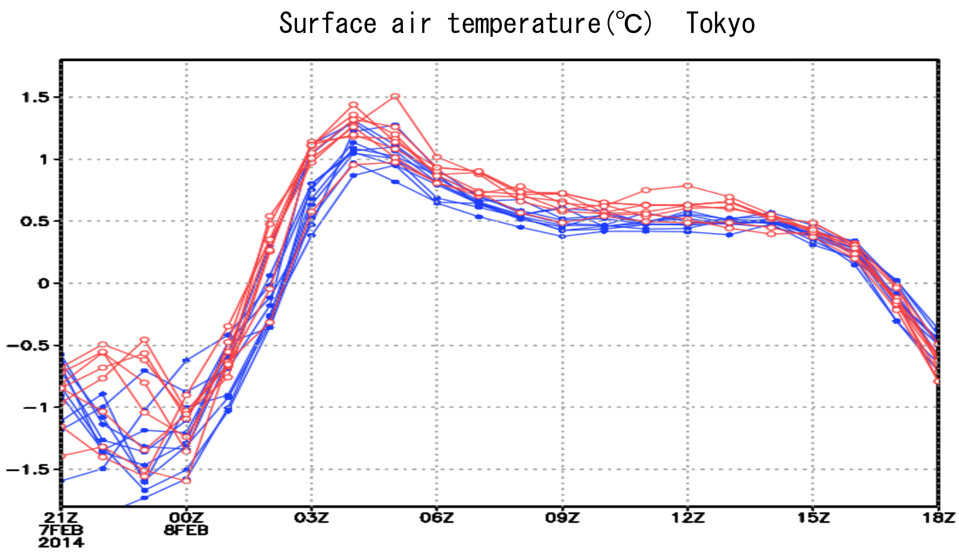


Figure. 1: Time-series of the simulated surface air temperature at Tokyo during the snowfall period from 21UTC February 7th 2014 to 18UTC Feb 8th 2014. 9 blue lines indicate CTL experiment. 9 red circles denote NLM experiments.

## References:

Skamarock, W, C., Klemp, J, B., Dudhia, J., Gill, D, O., Barker, D, M., Duda, M, G., Huang, X., Wang, W., Powers, J, G.: A description of the Advanced Research WRF Version 3, *NCAR Tech. Note* , NCAR/TN-475+STR, 1 pp, 2008.

Hayasaki, M., Kawamura, R., Mori, M., & Watanabe, M: Response of extratropical cyclone activity to the Kuroshio large meander in northern winter. *Geophysical Research Letters*, 2013, 40.11: 2851-2855.

Nakamura, H., Nishina, A., & Minobe, S: Response of storm tracks to bimodal Kuroshio path states south of Japan. *Journal of Climate* 2012 , 25(21), 7772-7779.

P5

# Sensitivity of coastal front simulation to thermal diffusivity in the PBL scheme

Kento Suzuki[1], Takeshi Yamazaki[1], Toshiki Iwasaki[1]

1. Department of Atmospheric Science, Graduate school of Science, Tohoku University

## Abstract

1. Introduction

"A coastal front is defined as a local front between warm air associated with an onshore wind and colder air trapped inland." "Coastal fronts are often formed over Kanto plain, an exposed region to southerly onshore winds during late autumn to winter season." [1] The forecasting of such phenomena is challenging at times. Furthermore, the numerical simulation of coastal front location over Kanto plain is frequently biased northward (inland) [2]. To our current knowledge, the cause of such bias is unknown. It could be due to grid size, physics parameterizations or other factors and needs further investigation. In this experiment, we focus on Planetary Boundary Layer (PBL) process under stable conditions. We conducted a case study on the sensitivity of coastal front simulation to thermal diffusivity.

2. Overview of Case Study

This case study is based during an extratropical cyclone (ex-TC) event that took place on 8$^{th}$ and 9$^{th}$ of March, 2018. An ex-TC passed over Sea of Japan while a coastal front was formed due to a warm southerly onshore wind interacting with colder air mass from the mountainous region.

3. Model configuration

We used JMA-NHM (Saito, et.al 2006) in this experiment. We conducted 250m grid scale simulation (including Kanto region) and used Deardorff [3][4] in the PBL scheme. Under stable condition ($d\theta_l/dz > 7K/km$), we applied the following; (1) constant thermal diffusivity (Ctl-Experiment), (2) thermal diffusivity reduced by a factor of 10 (S-Experiment) and (3) thermal diffusivity increased by a factor of 10 (L-Experiment).

4. Result

In figure 1 (middle), Ctl-Experiment shows that coastal front was formed over Kanto region, however, it was biased inland as compared to real observation. In figure 1 (right), the coastal front moved slightly south-eastward in S-Experiment. It is also observed that the coastal front moved slightly north-westward in L-experiment. This indicates that the thermal diffusivity affects vertical heat transport, which in turn affects the strength of cold air mass trapped inland. Nevertheless, the displacement of coastal front is relatively small compared to the bias between observation and Ctl-Experiment.

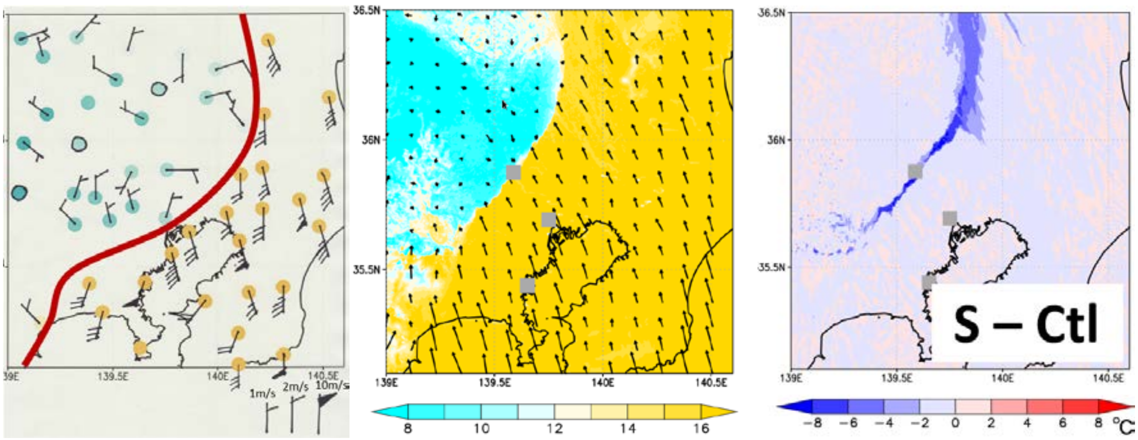


Figure 1. (left) Observed surface temperature and wind, (middle) simulated surface temperature and wind of Ctl-experiment, (right) simulated surface temperature anomaly between Ctl and S-experiment. Every figure is at 3:00, 9th March, 2018

5. Conclusion

The location of coastal front is not sensitive to thermal diffusivity as per this case study. It is insufficient to suggest that the bias in coastal front location is caused by the initial condition error or systematic error in the model. However, sensitivity to the thermal diffusivity may have relation with grid size, thus, future work is needed.

[References]

[1] Fumiaki Fujibe : Climatology of the Coastal Front in the Kanto Plain. *Papers in Meteorology and Geophysics Vol.41, No3, pp. 105-128, September 1990*

[2] Tokyo Aviation Weather Service Center, *WEATHER TOPICS Vol.*38, *May 2014*

[3] James W. Deardorff : Stratocumulus-capped mixed layers derived from a three-dimensional model. *Bound.-Layer Meteor*, ***18****, 495-527, 1980*

[4] JMA, Forecast Department, *Reports of Numerical Simulation, Vol.54 pp. 117-148, 2008*

P6

# Data assimilation and forecast experiments for the record-breaking rainfall event in Japan in July 2018 with NICAM-LETKF at 112-km and 28-km resolution

Koji Terasaki[1] and Takemasa Miyoshi[1,2,3,4,5]

[1]*RIKEN Center for Computational Science, Kobe, Japan*
[2]*RIKEN Interdisciplinary Theoretical and Mathematical Sciences Program, Kobe, Japan*
[3]*Prediction Science Laboratory, RIKEN Cluster for Pioneering Research, Kobe, Japan*
[4]*University of Maryland, College Park, Maryland, USA*
[5]*Japan Agency for Marine–Earth Science and Technology, Yokohama, Japan*

Email: koji.terasaki@riken.jp

## Abstract

In July 2018, the active Baiu front caused record-breaking rainfalls and disasters in broad areas in western Japan (Figure 1a). Total precipitation exceeded 1000 mm in some areas. This study performs data assimilation and forecast experiments using the NICAM-LETKF system (Terasaki et al. 2015, Terasaki et al. 2017) at 112-km and 28-km resolution with 32 ensemble members. We apply the relaxation to prior spread with a fixed parameter ($\alpha = 0.95$) for both resolution, although the parameter was manually tuned with only 112-km resolution by Kotsuki et al. (2017). We assimilated conventional observations and advanced microwave sounding unit-A (AMSU-A) radiances. We conducted data assimilation cycles for one month starting at 0000 UTC 10 June 2018 for both experiments. Also, we performed forecast experiments from different five initial conditions every day from 0000 UTC 1 July 2018 for both experiments.

Figures 1b and 1c show 6-hour accumulated precipitation from 1200 UTC 6 July 2018 to 1800 UTC 6 July 2018 (36 to 42 hours forecasts) for 112-km and 28-km forecast experiments, respectively, initialized at 0000 UTC 5 July 2018. JMA's radar observed the heavy rainfalls along the Baiu front extending from southwest to northeast in western Japan (Figure 1a). The 28-

km resolution experiment outperforms the 112-km resolution experiment for the location and intensity of the heavy rainfall, while forecasted precipitation is much less than the observation. The 112-km experiment also successfully reproduces the heavy rain by the Baiu front; however, the location is shifted northward compared with the observation and 28-km experiment. The locations of the Pacific and Okhotsk highs determine the location of the Baiu front. The 112-km resolution may be too course to resolve these phenomena sufficiently.

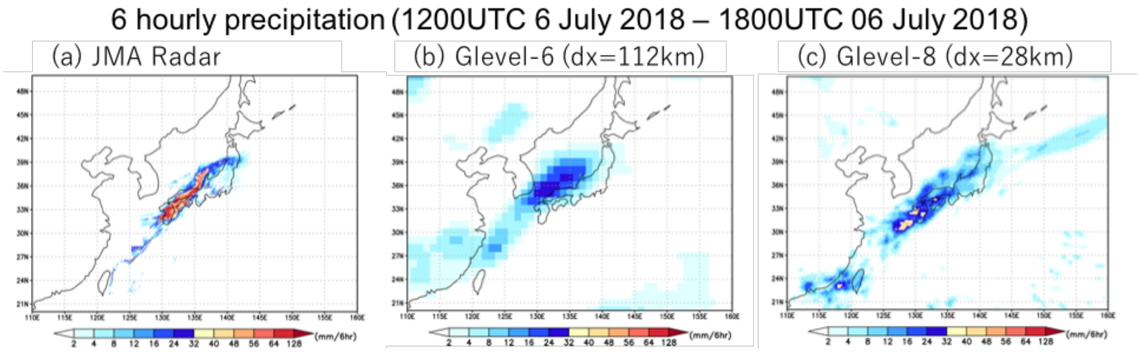


Fig. 1 6-hour accumulated precipitation from 1200 UTC 06 July 2018 to 1800 UTC 06 July 2018 . (a) JMA radar, (b) 112-km experiment, and (c) 28-km experiment, respectively. Initial time of the forecast experiments (b, c) is 0000 UTC 05 July 2018.

**References:**


Kotsuki, S., Y. Ota, and T. Miyoshi, 2017: Adaptive covariance relaxation methods for ensemble data assimilation: Experiments in the real atmosphere, *Quart. J. Roy. Meteor. Soc.*, **143**, 2001–2015, doi:10.1002/qj.3060.

Terasaki, K., M. Sawada, and T. Miyoshi, 2015: Local Ensemble Transform Kalman Filter Experiments with the Nonhydrostatic Icosahedral Atmospheric Model NICAM. *SOLA*, **11**, 23-26. doi:10.2151/sola.2015-006

Terasaki, K., and T. Miyoshi, 2017: Assimilating Advanced Microwave Sounding Unit-A Satellite Radiances with the NICAM-LETKF. *J. Meteorol. Soc. J.*, **95**, 433-446. Doi:10.2151/jmsj.2017-028.

P7

# Data Assimilation Experiments with Himawari-8 Optimal Cloud Analysis (OCA) Products

Michiko Otsuak[1], Hiromu Seko[1,2], Masahiro Hayashi[1], Ko Koizumi[1]

1.Meteorological Research Institute, Japan Meteorological Agency, Japan

2. Japan Agency for Marine-Earth Science and Technology, Japan

Email: motsuka@mri-jma.go.jp

## Abstract

The OCA is an algorithm used to extract the cloud parameters such as phase, cloud top pressure (CTP), cloud optical thickness (COT), and effective radius using an optimal estimation method (EUMETSAT 2011). Hayashi (2016) developed the OCA retrieval scheme using all the AHI (Advanced Himawari Imager) spectral measurement and evaluated them in comparison with A-train data sets and showed they were of sufficiently good quality. Himawari-8 OCA products can provide useful information on water vapor in the form of clouds with good horizontal resolution (0.02 degrees) and coverage including over the ocean. Our main purpose is to exploit them in mesoscale data assimilation and to improve initial conditions for short range forecasts of precipitation.

Cloud occurrence matchups against surface observation and sonde observations indicated that OCA detected clouds better at high levels than at middle and low levels. Cloud layers inferred from sonde observations were determined using threshold values of relative humidity (RH) depending on heights (Zhang et al. 2010). Cloud fractions of OCA and surface observations were well correlated with a correlation coefficient of 0.78. Cloud types observed at surface observations overall corresponded with OCA COT and CTP values as described in ISCCP classification (Rossow and Schiffer 1991) in case of no overlapping cloud layers.

OCA data were assimilated as pseudo RH. While cloud top heights (CTH) were estimated by OCA, corresponding cloud base heights (CBH) were inferred by subtracting cloud geometric thickness (CGT) from CTH. For liquid clouds, CGT is obtained as the ratio between the liquid water path (LWP) and the cloud-averaged liquid water content (LWC). Where cloud layers were detected from CBH to CTH,

pseudo RH values were set around 90 % slightly varied with heights (Zhang et al. 2010). Only liquid clouds having COT below 50 and CTP below 440 hPa level were targeted for assimilation in order to avoid OCA data with large uncertainties in the presence of multilayered clouds or deep convections.

Assimilation experiments were conducted with JNoVA (JMA-NHM based variational analysis data assimilation) using pseudo RH derived from Himawari-8 OCA for a heavy rainfall event on 9 -10 Sep. 2015. In TEST experiment, the pseudo RH were assimilated for four forecast-analysis cycles of JNoVA (21:00 on $8^{\text{th}}$ to 09:00 UTC on $9^{\text{th}}$ ), during which one typhoon was passing over and another was approaching to Japan, together with other observational data used for operational JMA NWP. Only operational data were assimilated in CNTL experiment. The analyses after the four cycles of TEST showed significant increase in water vapor at low to middle levels where OCA pseudo RH were assimilated. The extended 39-h precipitation forecasts also showed differences in intensity and distribution of rainfalls from CNTL, suggesting a promising impact of OCA data.

**References:**


EUMETSAT: ATBD for optimal cloud analysis product. EUM/MTG/DOC/11/0654, 2011.

Hayashi, M.: Two-layer cloud retrieval using visible to infrared bands of Himawari-8. *EUMETSAT meteorological satellite conference 2016*.

Rossow, W. B. and R. A. Schiffer: ISCCP cloud data products. *Bull. Amer. Meteor. Soc.*, **72**, 1991, doi:10.1175/1520-0477(1991)072<0002:ICDP>2.0.CO;2.

Zhang, J., H. Chen, Z. Li, X. Fan, L. Peng, Y. Yu, and M. Cribb: Analysis of cloud layer structure in Shouxian, China using RS92 radiosonde aided by 95 GHz cloud radar. *J. Geophys. Res.*, **115**, 2010, doi:10.1029/2010JD014030.

P8

# Precipitation nowcasting with Phased-Array Weather Radar: a case of July 2018 record-breaking rainfall in Western Japan

Shigenori Otsuka[1,2], Marimo Ohhigashi[1], Yutaka Ishikawa[1], Shinsuke Satoh[3], and Takemasa Miyoshi[1,2,4,5,6]

1. RIKEN Center for Computational Science
2. RIKEN Interdisciplinary Theoretical and Mathematical Science Program
3. National Institute of Information and Communications Technology
4. RIKEN Cluster for Pioneering Research
5. University of Maryland
6. Japan Agency for Marine-Earth Science and Technology

Email: shigenori.otsuka@riken.jp

## Abstract

The Phased-Array Weather Radar (PAWR) can observe the whole sky much more frequently and densely than the conventional parabolic-antenna radars. At RIKEN we have been operating an optical-flow-based precipitation nowcasting system in real time with a PAWR since July 2017 (Otsuka et al. 2016).

On 4-7 July 2018, a Baiu front caused torrential rains in Kansai area, Japan. During this period, a PAWR installed at Kobe Branch of the National Institute of Information and Communications Technology successfully captured details of the rain system, and our three-dimensional precipitation nowcasting system produced 30-second-update 10-minute predictions at 250-m resolution. Figure 1 shows an example of 5-minute nowcast initialized at 14:21:30 JST 6 July 2018. The motion of a convective rain band embedded in a widespread stratiform rain area is captured well by the nowcast. At the same time, small-scale structures such as each convective cell in the rain band changes rapidly in the observations. Figure 2 shows the mean threat scores as a function of forecast time for 1000-1500 JST 6 July 2018. The nowcast clearly outperforms the Eulerian persistence forecasts at the two thresholds of 10 and 30 mm/h.

In this presentation we will show preliminary analyses on the structure of observed rain systems during this event.

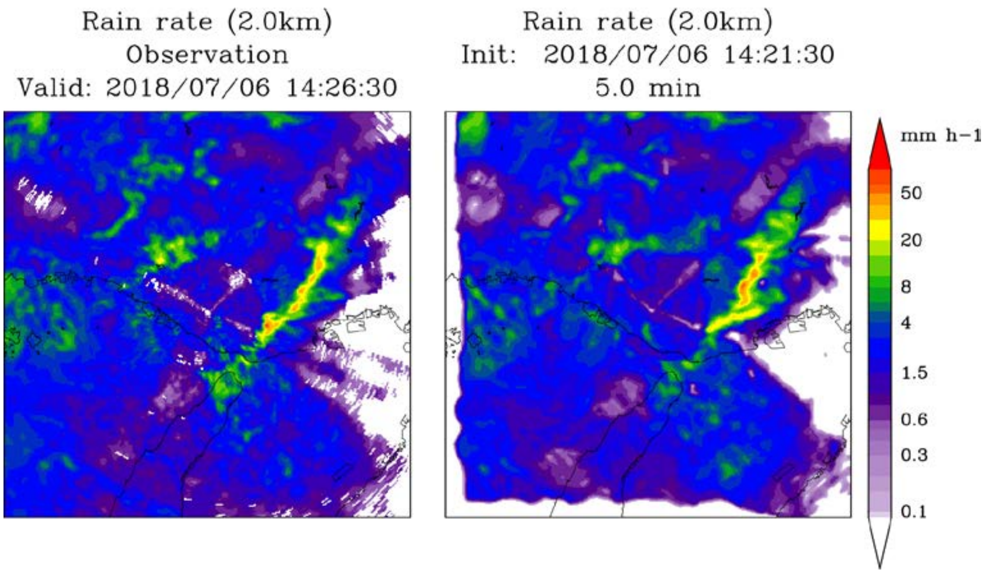


Fig. 1: (left) Kobe PAWR rain rate at the 2 km altitude at 14:26:30 JST 6 July 2018. (right) Corresponding five-minute nowcast initialized at 14:21:30 JST.

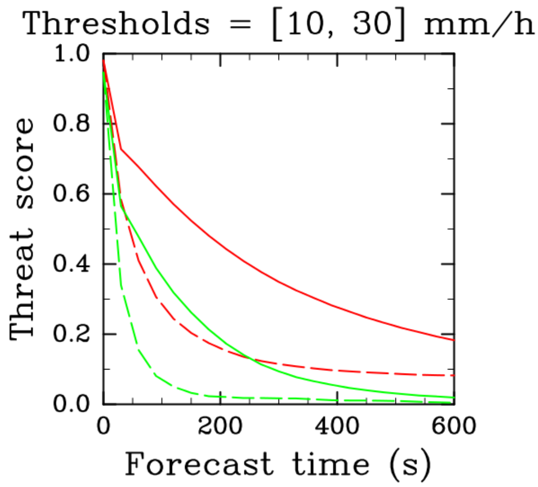


Fig. 2: Mean threat scores as a function of forecast time for 1000-1500 JST 6 July 2018. The solid lines show the nowcasts, and the dashed lines show Eulerian persistence forecasts. Red: 10 mm/h, green: 30 mm/h.

**References:**


Otsuka, S., G. Tuerhong, R. Kikuchi, Y. Kitano, Y. Taniguchi, J. J. Ruiz, S. Satoh, T. Ushio, and T. Miyoshi, 2016: Precipitation nowcasting with three-dimensional space-time extrapolation of dense and frequent phased-array weather radar observations. *Wea. Forecasting*, **31**, 329-340. doi: 10.1175/WAF-D-15-0063.1.

P9

# Assimilating every 30-second phased array weather radar data in a torrential rainfall event on July 6, 2018 around Kobe city

Yasumitsu Maejima[1], Shigenori Otsuka[1] and Takemasa Miyoshi[1, 2, 3]

1. RIKEN, Center for Computational Science
2. University of Maryland, College Park
3. Japan Agency for Marine-Earth Science and Technology

## Abstract

To investigate the impact of every 30-second phased array weather radar (PAWR; Yoshikawa et al. 2013, Ushio et al. 2014) observation on a simulation of a severe rainfall event occurred on July 6, 2018 around Kobe city, we perform 30-second-update 100-m-mesh data assimilation (DA) experiments using the Local Ensemble Transform Kalman Filter (LETKF; Hunt et al. 2007) with the Scalable Computing for Advanced Library and Environment (SCALE; Nishizawa et al. 2015) regional numerical weather prediction model. Two experiments were performed: the test experiment with every 30-second PAWR observation (TEST), and the other without observation (NO-DA).

Figure 1 shows radar reflectivity at the 2-km elevation at 1040 JST on July 6, 2018 after 50 LETKF cycles. The TEST analysis shows intense rainfalls with detailed structure of active convection, better matching with the PAWR observation compared to NO-DA analysis (Fig. 1).

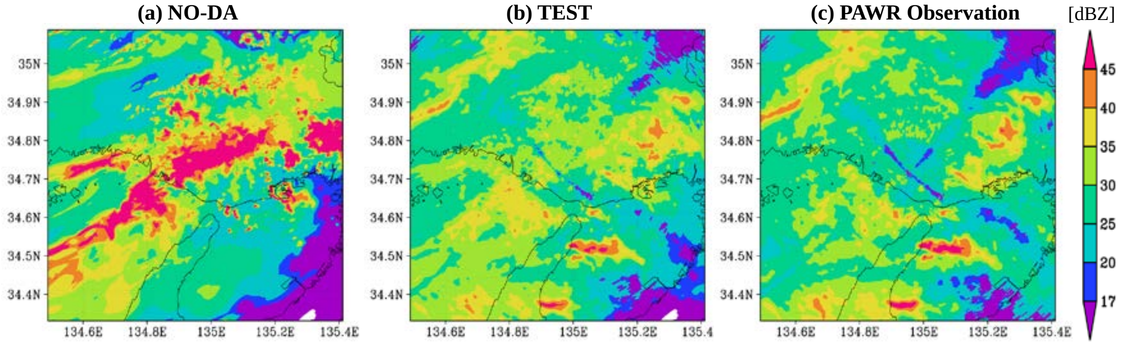


Fig.1: Radar reflectivity at the 2-km elevation at 1040 JST on July 6, 2018 after 50 LETKF cycles for (a) NO-DA analysis, (b) TEST analysis and (c) PAWR observation.

Figure 2 shows the time series of the root mean squared error (RMSE) of radar reflectivity at the 2-km elevation. The black and blue lines show the ensemble mean of the analysis of NO-DA and TEST, respectively. Consistently with Fig. 1, TEST analysis is clearly better than NO-DA analysis. The red line shows a forecast initialized by the ensemble mean of the TEST analysis at 1040 JST. Compared with NO-DA, the forecast is skillful for 20 minutes, although the skill is decreased rapidly. The results suggest that the PAWR DA have a potential to improve the numerical simulation for this torrential rainfall event.

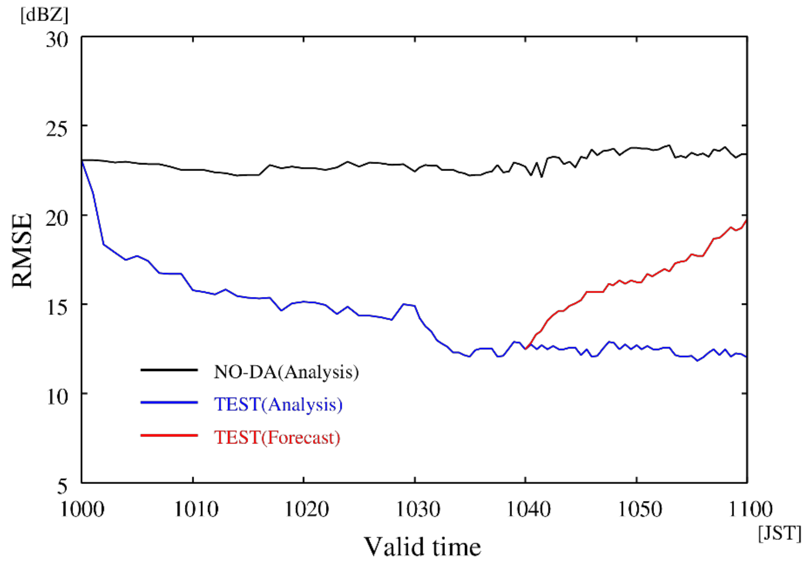


Fig. 2: Time series of RMSE for radar reflectivity [dBZ] at the 2-km elevation on July 6, 2018. Black, blue and red lines correspond to the NO-DA analysis, TEST analysis, and TEST forecast initialized at 1040 JST, respectively.

**References:**

Hunt, B. R., E. J. Kostelich, and I. Szunyogh, 2007: Efficient data assimilation for spatiotemporal chaos: A local ensemble transform Kalman filter. *Physica D*, **230**, 112–126.

Nishizawa, S., H. Yashiro, Y. Sato, Y. Miyamoto, and H. Tomita, 2015: Influence of grid aspect ratio on planetary boundary layer turbulence in large-eddy simulations. *Geosci. Model Dev.*, **8**, 3393−3419.

Ushio, T., T. Wu, and S. Yoshida, 2014: Review of recent progress in lightning and thunderstorm detection techniques in Asia. *Atmos. Res.*, **154,** 89–102.

Yoshikawa, E., T. Ushio, Z. Kawasaki, S. Yoshida, T. Morimoto, F. Mizutani, and W. Wada, 2013: MMSE beam forming on fast-scanning phased array weather radar. *IEEE Trans. Geosci. Remote Sens.*, **51**, 3077–3088.

P10

# Fine-scale Structure of Mesoscale-beta-scale vortices that caused tornado-like vortices

Eigo Tochimoto[1], Sho Yokota[2], Hiroshi Niino[1], Wataru Yanase[2]

1. Atmosphere and Ocean Research Institute, the University of Tokyo, Japan

2. Meteorological Resaerch Institute, Japan Meteorological Agency

Email: tochimoto@aori.u-tokyo.ac.jp

## Abstract

A sudden gusty winds caused by meso-$\beta$-scale vortex (MBV) of 30-50 km diameter occurred at the southwestern part of the Sea of Japan between 0300 and 0400 JST (Japan Standard Time; UTC+9 hour) on 1 September 2015. The MBV formed in the northeastern part of the center of extratropical cyclones. A C-band Doppler radar of Japan Meteorological Agency (JMA) detected spiral-shaped reflectivity patterns associated with the MBV. Couplet of positive and negative Doppler velocities exceeding 50 m s-1was observed near the center of the spiral-shaped reflectivity pattern. The observed convective system is not associated with a quasi-linear convective system nor pre-existing mesoscale convective complexes. Thus, to our knowledge, this kind of MBV and the associated strong gusty winds due to embedded tornado-like vortices over the oceans have not been reported previously, yet they can be a serious threat to marine traffic.

A triply-nested numerical simulation using JMA non-hydrostatic model was performed to clarify the fine structure and evolution of the MBVs that caused the damaging gusty winds. The simulations with the finest horizontal resolution of 50m and 100 vertical levels successfully reproduced the MBV with spiral-shaped precipitation systems and associated tornado-like vortices (TLVs) within the MBV. The simulated MBV had the maximum vertical vorticity near the surface. A vorticity budget analysis and a circulation analysis show that the near-surface vorticity of the MBV is strengthened by stretching of vertical vorticity associated with horizontal shear between northeasterly and southeasterly winds in the EC. TLVs with maximum vorticity exceeding 1 s-1grew and decayed repeatedly near the surface in the region of the horizontal shear. It is suggested that TLVs were generated and strengthened by the shear instability. The simulated maximum wind speed near the surface were about 50 m s-1, which is

comparable to Japanese Enhanced Fujita scale of 1~2.

Similar MBVs have been detected with radar observations over the oceans around Japan on 21 August 2011, and 16 October 2016. The MBV in 2011 also caused a gusty wind, resulting in a shipwreck. Unlike the MBV in 2015, these MBVs are seem to be associated with liner-shaped convective systems. Similar triply-nested simulations succeeded in reproducing fine structures of MBVs and associated strong TLVs. The locations of TLVs with respect to the MBV center, however, varies from case to case: a TLV in August 2011 formed in the southeast of the MBV, and TLVs in October 2016 formed in west and east of the MBV. Thus, TLVs in MBVs seem to occur in various regions with respect to the MBV center. The circulation analysis show that the source of near-surface strong vorticity for both MBVs in 2011 and 2016 is due to environmental circulation.

P11

# 30-second cycle LETKF assimilation of dual phased array weather radar observations to short-range convective forecasts

James Taylor[1], Guo-Yuan Lien[1], Yasumitsu Maejima[1], Shinsuke Satoh[2], Takemasa Miyoshi[1]

1. RIKEN Center for Computational Science, Kobe, Japan
2. NICT, Koganei, Japan

The assimilation of Doppler velocity and reflectivity observations from phased array weather radar (PAWR) have been widely studied for the use of short-range numerical weather prediction (NWP) and have been found to have positive impact to analyses and forecasts e.g. Maejima et al. 2017. However, these studies assimilated observations from a single PAWR and the use of multiple PAWR observations for NWP has not yet been explored. With the recent development of PAWR at sites in Osaka and Kobe a common observation region exists where we are able to observe convective storms across an area where they can develop very rapidly bringing intense, hazardous rainfall. This study represents the first attempt at assimilating dual PAWR observations for the purpose of improved short-range weather forecasts of a sudden convective rainfall event. We focus on a case that occurred on 20 August 2016, which generated heavy rainfall and was well observed by both radars. Simulations are performed with 30-second-cycling of PAWR observations within a high-resolution 100-m mesh using the SCALE-LETKF system (Lien et al., 2017). We aim to develop an effective data assimilation method which fully exploits the availability of having two PAWR systems to observe a single convective rainfall event and show how the data can be optimally combined to improved analyses and short-range forecasts compared to assimilating observations from a single PAWR.

## References

Lien, G.-Y., T. Miyoshi, S. Nishizawa, R. Yoshida, H. Yashiro, S. A. Adachi, T. Yamaura, and H. Tomita, 2017: The near-real-time SCALE-LETKF system: A case of the September 2015 Kanto-Tohoku heavy rainfall. *SOLA*, 13, 1-6. doi:10.2151/sola.2017-001

Maejima, Y., Kunii, M., Miyoshi, T. 2017: 30-second-Update 100-m-Mesh Data Assimilation Experiments: A Sudden Local Rain Case in Kobe on 11 September 2014. SOLA, 13, 174–180, doi:10.2151/sola.2017-032

P12

# Surface Flux Parameterization for Large Eddy Simulation

Junshi Ito[1,2], Hiroshi Niino[1], Hideaki Mouri[2]

1. Atmosphere and Ocean Research Institute, the University of Tokyo, Japan

2. Meteorological Research Institute, Japan Meteorological Agency, Japan

Email: junshi@aori.u-tokyo.ac.jp

## Abstract

Atmospheric large eddy simulation (LES) need a surface flux parameterization of turbulent transports near the ground. Conventional parameterizations used for Reynolds- Averaged Navier–Stokes simulation may not be correct for LES: the grid values of wind speed in LES contain turbulence fluctuation, so that they may be inappropriate to substitute in the surface flux parameterization. A sensitivity experiment with an atmospheric LES shows that the issue in the surface flux parameterization is relatively unimportant to domain-averaged wind speeds but significant for their variations.

The results of direct numerical simulation (DNS) and wind tunnel experiments are examined to how surface momentum flux relates to wind speeds in turbulent boundary layers. The surface flux hardly correlates with wind speed fluctuations due to turbulence. Both DNS and wind tunnel experiments suggest temporal (spatial) filtering over the correlation time (length) is required to rationalize the conventional parameterization.

Considering temporally filtered wind speed in the surface flux parameterization is a plausible modification on numerical weather prediction models. Thus, modified parameterization is implemented in LES. Its result is shown to realize more reasonable vertical profiles of wind speed variations in accord with the wind tunnel experiments: the log-law for the wind speed variations (Marusic et al., 2013) is realized.

**References:**

Marusic, I., J. P. Monty, M. Hultmark, and A. J. Smits (2013), On the logarithmic region in wall turbulence, J. Fluid Mech., **716**, R3, doi:10.1017/jfm.2012.511.

P13

# LES analysis of the effect of source heights on the longitudinal distribution of plume concentration in the convective boundary layer capped by a temperature inversion

Hiromasa Nakayama[1], Tetsuya Takemi[2]

1. Japan Atomic Energy Agency, Ibaraki, Japan

2. Disaster Prevention Research Institute, Kyoto University, Kyoto, Japan

Email: nakayama.hiromasa@jaea.go.jp

## Abstract

A convective boundary layer (CBL) capped by a temperature inversion is one of common cases of atmospheric boundary layers during daytime conditions. With solar heating after sunrise, large-scale convective flows are generated, which leads to substantial plume meandering. Consequently, a part of the plume suddenly touches the ground with high concentrations. Fedorovich and Thater (2002) conducted wind tunnel experiments and investigated the influence of different plume source heights on the longitudinal distribution pattern of concentration in a CBL capped by a temperature inversion. However, the properties of plume dispersion have not been fully discussed in conjunction with the turbulence characteristics with thermal effects.

With the rapid development of computational technology, large-eddy simulation (LES) technique has been recognized as an effective tool for providing a better understanding of physical mechanism of airflow motions, heat, and mass transfer. In this study, we perform LESs of plume dispersion in the CBL capped by a temperature inversion and clarify the mechanism of the longitudinal distribution of concentration depending on different source heights.

The model used here is LOcal-scale High-resolution atmospheric DIspersion Model using LES (LOHDIM-LES) developed by Japan Atomic Energy Agency (Nakayama et al., 2016). The model size and the number of grid points are $12\delta \times 5\delta \times 3\delta$ (δ: the inversion layer height) and $300 \times 250 \times 94$ in the streamwise, spanwise and vertical directions, respectively. The Reynolds numbers $Re_\delta$ and the bulk Richardson number $Ri_\delta$ is set to 12,000 and -0.45 which are almost the same values as those of the wind tunnel experiments (Ohya and Uchida, 2004).

In order to simulate plume dispersion in a CBL flow by LES, first, in the driver region, the very weak unstable boundary layer flow with an inversion part is generated by the

turbulent inflow technique. Then, the instantaneous wind velocities and temperature are imposed at the inflow boundary of the main analysis region. The release points are located at a downwind distance of $6\delta$ from the inlet boundary of the driver region and are elevated with three different heights of $h_s/\delta = 0.16,\ 0.50$, and 0.95, respectively. Here, $h_s$ is the source height.

In our LES results, vertical profiles of the mean velocity and temperature are nearly constant within the CBL due to the large-scale convective flows. The turbulence intensity for the vertical component also shows nearly constant in the main part of the CBL ($0.2 < z/\delta < 0.6$) due to the buoyancy-driven turbulent flows. However, the vertical turbulent motions begins to be constrained by the inversion layer. The turbulence intensity gradually decreases in the upper part ($0.6 < z/\delta < 1.0$) and rapidly decreases in the inversion layer ($1.0 < z/\delta$). These turbulence characteristics are in good agreement with the wind tunnel experiments of Ohya and Uchida (2004).

Focusing on the plume dispersion behaviors, it is found that for the case of $h_s/\delta = 0.16$ the plume is rapidly dispersed in the vertical direction with a downwind distance due to the buoyancy-driven turbulent flows. For the case of $h_s/\delta = 0.5$, the plume is also rapidly dispersed near the source location. However, at a large downwind distance from the source, the upward plume spreads are constrained by the inversion layer. For the case of $h_s/\delta = 0.95$, the vertical plume spreads are highly constrained due to the capping effects and the high concentration regions are formed for the streamwise direction at the release height. However, at a large downwind distance from the source, a part of the plume begins to touches the ground due to the large-scale convective flows. It is concluded from these results that the longitudinal distribution patterns depending on the different source heights are clarified in conjunction with the turbulence characteristics of the inversion-capped CBL flow by the LES.

**References:**

Fedorovich. E. and J. Thater: A wind tunnel study of gaseous tracer dispersion in the convective boundary layer capped by a temperature inversion, *Atmos Envi.*, **36**, 2245-2255, 2002.

Nakayama, H, T. Takemi and H. Nagai: Development of local-scale high-resolution atmospheric dispersion model using large-eddy simulation Part 5: Detailed simulation of turbulent flows and plume dispersion in an actual urban area under real meteorological conditions, *J Nucl Sci Technol.,*, **53**, 887-908, 2016.

Ohya, Y., and Uchida, T.: Laboratory and numerical studies of the convective boundary layer capped by a strong inversion, *Bound.-Layer Meteor.*, **112**, 223-240, 2004.

P14

# Intercomparison of rainfall simulations using different bulk microphysical models

Yoshinori Yamada

Meteorological Research Institute, Tsukuba, Ibaraki, 305-0052, Japan

E-mail: yyamada@mri-jma.go.jp

## Abstract

### 1. Introduction

High resolution numerical models are now available for the forecast and simulation of localized heavy rainfalls. It is not, however, so many studies focusing on the difference in the simulated precipitation fields depending on microphysical models. This paper presents an intercomparison of rainfall simulations using different three bulk models for a case of a catastrophic heavy rain fall event from 6th July, 2018 to 8th in the western part of Japan.

### 2. Outline of the experiments

Three bulk microphysical models are used in this study. Two of those are from Ikawa and Saito (1987) and Yamada (2016). Both models classify water substances into six species (water vapor, cloud water, rain, cloud ice, snow, and graupel), the latter is, however, more sophisticated and high in degree of freedom. In the rest (hereafter Y2018) of the models, water is categorized into five types of water vapor, cloud water, rain, “snow crystal”, and graupel. The category of snow crystal includes pristine ice, snow, and rimed ice particles except for graupel. This classification resembles that in Morrison and Grabowski (2008), the category of graupel, however, remains because it is not suitable to represent a drop size distribution for an ensemble of snow crystals and graupels, both of which have very different properties. The ice phase model of Y2018 is similar to that in Yamada (2016).

The two-moment scheme of warm rain by Cohard and Pinty (2000) is employed. The analytical self-collection equation for rain drops (Verlinde and Cotton 1990) is used instead except for the model of Ikawa and Saito (1987).

The simulations are made using JMA-NHM (Saito et al. 2006) with a horizontal resolution of 0.5 km for a model domain of 450 km x 450 km centered at (132.66 E, 34.25 N). Number of vertical layers was 60, and the top of the model domain was set to 21.8 km. The model run started at the initial time of 06 UTC on Jul. 6 up to 6 hours. The initial and boundary conditions were supplied from the meso-analysis of Japan Meteorological Agency. The boundary layer model for the grey zone (Ito et al. 2015) was used. Two-moment ice phase models is used throughout, while warm rain model is either one- or two-moment.

## 3. Results

Figure 1 shows hourly rainfall at forecast hour = 4. All of the simulated rainfall fields represent a band-like precipitation pattern. The difference in the one- and the two-moment model of the warm phase brought about contrasts in the rainfall amounts. It is also found that the difference in the ice phase model does not bring about significant differences in the simulated rainfall amount for this heavy rainfall event.

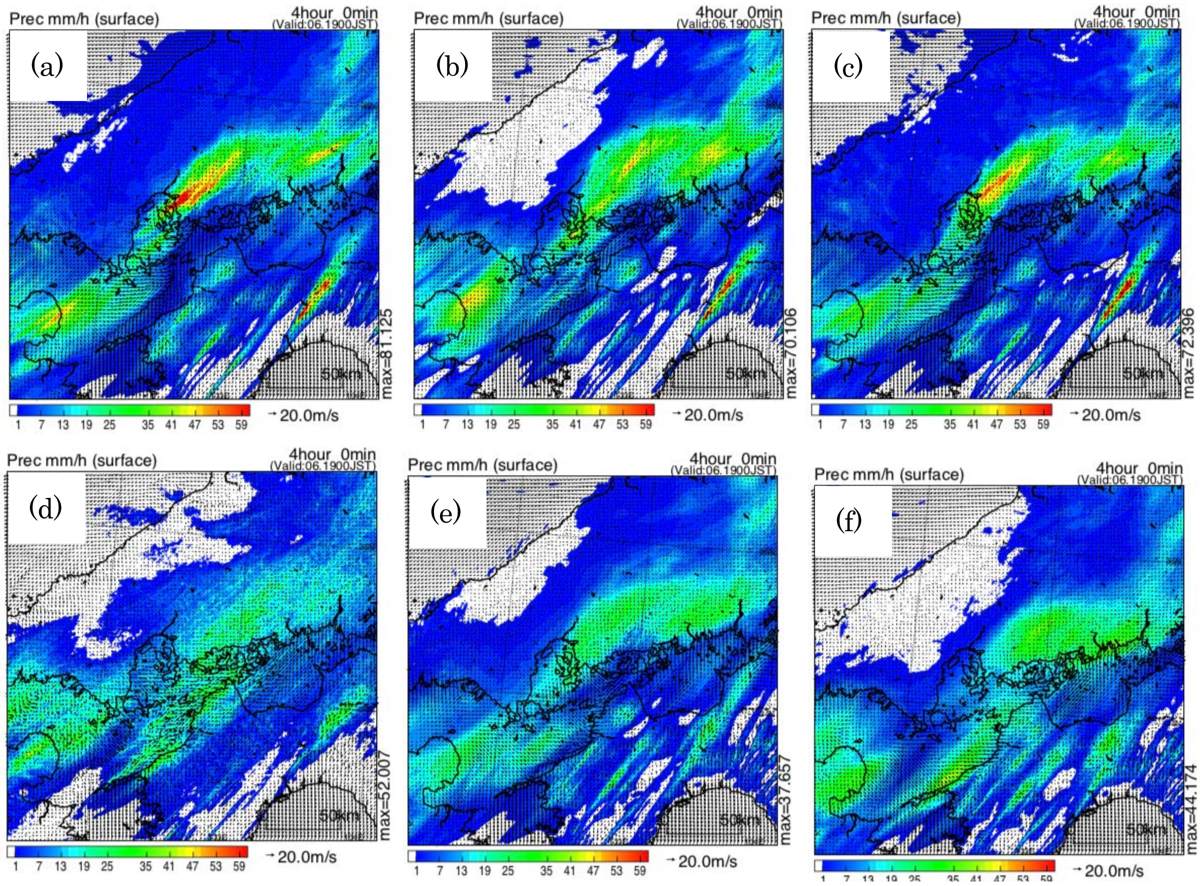


Fig. 1 Simulated hourly rainfall amount in mm. Upper panels: results using one-moment model of warm phase. (a): Ikawa and Saito, (b) Yamada (2016), (c) Y2018. Lower panel: results using two-moment model of warm phase. (d): Ikawa and Saito, (e) Yamada (2016), (f) Y2018.

## References:


Ito, J., H. Niino, M. Nakanishi, and C.-H. Hoeng, 2015: An extension of the Mellor–Yamada model to the terra incognita zone for dry convective mixed layers in the free convection regime. *Bound.-Lay. Meteorol.*, **157**, 23-43.

Morrison, H. and W. W. Grabowski, 2008: A novel approach for representing ice microphysics in models: Description and tests using a kinematic framework. *J. Atmos. Sci.*, **65**, 1528 – 1548.

Saito, K., T. Fujita, Y. Yamada, J. Ishida, Y. Kumagai, K. Aranami, S. Ohmori, R. Nagasawa, S. Kumagai, C. Muroi, T. Kato, H. Eito, and Y. Yamazaki, 2006: The Operational JMA Nonhydrostatic Mesoscale Model. *Mon. Wea. Rev.*, **134**, 1266-1298.

P15

# Revisit of the fixed anvil temperature hypothesis from nonhydrostatic global simulations

*Akira T. Noda[1], T. Seiki[1], M. Satoh[1,2] and Y. Yamada[1]

[1]Japan Agency for Marine-Earth Science and Technology, Japan

[2]Atmosphere and Ocean Research institute, The University of Tokyo, Japan

(Akira T. Noda, a_noda@jamstec.go.jp)

## 1. Introduction

*Hartmann and Larson* [2002] proposed a constraint of a response of high clouds to global warming, termed the fixed-anvil-temperature (FAT) hypothesis. The hypothesis states that cloud-top temperature, $T_{CT}$, remains nearly constant despite the increase in surface temperature due to global warming. The validity of the FAT hypothesis depends on the magnitude of the changes of cloud-top temperature. However, it has not been well recognized the extent to which changes can be regarded as *small* or *large* enough. We investigate the relative components of the changes of outgoing-longwave radiation (OLR) at the top of the atmosphere (TOA) by decomposing the contributions into $T_{CT}$, cloud optical thickness (or cloud emissivity, $\varepsilon$), and clear-sky OLR, $F^{CLR}$.

## 2. Data

NICAM is used in the present study. The model configuration used was the same as Noda et al. [2014, JCLI, 2015, JMSJ], with mesh intervals of approximately 7 km and a time integration period extended to a full year (1 June 2004-31 May 2005). In the following analysis, we defined a high-cloud region as one where the modeled OLR at TOA was less than 210 W m$^{-2}$, and cloud sizes are shown as an equivalent radius of a circle, and thus the minimum radius is approximately half of the model grid size [Noda et al., 2012, JCLI]. We focus mostly on the tropical and subtropical regions between 30°S and 30°N, which will be referred to as 'low latitudes' hereafter.

## 3. Diagnosis of OLR

To evaluate what factors contribute to the net OLR change, we derive a diagnostic equation of OLR at the TOA, $F$ (W m$^{-2}$), in terms of $T_{CT}$ (K), $\varepsilon$, and $F^{CLR}$ (W m$^{-2}$). We begin with an approximation of OLR as

$$F \simeq \sigma\varepsilon T_{CT}^4 + F_{CB} \simeq \sigma\varepsilon T_{CT}^4 + (1-\varepsilon)F^{CLR} \quad (1)$$

where $F_{CB}$ (W m$^{-2}$) is the upwelling longwave radiation from the bottom level of a high cloud, and $\sigma(= 5.67\times10^{-8}\mathrm{Wm^{-2}K^{-4}})$ is the Stefan-Boltzmann constant. We calculated $\varepsilon$ using an approximation proposed by *Fu and Liou* [1993] as

$$\varepsilon = 1 - exp(-a\tau) \quad (2)$$

where $a$=0.79. $\tau$ is an optical depth. Thus, OLR at TOA is approximately diagnosed from equation (1) by determining the cloud top temperature $T_{CT}$. Conventionally, the $T_{CT}$ value is often defined at the level where optical depth from cloud top $\tau_c$ reaches 0.1 [e.g., *Hartmann and Larson*, 2002]. In this study, however we use an empirical formula instead of the constant value of 0.1 as

$$\tau_c = \max\left(min\left(\frac{\tau_2-\tau_1}{F_2-F_1}(F-F_1),\tau_2\right),\tau_1\right) \quad (3)$$

where ($F_1$, $\tau_1$)=(200, 0.1) and ($F_2$, $\tau_2$)=(185, 0.4). These values are derived from a trial-and-error approach to diagnose a simulated relation between OLR and cloud radius. The response of OLR to global warming, $\Delta$, can be approximated as

$$\Delta\bar{F}^{(i)} \simeq \left(\frac{\partial F}{\partial \varepsilon}\right)_{T_{CT},F^{CLR}} \Delta\bar{\varepsilon}^{(i)} + \left(\frac{\partial F}{\partial T_{CT}}\right)_{\varepsilon,F^{CLR}} \Delta\overline{T_{CT}}^{(i)} + \left(\frac{\partial F}{\partial F^{CLR}}\right)_{T_{CT},\varepsilon} \Delta\overline{F^{CLR}}^{(i)}$$

$$\equiv F_\varepsilon \Delta\bar{\varepsilon}^{(i)} + F_T \Delta\overline{T_{CT}}^{(i)} + F_F \Delta\overline{F^{CLR}}^{(i)}. \quad (4)$$

An overbar with a prefix, $i$, denotes an average over $i$-th cloud area. Those values are hereafter shown with being binned at cloud radius. Using the above formula, one can evaluate the contributions of $\varepsilon$, $T_{CT}$, and $F^{CLR}$ to changes of $F$.

## 4. Results

Figure 1 shows each contribution of the terms in Eq. 4 on OLR as a function of cloud size. From CTL to GW (Fig. 1a), OLR changes positively by 1.0–3.5 W m$^{-2}$ for the clouds with $r$>50 km for the actual $\Delta F$. The contribution of the three terms to the net OLR change clearly varies depending on the radius. The change of cloud emissivity is largest at approximately $r$=90 km, and then decreases with increasing radius. In contrast, the effect of the changes of $T_{CT}$ becomes stronger with increasing radius. In particular, for $r$>340 km, the contribution magnitude becomes comparable to that of cloud emissivity (blue and green lines, respectively). In contrast to the above two terms, the $F^{CLR}$ contribution is very small: the term is negative at every radius, and its amplitude increases slightly with increasing cloud radius by $r$=700 km.

Considering the net contributions (Fig. 1b), the changes in $\varepsilon$ strongly contribute to the net OLR change by $r$=1800 km due to changes of smaller clouds. In contrast, the contribution of $T_{CT}$ increases gradually, nearly constantly with radius, eventually slightly exceeding that of $\varepsilon$. The effects of changes in $\varepsilon$ and $T_{CT}$ are nearly comparable with each other, and the changes in $F^{CLR}$ have a much weaker effect.

## 5. Summary

We have argued for the importance of the FAT hypothesis based on the high-resolution GCM data, in which cumulus parameterization was not used, particularly focusing on the dependency on high cloud size. The present study suggests that the extent to which the FAT hypothesis holds true can depend on cloud size. That is, for smaller cloud sizes (e.g., less than approximately 340 km in the present case), the contribution of $T_{CT}$ is of secondary importance, and the contribution of cloud emissivity is more important. In contrast, for clouds larger than 340 km, the contribution of cloud emissivity is comparable to that of $T_{CT}$, and thus, both of the two components become equally important. The role of $F^{CLR}$ is smaller than those of the two previous factors over the low latitudes. The changes of $F^{CLR}$ depend weakly on cloud radius. In addition, we also showed dependency of the responses of precipitable water, $\tau$, $\varepsilon$, $F_{CLR}$, and $T_{CT}$ to global warming on cloud radius.

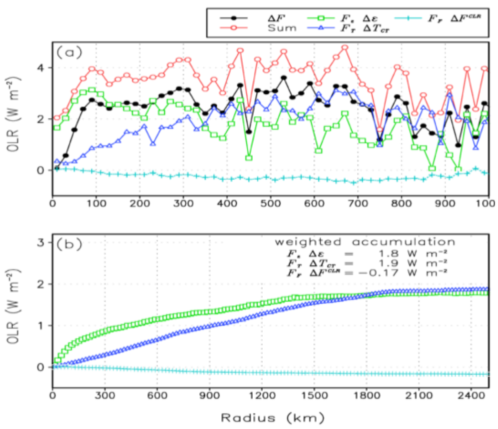


Figure 1. Budget analysis of OLR changes due to global warming binned by cloud size (20 km bins), showing (a) mean values for each cloud size, and (b) their area-ratio-and-frequency-of-occurrence-weighted accumulation in the $x$ (radius) direction. The original OLR values (black), diagnosed values from Eq. 4 (red), and the contributions of each RHS term (green, blue and sky blue) are plotted.

P16

# High resolution simulation of the west Japan heavy rainfall in July 2018

Tsutao Oizumi[1,4], Kazuo Saito[2,3,4], Le Duc[1,4], Junshi Ito[2,4]

1 Japan Agency for Marine-Earth Science and Technology, Japan

2. Japan Meteorological Business Support Center, Japan

3. Atmosphere and Ocean Research Institute, the University of Tokyo, Japan

4. Meteorological Research Institute, Japan

Email: oizumi@jamstec.go.jp

## Abstract

Several landslides and floods caused by heavy rainfall in west Japan, on July 5th – 8th, 2018. To mitigate the damages of heavy rainfall and evacuate residents in a timely fashion, an accurate numerical weather prediction (NWP) system is vital. In the previous heavy rainfall event in Izu Ohsima in October 2013, the authors showed importance of grid spacing, planetary boundary layer (PBL) schemes, terrain data and model domain size (Oizumi et al., 2013)

In this study, we conducted an ultra-high resolution numerical weather prediction (NWP) simulations with a large domain area to this west Japan rainfall event in July 2018. Several important model factors (grid spacing, model domain size) influencing heavy rainfall forecasting in NWP models were investigated. An optimized version of NHM (Oizumi et al. 2015) for the K computer was used to this study with the model domains presented in Fig. 1. The model settings are listed in Table 1.

Fig. 2 shows the Radar-AMeDAS precipitation results. Fig.3 shows the results of 5-, 2-km and 500-m grid spacing models with the large and small model domain experiments. The result showed the 2-km resolution models showed better precipitation performance than 5-km resolution models. And the 500-m resolution models with both model domains showed better precipitation performance than 2-km resolution models. The 2-km and 500-m resolution models with the large model domain shows better performance than those with the small domain. Overall, the results indicated that using a high-resolution model (500 m grid spacing) with a large domain area provides an advantage for simulating torrential rain events.

Table 1. List of experiments using the large and small domain area

| Experimental name | Grid spacing (m) | Time step (s) | Domain | Number og grids | Vertical level | Turbulence closure model | Cumulus parametrization | W threshhold (m/s) |
|---|---|---|---|---|---|---|---|---|
| KF5kmMY | 5,000 | 24 | LFM | 321 × 221 | 50 | MYNN3 | CM with KF | 3 |
| CM2kmMY | 2,000 | 10 | LFM | 800 × 550 | 60 | MYNN3 | CM | 5 |
| CM500mDD | 500 | 2 | LFM | 3197×2197 | 85 | DD | CM | no |
| KF5kmMY_L | 5,000 | 24 | LFM | 633 × 521 | 50 | MYNN3 | CM with KF | 3 |
| CM2kmMY_L | 2,000 | 10 | LFM | 1581 × 1301 | 60 | MYNN3 | CM | 5 |
| CM500mDD_L | 500 | 2 | LFM | 6321×5201 | 85 | DD | CM | no |

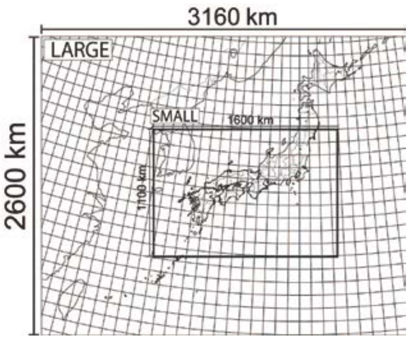


Fig. 1. Model domains used: large: 3160-2600 km, small:1600-1100 km.

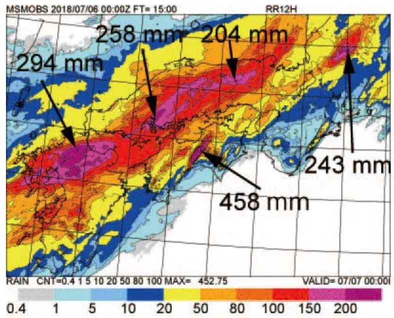


Fig. 2. Observed 12-hour precipitation from 1200 JST on July 6th to 0000 JST on July 7th

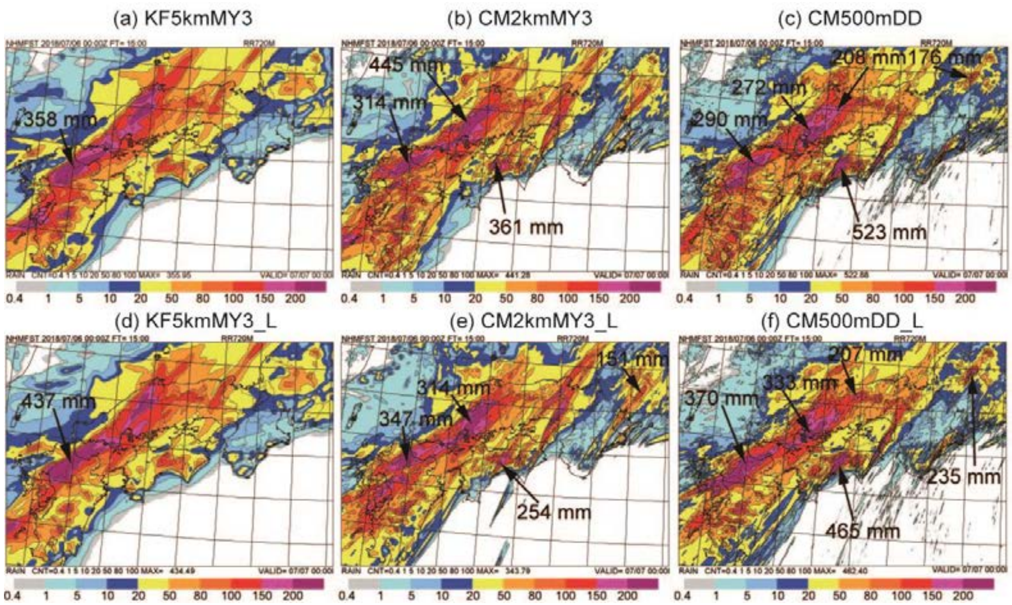


Fig. 3 12-hour precipitation from 1200 JST on July 6th to 0000 JST on July 7th. (a)-(c) are the small model domain results and (d)-(f) are the large model domain results.

## References:

Oizumi, T., T. Kuroda, K. Saito, J. Ito, and S. Hayashi, 2015: Performance tuning of the JMA-NHM for the K supercomputer. *WGNE Blue Book*, 3-09.

Oizumi, T., K. Saito, J. Ito, T. Kuroda, and L. Duc, 2018: Ultra-high-resolution numerical weather prediction with a large domain using the K Computer: A case study of the Izu Oshima heavy rainfall event on October 15-16, 2013. *J. Meteor. Soc. Japan*, **96**.

P17

# Development and validation of a diagonal ensemble transform Kalman filter

Le Duc[13], Kazuo Saito[23], and Daisuke Hotta[3]

1. Japan Agency for Marine-Earth Science and Technology, Japan

2. Atmosphere and Ocean Research Institute, the University of Tokyo, Japan

3. Meteorological Research Institute, Japan

Email: leduc@jamstec.go.jp

## Abstract

A variant of the ensemble transform Kalman filter (ETKF) has been developed with the following property: analysis perturbations run independently from each other. The independence of each perturbation helps to maintain physical structures of perturbations associated with large-scale systems like tropical cyclones or fronts in a consistent and coherent manner through multi assimilation cycles. This property dictates a special form for the ensemble transform matrix (ETM) in ETKF: that is a scalar multiple of the identity $\mathbf{I}$. Therefore, this variant of ETKF is called the diagonal ETKF.

In this study, we show that the diagonal ETKF can be derived from the two very different approaches: (1) the diagonally predominant property of the unique positive symmetric ETM $\mathbf{T}^s$, i.e. the diagonal elements are at least an order of magnitude larger than the off-diagonal elements; and (2) constant inflation functions, i.e. the spectrum of $\mathbf{T}^s$ is replaced by a constant function. Experiments using real observations show that the diagonal ETM produces forecasts better than the ones obtained from the conventional ETM $\mathbf{T}^s$.

P18

# 4DEnVar with Iterative Calculation of Nonlinear Nonhydrostatic Model Compared to En4DVar


Sho Yokota[1], Ko Koizumi[1], Masaru Kunii[2,1], and Kosuke Ito[3,1]

1. Meteorological Research Institute, Japan Meteorological Agency

2. Numerical Prediction Division, Forecast Department, Japan Meteorological Agency

3. University of the Ryukyus

Email: syokota@mri-jma.go.jp


## 1. Introduction

En4DVar and 4DEnVar are two popular variational data assimilation methods that use the ensemble-based forecast error covariance. While En4DVar calculates the gradient of the cost function with the adjoint of tangent linear forecast model, 4DEnVar calculates it with the ensemble perturbations. To compare between En4DVar and 4DEnVar, we developed these two methods based on JMA nonhydrostatic model (NHM)-based 4DVar data assimilation system (JNoVA), which iteratively calculates the nonlinear NHM to gain the cost function.

## 2. Formulation

In JNoVA, to gain the analysis $\mathbf{x}_t = M_t\,(\mathbf{x}_0^f + \mathbf{U}\mathbf{v})$, the cost function

$$J(\mathbf{v}) = \frac{1}{2}\mathbf{v}^T\mathbf{v} + \frac{1}{2}\sum_t [HM_t(\mathbf{x}_0) - \mathbf{y}_t]^T \mathbf{R}_t^{-1} [HM_t(\mathbf{x}_0) - \mathbf{y}_t] \qquad (1)$$

is minimized using the gradient of the cost function

$$\nabla J(\mathbf{v}) = \mathbf{v} + \sum_t \mathbf{U}^T\mathbf{M}_t^T\mathbf{H}^T\mathbf{R}_t^{-1}[HM_t(\mathbf{x}_0) - \mathbf{y}_t], \qquad (2)$$

where $\mathbf{x}_0^f$ is the first guess, $\mathbf{U}$ is the square root of the climatological background error covariance, $M_t$ and $\mathbf{M}_t$ are the nonlinear forecast model and its tangent linear version, respectively, $H$ and $\mathbf{H}$ are the observation operator and its tangent linear version, respectively, and $\mathbf{y}_t$ and $\mathbf{R}_t$ are the observation and the observation error covariance in time $t$, respectively. In En4DVar, $\mathbf{U}$ is replaced by initial ensemble perturbations $\mathbf{X}_0=[\delta\mathbf{x}_0^{(1)}\ldots\delta\mathbf{x}_0^{(N)}]/(N-1)^{1/2}$. In 4DEnVar, furthermore, $\mathbf{X}_0^T\mathbf{M}_t^T$ in Eq. (2) is replaced by perturbations of ensemble forecasts $\mathbf{X}_t^T$. Therefore, the nonlocal gradient of the cost function can be reflected in the analysis of 4DEnVar without the adjoint model $\mathbf{M}_t^T$ compared to En4DVar.

## 3. Data Assimilation Experiments with Lorenz-63 model and JNoVA

To clarify the advantage of 4DEnVar compared to En4DVar, we conducted the data assimilation experiments with the Lorenz-63 model (the number of ensemble members: 3). The result showed that 4DEnVar can further minimize the cost function than En4DVar if the gradient of the cost function is nonlinear and the ensemble perturbations are appropriate (Fig. 1).

In the single observation assimilation experiments with JNoVA, the analysis of 4DEnVar was different from that of En4DVar (Fig. 2). In both analyses, however, the observation was assimilated as expected. The difference between En4DVar and 4DEnVar is probably caused by the nonlinearity of the NHM.

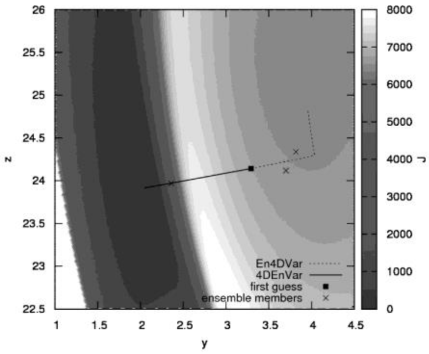


Fig.1. The cost function (shaded) and the trajectory of its minimization by En4DVar (dotted line) and 4DEnVar (solid line) with the Lorenz-63 model. ■ and × are points of the first guess and the three members, respectively.

## 4. Summary

We developed En4DVar and 4DEnVar based on JNoVA and examined the difference of them. As a next step, we will develop the time evolution of the climatological background error covariance to improve the hybrid of forecast error covariance in 4DEnVar.

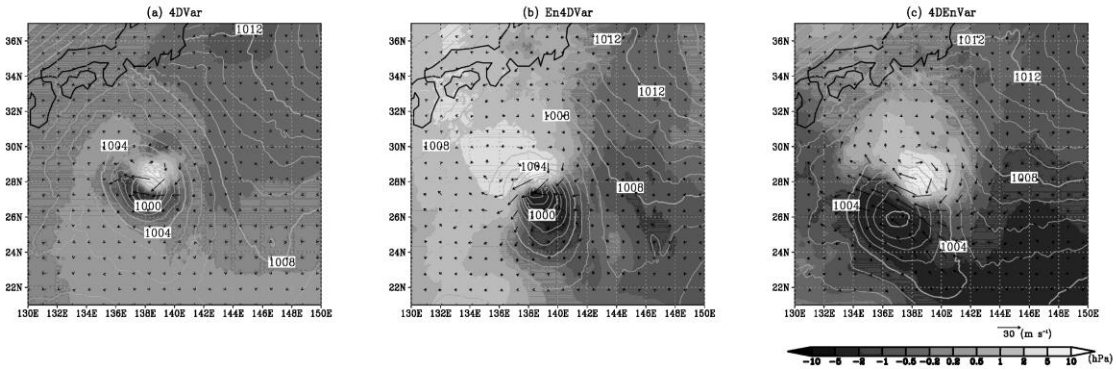


Fig.2. The analysis increments of horizontal wind (arrows, m s$^{-1}$, 1180-m height) and surface pressure (shaded, hPa) along with the analyzed surface pressure (contours, hPa) at the time of observation in the single observation assimilation experiment with JNoVA (a: 4DVar; b: En4DVar; c: 4DEnVar). In each experiments, zonal wind –30.0 m s$^{-1}$ (innovation: –47.7 m s$^{-1}$) is assimilated in (138.7E, 27.7N) at 1180-m height at the end of the 3-hour assimilation window and the number of ensemble members is 50.


**Acknowledgement:**

This work was supported in part by “social and scientific priority issues (Theme 4) to be tackled by using post K computer of the FLAGSHIP2020 Project” (Project ID: hp160229, hp170246, hp180194) and JSPS KAKENHI Grant Number JP16K17804 and JP16H04054.

# Ensemble-based Singular Value Decomposition Analysis to Clarify Relationship between the Atmospheric State and the Hydrometeors

Sho Yokota[1], Hiromu Seko[1,2], Nobuhiro Nagumo[1], Hiroshi Yamauchi[3,1], Rei Kudo[1], Tetsu Sakai[1], Yoshinori Shoji[1], Takuya Kawabata[1], Yasutaka Ikuta[4,1], and Hiroshi Niino[5]

1. Meteorological Research Institute, Japan Meteorological Agency
2. Japan Agency for Marine-Earth Science and Technology
3. Administration Division, Observation Department, Japan Meteorological Agency
4. Numerical Prediction Division, Forecast Department, Japan Meteorological Agency
5. Atmosphere and Ocean Research Institute, The University of Tokyo

Email: syokota@mri-jma.go.jp

## 1. Introduction

To improve the accuracy of numerical forecasts of local rainfalls through assimilation of observations associated with rainfall, it is important to understand the relationship between the atmospheric state around the precipitation and the hydrometeors in the precipitation. To investigate such relationship statistically, we performed the singular value decomposition (SVD) of the ensemble-based cross-covariance matrix between the atmospheric state and the hydrometeors using 301-member ensemble forecasts of a local rainfall occurred on the Kanto Plain at about 1430JST on 4 August 2016.

## 2. Data Assimilation with NHM-LETKF System

The 301-member initial states of the ensemble forecasts at 1430JST were created by the JMA nonhydrostatic model-based local ensemble transform Kalman filter (NHM-LETKF[1]) with the 1-km horizontal grid interval. In NHM-LETKF, data observed by four C-band radars, GNSS, and a water vapor Raman Lidar were assimilated with the 10-min assimilation window from 1400JST. The additive ensemble perturbations correlated to the atmospheric state were used for the assimilation of the radar reflectivity[2].

## 3. SVD Analysis for the Local Rainfall

We created the ensemble-based cross-covariance matrix between the atmospheric state and the hydrometeors $\mathbf{XY}^T$ and calculated its singular values $d_i$ and singular vectors of the atmospheric state $\mathbf{u}_i$ and the hydrometeors $\mathbf{v}_i$ as $\mathbf{XY}^T = \sum_{i=1}^{301} d_i \mathbf{u}_i \mathbf{v}_i^T$. Here, $\mathbf{X} = [\delta\mathbf{x}_1 \dots \delta\mathbf{x}_{301}]/\sqrt{300}$ is the matrix of 301-member ensemble perturbations of zonal wind ($U$), meridional wind ($V$), vertical wind ($W$), potential temperature (PT), pressure ($P$), and water vapor mixing ratio (QV) and $\mathbf{Y} = [\delta\mathbf{y}_1 \dots \delta\mathbf{y}_{301}]/\sqrt{300}$ is that of mixing ratio of cloud water, cloud ice, rain, snow, and graupel at the time of the rainfall (1450JST). The squared covariance fraction of the first mode was about 50%. The heterogeneous correlation maps of the first mode indicated that the hydrometeors in the rainfall were mainly correlated with the convergence of the horizontal wind and humid air below the 2-km height especially before the rainfall (Figs. 1 and 2). It means that correcting the atmospheric state below the 2-km height through the hydrometeor data assimilation is effective for rainfall forecasts.

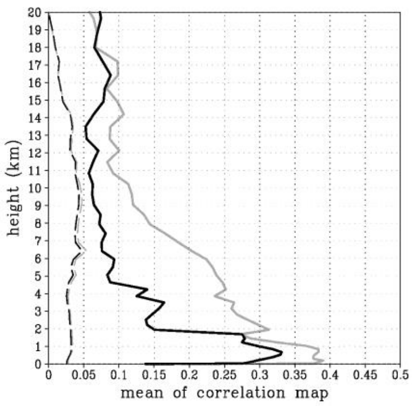


Fig.1. Vertical profile of heterogeneous correlation map of $\mathbf{u}_1$ (solid) and $\mathbf{v}_1$ (dotted) averaged horizontally in the square region (22km × 22km). Black and gray mean the atmospheric states $\mathbf{X}$ at 1430 and 1450JST were used for SVD, respectively.

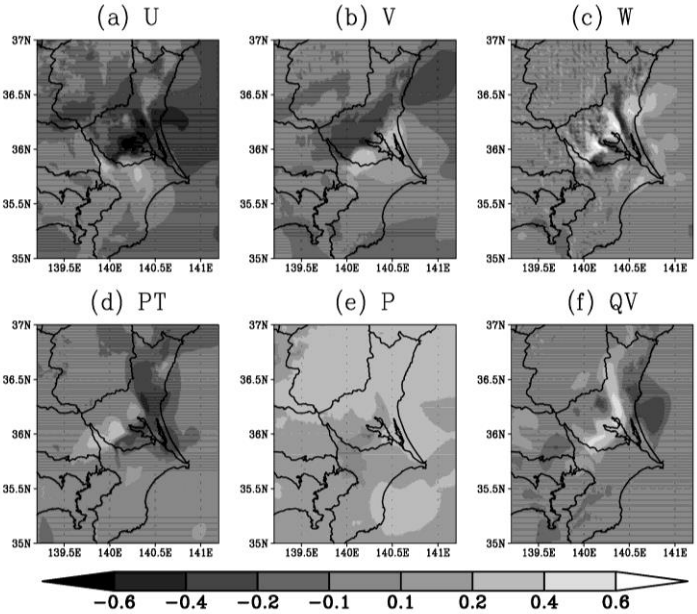


Fig.2. Heterogeneous correlation map of $\mathbf{u}_1$ at 0.4-km height. The atmospheric state $\mathbf{X}$ before the rainfall (1430JST) was used for SVD.

**Acknowledgement:**
This work was supported in part by "social and scientific priority issues (Theme 4) to be tackled by using post K computer of the FLAGSHIP2020 Project" (Project ID: hp160229, hp170246, hp180194) and JSPS KAKENHI Grant Number JP16K17804 and JP17H00852.

**References:**
[1] Kunii, M. (2014). Mesoscale data assimilation for a local severe rainfall event with the NHM–LETKF system. *Wea. Forecasting*, **29**, 1093–1105.
[2] Yokota, S., H. Seko, M. Kunii, H. Yamauchi, and E. Sato (2018), Improving short-term rainfall forecasts by assimilating weather radar reflectivity using additive ensemble perturbations. *J. Geophys. Res.*, **123**, 9047–9062.

P20

# Dense precipitation radar data assimilation with an ensemble Kalman filter: an observing system simulation experiment for a typhoon case

Atsushi Okazaki[1], Takumi Honda[1], Shunji Kotsuki[1], Takemasa Miyoshi[1]
1. RIKEN Center for Computational Science, Japan
Email: atsushi.okazaki@riken.jp

**Abstract**

Precipitation radar observations have been playing an important role in meteorology through providing valuable information such as precipitation nowcast. Recently, such observations started to be used in the field of numerical weather prediction. Previous studies showed some success in data assimilation of radar reflectivity for convective-scale and tropical cyclone analyses. Nevertheless, it is still difficult to build a general approach to data assimilation of radar reflectivity due to various factors such as the non-diagonal observation error covariance matrix, complex observation operator, and strong nonlinearity and model errors in the moist physical processes. In this study, we aim to develop a method to effectively assimilate radar reflectivity data. We perform an observing system simulation experiment, in which we assume that reflectivity data are available at all model grid points, using the SCALE-LETKF system (Lien et al., 2017) and a satellite simulator known as the Joint-Simulator (Hashino et al., 2013). As the first step, we focus on a case of Typhoon Soudelor (2015), the strongest typhoon in the West Pacific in 2015. In the presentation, we will show the impact of dense radar observations on the analyses and forecasts of Typhoon Soudelor.

**References:**

Lien, G.-Y., T. Miyoshi, S. Nishizawa, R. Yoshida, H. Yashiro, S. A. Adachi, T. Yamaura, and H. Tomita, 2017: The near-real-time SCALE-LETKF system: A case of the September 2015 Kanto-Tohoku heavy rainfall. *SOLA*, 13, 1-6. doi:10.2151/sola.2017-001

Hashino, T., M. Satoh, Y. Hagihara, T. Kubota, T. Matsui, T. Nasuno and H. Okamoto, 2013: Evaluating cloud microphysics from NICAM against CloudSat and CALIPSO, *Journal of Geophysical Research: Atmospheres*, 118, 377 7273-7292, doi: 10.1002/jgrd.50564

P21

# Assimilating every-10-minute Himawari-8 infrared radiances to improve convective predictability

Yohei Sawada[1,2], Kozo Okamoto[1,2], Masaru Kunii[1,3],
and Takemasa Miyoshi[2,4,5,6,7]

[1] Meteorological Research Institute, Japan Meteorological Agency, Tsukuba, Japan

[2] RIKEN Center for Computational Science, Kobe, Japan

[3] Numerical Prediction Division, Japan Meteorological Agency, Tokyo, Japan

[4] RIKEN Interdisciplinary Theoretical and Mathematical Sciences Program, Kobe, Japan

[5] Prediction Science Laboratory, RIKEN Cluster for Pioneering Research, Kobe, Japan

[6]Department of Atmospheric and Oceanic Science, University of Maryland, College Park, Maryland, USA

[7]Japan Agency for Marine-Earth Science and Technology (JAMSTEC), Yokohama, Japan

Email: ysawada@mri-jma.go.jp

## Abstract

Improving the predictability of sudden local severe weather is a grand challenge for numerical weather prediction. Recently, the capability of geostationary satellites to observe infrared radiances has been significantly improved, and it is expected that the 'Big Data' from the new generation geostationary satellites contribute to improving convective predictability. We examined the potential impacts of assimilating frequent infrared observations from a new generation geostationary satellite, Himawari-8, on convective predictability. We implemented the real-data experiment in which Himawari-8 all-sky moisture sensitive infrared radiances of band 8 (6.2μm) and band 10 (7.3μm) were assimilated into the high-resolution (2km) limited area model every 10 minutes. The frequent infrared observations from Himawari-8 improve the analysis and forecast of isolated convective cells and sudden local severe rainfall induced by weak large-scale forcing (Figure 1). The results imply that satellite data assimilation can contribute to better forecasting severe weather events in smaller spatiotemporal scales than the previous studies.

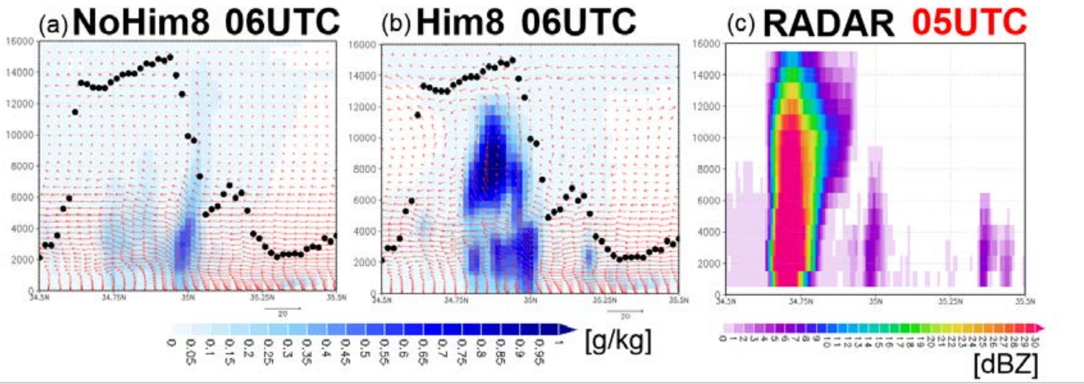


**Figure 1.** Vertical cross section of total condensate mixing ratio and wind vectors. Values are averaged from 135.5E to 135.75E. Black dots show cloud heights from the Himawari-8 Optimal Cloud Analysis (OCA) data. (a) The NoHim8 experiment in which only conventional observations are assimilated. (b) same as (a) but for the Him8 experiment in which Himawari-8 radiances are assimilated every 10 minutes. (c) radar reflectivity observations from the JMA's radar. Note that the time of (c) is different from the others.